Slope Stability Analyses of Selected Road-Cut Slope Section from Agarfa Town-Wabe River Bridge, Bale Zone, Southeastern Ethiopia

Dita Amano Merga

A Thesis Submitted to the Department of Applied Geology

School of Applied Natural Science

Office of Graduate Studies

Adama Science and Technology University

July, 2023

Adama, Ethiopia

Slope Stability Analyses of Selected Road-Cut Slope Section from Agarfa Town-Wabe River Bridge, Bale Zone, Southeastern Ethiopia

Dita Amano Merga

Advisor

Yadeta Chemdesa (Ph.D.)

Co-Advisor

Tola Garo (MSc.)

A Thesis submitted to the Department of Applied Geology

School of Applied Natural Science

Presented in Partial Fulfilment of the Requirement for the Degree of Master's in Engineering Geology

Office of Graduate Studies

Adama Science and Technology University

July, 2023

Adama, Ethiopia

DECLARATION

I hereby declare that this Master thesis entitled "**Slope Stability Analyses of Selected Road-Cut Slope Section from Agarfa Town-Wabe River Bridge, Bale Zone, Southeastern Ethiopia**" is my own work and has not been submitted to any university for similar purpose. The references used in this proposal are duly recognized by proper citations.

Dita Amano ________________________ ________________

Name of student Signature Date

RECOMMENDATION OF ADVISORS

I, the major advisor of this thesis, hereby certify that we read the revised version of the thesis entitled "**Slope Stability Analyses of Selected Road-Cut Slope section from Agarfa Town-Wabe River bridge, Bale zone, Southeastern Ethiopia**" was prepared under our guidance by **Dita Amano** and submitted in the partial fulfillment of the requirements for the degree of Masters of science in Engineering Geology. Therefore, we recommend the submission of a revised version of the thesis to the department following the applicable procedures.

___________________________	________________________	________________
Major Advisor	Signature	Date
__________________________	________________________	________________
Co-advisor	Signature	Date

APPROVAL PAGE

We, the advisors of the thesis entitled "Slope Stability Analyses of Selected Road-Cut Slope Section from Agarfa Town-Wabe River Bridge, Bale Zone, Southeastern Ethiopia'' and developed by Dita Amano Merga, hereby certify that the recommendation and suggestions made by the board of examiners are appropriately incorporated into the final version of the thesis.

Major Advisor:	Signature	Date
Co-advisor:	Signature	Date

We, the undersigned, members of the Board of Examiners of the thesis by have read and evaluated his thesis entitled "**Slope Stability Analyses of Selected Road-Cut Slope Section from Agarfa Town-Wabe River Bridge, Bale Zone, Southeastern Ethiopia** and examined the candidate during open defense. This is, therefore, to certify that the thesis has been accepted in partial fulfillment of the requirement of the Degree of Master of Science applied Geology.

Chairperson:	Signature	Date
Internal Examiner:	Signature	Date
External Examiner:	Signature	Date

Finally, approval and acceptance of the thesis is contingent upon submission of its final copy to the Office of Postgraduate Studies (OPGS) through the Department Graduate Council (DGC) and School Graduate Committee (SGC).

Department Head:	Signature	Date
School Dean:	Signature	Date
Office of Postgraduate Studies, Dean:	Signature	Date

ACKNOWLEDGEMENT

First of all, I would like to express my deep gratitude and praises to the Almighty God for all good graces and mercies he granted me in my life and throughout my thesis work successful. Next, I would like to express my sincere gratitude to my advisor, Dr. Yadeta Chemdessa, for his guidance, support, and encouragement throughout my research. His expertise, insights, and feedback have been invaluable in shaping my work and helping me to achieve my goals.

I would also like to thank my co-advisor, Mr. Tola Garo, for his contributions to my research. His knowledge, and guidance have been instrumental in helping me to navigate the challenges of my research.

I am grateful to the school of applied natural science and staff of the applied geology department for their support and encouragement throughout my studies. Their dedication to teaching and research has inspired me to pursue my own academic and professional goals

I would like also to thank Addis Ababa Science and Technology University the School of Civil and Architectural engineering Geotechnical Laboratory department of mining engineering for the material and laboratory support they contribute for me to accomplish this thesis. I would like to forward my appreciation to Ethiopian Institute of Geological Survey and National Metrological Agency for providing me necessary data for this research works.

I would like to thank my family and friends for their unwavering support and encouragement throughout my academic journey. Their love, encouragement, and understanding have been a constant source of strength and motivation for me.

Finally, I would like to thank Adama Science and Technology University for its financial support.

Table of Contents

LIST OF FIGURES

LIST OF TABLES

LIST OF ABBREVIATIONS AND ACRONYMS

FOS = Factory of Safety

FEM = Finite Element Method

JV = Volumetric Joint Count

JS = Joint set

SF = Slope Face

SRF = Stress reduction factor

DD = Dip direction

DA = Dip angle

LEM = Limit Equilibrium Method

RMR = Rock Mass Rating

RQD = Rock Quality Destination

RSS = Road slope section

SMR = Slope Mass Rating

UCS = Uniaxial compressive Strength

USCS = Unified Soil Classification Systems

ABSTRACTS

*Infrastructure development is crucial for a country's economic, social, and cultural evolution. It involves not only construction but also sustainable practices that can boost the economy. However, the construction of civil engineering infrastructure such as roads, buildings, dams, and open-pit mines is often hindered by the instability of slopes along road cuts. This issue can have serious consequences for lives, properties, traffic flow, and car accidents***.** *The road which connects Agarfa town to Wabe river bridge passes steep slope landscape to gentle slope with main to minor valleys and prone to slope stability failure. The study area was along a road between Agarfa town to Wabe river bridge. The aim of this study was to assess the stability of selected road sections by analyzing the geological and geotechnical properties of the materials that determine the FOS of the critical slope sections and proposing remedial measure. This study identifies eight different slope section out of these two structural controls (R1SS2 and R3SS2), three heterogenous rock slope R2SS1, R3SS1 and R5SS2 and other rock slope was homogenous basaltic slope (R4SS2) and two soil slope section (clay and silt clay) soils. From the field observation and kinematic analysis was show that different mode of failure such as planar, wedge and toppling occur at slope section R1SS2 and R3SS2. The FOS determined by deterministic methods such as Rocplane and swedge software. The stability analysis was conducted under four different scenarios, including static dry, dynamic dry, static saturated, and dynamic saturated conditions. Additionally, the soil laboratory test was conducted for four soil test pits to determining of shear parameter and for classification. From four soil sample two of them were homogenous soil slope (SS1 and SS3) and the other two was from heterogenous slope section (SS2 and SS4). The cohesion and frictional angle of the soil samples obtained from direct shear tests for SS1, SS2, SS3 and SS4 were 45.31K KN/m2, 38.68 KN/m2, 18.47 KN/m2, 17.65 KN/m2 and 19.16°, 19.22°, 23.21°, and 24.88°, respectively. Liquid limit, plastic limit and plastic index of SS1 were 73.5, 36 and 37.5, For SS2 were 68.9, 33 respectively. The study conducted slope stability analyses using deterministic, limit equilibrium and finite elements methods under different static and saturation conditions. The results showed that most of critical rock and soil slopes were unstable under static saturated and dynamic saturated conditions compared to static dry and dynamic dry conditions. The analyses identified rainfall, groundwater, and unfavorable orientation of rock discontinuities as causative factors for critical slope failures. Based on the findings, the study* recommends remedial measures such as increasing the benching, lowering the slope angle and proper drainage systems in the critical slope failure sections.

Key words*: Factory of safety (FOS), stability analysis, kinematic analysis, deterministic, limit equilibrium and finite element methods*

CHAPTER ONE

1. INTRODUCTION

1.1 Background of the Study

Slope stability refers to the ability of a sloped ground or rock face to withstand and receive movement (Bayou, 2020). Slope stability analysis is an important tool for designing and constructing slope area (Bekele, 2022; Lamessa, 2019; Torabi-Kaveh et al., 2023a). Instability of slope is one of the most frequent natural disasters that can lead to huge loss of properties and human life in danger (Göktepe & Keskin, 2018). According to (Bekele & Meten, 2022) slope instability is one of the most important concerns among researchers and professionals in rock and soil slope engineering. The problem of the instability of slopes, both natural and artificial slopes, in connection with the construction of civil projects such as roads and railways, is of particular concern to project managers (Torabi-Kaveh et al., 2023b). The slope failures are natural occurrences that commonly occur along cut slopes of road built in hilly areas of the world causing the loss of life, injury, and significant property damage each year (Cao *et al*., 2016). Natural disasters such as landslides, soil collapse, and slope failures regularly occur throughout the world. These frequently occur as a result of a lack of forethought while dealing with sloping terrain (Habtemariam *et al*., 2022). According to (Kabeta *et al*., 2020) the Ethiopian highlands are highly vulnerable to slope instability due to land use change, including heavy rainfall and road construction impacts. The majority of the Ethiopian plateau's north, south, and western regions have a history of slope instability due to mountain and roadside cutting, both in the surface materials and at bedrock Kiros *et al*., (2020).

The study area is a part of the southeast Ethiopia plateau, where rugged topography mountains are present. The most crucial aspects of rock and soils slope stability are the characteristics and orientation of a discontinuity in the rock mass (Vatanpour *et al.,* 2014). The direction of the rock mass's discontinuity affects the slope's stability. Due to the presence of irregularly oriented discontinuities in the rock and soil mass, the slopes along the road cut may fail. The limit equilibrium, kinematic, and finite element approaches are only a few of the analytical and numerical modeling techniques that a number of scholars (Sarkar & Chakraborty, 2021) have used to assess slope stability. Slope stability evaluations using the limit equilibrium method or the finite element approach using the shear strength reduction (SSR) technique can be performed to analyze the factor of safety (Hussain et al., 2019; Siddque & Pradhan, 2018; Tiwari et al., 2020). The factor of safety (FOS) is the ratio of resisting forces to driving forces that describes the slope stability Komadja et al., (2020). A lot of authors of use the Morgenstern and Price (1965) method due to its ability to accommodate any form of slip surface, as well as the accurate comprehensive equilibrium parameters established by Zheng (2012). To asses and analyze stability of the slope, some of the methods such as: Kinematic, Deterministic, Probabilistic and Numerical methods (Hoek and Bray, 1981; Abramson *et al*., 2002; Wyllie and Mah, 2004; as cited in (Lamessa, 2019) were used frequently. Therefore, it is necessary to identify and analyze stability of the slope and this study used kinematic, deterministic and Numerical methods to evaluate the stability of the slopes and possible remedial measures were recommended based on the analyses result.

1.2 Statement problems

Slope stability is the resistance of inclined surface to failure by sliding or collapsing (Khanna & Dubey, 2021). This can cause damage to human beings as well as properties. Such areas have to be clearly identified including the different processes that cause the failure, mechanism of failure and the possible remedial measures for that landslide problem. The study was conducted on a road that connects Agarfa town to Wabe river bridge in Oromia, Southeastern Ethiopia. The road was constructed in 2015 E.C. to facilitate transportation between Bale zone and East Arsi zone. However, the road has been facing frequent slope instability problems due to soil and rock slope failures. The study aimed to identify and analyze the slope stability problems along the selected road section using various methods such as kinematic, limit equilibrium, and finite element methods. The study also recommended remedial measures based on the analysis results. The road is situated in a rugged landscape and has complex geology, including aphanitic basalts on the upper slope section within columnar joint shape and other slightly to highly weathered pyroclastic rock. Therefore, it is crucial to consider the stability of the proposed area before designing an artificial or natural slope. No research or investigation has been conducted on slope stability along the road segment to identify, analyze, and recommend appropriate mitigation measures.

1.3 Objectives

1.3.1 General objective

The general objective of this study was to identify and analyze slope instability problems along the road section from Agarfa town to the Wabe river bridge, Oromia, Southeastern Ethiopia

1.3.2 Specific objective

- To detect possible slope instability issues on road segments.
- To assess the geological and geotechnical characteristics of soils and rocks in crucial slope sections.
- To identify the mode of failure, calculate the safety factor (stress reduction factor), and assess the likelihood of failure for the critical slope section.
- To identify the factors that trigger or contribute to slope instability.
- To suggest potential corrective actions to reduce risks associated with the unstable slope.

1.4 Significance of the study

Road and highway networks play a vital role in remote areas for transportation, public network, and all kind of socio-economic activities. Slope failure is a great problem in the highlands of Ethiopia along road sections. This kind of phenomenon can affect traffic circulation even causing car accidents. The investigation of slope stability is an important aspect in the design and construction of highways and roadways in hilly terrain. Inadequate input or considerations of critical geologic features or structures associated with a particular slope can lead to slope failure with accompanying serious consequences. Therefore, detailed investigations of slope failure cause and assessment of triggering factors should be carried out in the study area.

The significance of the study is to differentiate the possible causes of slope failure and also to predict future problem conditions. This study also contributes to reducing the damages caused by slope failure in the form of movements. Later, the study can provide a proper remedial measure for the stability of slopes. Moreover, the present study may be helpful to researchers, individuals, or organizations, intending to carry out similar types of studies.

1.5 Limitations of the study

The study area is geologically very complex, with various orientations and the total road crosses slopes ranging from very steep to near-gentle. However, due to time, resource, and financial constraints, the present study was only able to identify eight critical slope sections on this road. Furthermore, the present study lacks sufficient secondary data, such as drill log geophysical data, geotechnical reports, and trial test pit depth, to fully understand the subsurface geology.

CHAPTER TWO

2. LITERATURE REVIEW

2.1 Introduction

The most parts of the world, slope failures represent a significant natural hazard. Slope stability problems are common in the construction of highways, canals, and dams, as well as some natural slopes that may become unstable due to the presence of water that affecting soil properties. Ground slope instability, rock slope instability, surface flooding, and soil erosion, as well as natural geological variations all-cause damage to constructed infrastructure such as roads, buildings, and dams in Ethiopia (Bekele, 2022). Generally, a slope failure can be defined as a downward movement soil or rock. Slope failures are also referred to as mass wasting. Slope failures can occur suddenly in one easily recognized movement, or may occur over a period of many years. Slope failures can occur without warning, but typically they give early warning signs, such as; surface cracks and tilted fence posts, poles, and trees. However, the problem of slope instability was also widespread along roads that the pass country mountainous region. According to (Woldearegay, 2013) rainfall-induced slope failures are common in hilly and mountainous terrains of Ethiopia characterized by a variety of topographical, geological, hydrological (surface and groundwater) and land-use conditions.

2.2 Slope stability studies in Ethiopia

In Ethiopia the problem of slope instability is wide spread mainly along the roads which cross through mountainous region of the country. To investigate the causative factor and recommend possible remedial measures different researchers did different investigations Lamessa (2019). As cited by Ofori *et al*. (2020) limit equilibrium method slope stability analyses conducted along the main road from Gohatsion to Dejen towns by identifying geological and geotechnical properties of geological material that compose the slope section. The study identified slope instability problems in the form of rockfall, toppling, planar, and wedge mode of rock failure in rock slope sections and circular mode of failure in the soil slope section. The problems were severe in the area on the sides of the road mainly during the rainy season.

2.3. Factors governing slope stability

The diverse topographical features of the Earth's surface are possible only because the shear strength of the soil exceeds the shear stresses due to gravity and other loads. Slope failures can occur not only in the steepest slope, but also in relatively shallow slopes. Factors leading to instability can generally be classified based on the effect they have on slopes (Yokota &

Iwamatsu, 2000). According to (Chala, 2017) governing factors are generally divided into internal factors such as gravity, geometry of the slope, potential failure planes, surface drainage, groundwater conditions, mineral composition, and shear strength parameters of material which compose the slope and external factors which are seismicity, rainfall and human activities. Each type of the governing factor is discussed as follow:

2.4 Internal factors

2.4.1 Gravity

The main force responsible for mass movement is gravity. Gravity is the force that acts everywhere on the Earth's surface, pulling everything in a direction toward the center of the Earth. On a flat surface the force of gravity acts downward. So long as the material remains on the flat surface it will not move under the force of gravity. Of course, if the material forming the flat surface becomes weak or fails, then the unsupported mass will move downward. On a slope, the force of gravity can be resolved into two components: a component acting perpendicular to the slope and a component acting tangential to the slope.

The perpendicular component of gravity, gp, helps to hold the object in place on the slope. The tangential component of gravity, gt, causes as shear stress parallel to the slope that pulls the object in the down-slope direction parallel to the slope.

- On a steeper slope, the shear stress or tangential component of gravity, gt, increases, and the perpendicular component of gravity, gp, decreases. The forces resisting movement down the slope are grouped under the term *shear strength* which includes frictional resistance and cohesion among the particles that make up the object.
- When the sheer stress becomes greater than the combination of forces holding the object on the slope, the object will move down-slope.
- Alternatively, if the object consists of a collection of materials like soil, clay, sand, etc., if the shear stress becomes greater than the cohesion forces holding the particles together, the particles will separate and move or flow down-slope

Thus, downslope movement is favoured by steeper slope angles which increase the shear stress, and anything that reduces the shear strength, such as lowering the cohesion among the particles or lowering the frictional resistance.

2.4.2 Geometry of the slope

Parameters which are considered as geometry of the slope, especially for rock slope are; dip and dip direction of the slope and failure plane, slope height, upper slope dip, tension crack

(Lamessa, 2019). Each of the parameters has their own effect on to the stability of the slope either in individually or collectively. Most of the time, steeper slope causes the slope to be unstable (Wyllie, 2014). In general, the steeper the slope, the more slope instability due to the higher shear induced by gravity, although various types of slope failure are related to certain slope range.

2.4.3. Potential failing planes

One of the factors which determine the stability of the rock and soil slope is potential failure plane. In rock slope failure, persistence of discontinuities such as joint, fault and shear plane act as failure plane along which the slope will fail. Sometimes, hard strata on which weak layer of the soil rest may serve as failure plane of soil slope. For specific mode of rock slope failure to occur, dip of the potential failure plane should be less than dip of the slope face but greater than friction angle along failure plane Hoek and Bray (1981); Willy and Mah (2004), as cited in (Bekele, 2022).

2.4.4 Surface water drainage

According to Ofori *et al*. (2020) Surface water drainage and groundwater conditions are the main slopes destabilizing factors by decreasing shear strength and increasing the shear stress applied to the failure plane. Surface water which infiltrates into the slope mainly through tension cracks will produce water force, increasing weight over the slope face and lubricate the failure plane which later enhances slope instability (Bekele, 2022; Hoek et al., 1995).

2.4.5 The parameter that describes the shear strength of the material that makes up the slope

The influence the shear strength parameters of soil on the slope stability are very important, especially when changing the cohesion. After determining the correct values, the shear strength parameters, you can calculate correct value of the factor of safety of soil for the optimal design of slope without failure.

Shear strength parameters are the parameters that describe the resistance of a material to sliding along a plane or surface. The materials that compose a slope can have different shear strength parameters depending on their composition and properties.

Some common materials that can compose a slope and their corresponding shear strength parameters are (Mite *et al*., 2020):

1. Rock: The shear strength of rock depends on its type, structure, and degree of weathering. The shear strength parameters of rock include cohesion and angle of internal friction.
2. Soil: The shear strength of soil depends on its type, density, moisture content, and other factors. The shear strength parameters of soil include cohesion, angle of internal friction, and angle of dilation.
3. Vegetation: The presence of vegetation on a slope can increase its stability by providing root reinforcement and increasing soil cohesion.
4. Water: The presence of water can decrease the shear strength of soil and rock by reducing cohesion and increasing pore pressure.

It is important to consider the shear strength parameters of the materials that compose a slope when assessing its stability and designing measures to prevent slope failure.

2.5 External factors

2.5.1 Rainfall

Rainfall is one of the most significant triggering factors for slope failure occurrence in the tropical regions. The mechanism of rainfall induced slope failure is as follows: rainfall infiltration results in a reduction of matric suction in soil which in turn reduces the soil shear strength, and subsequently triggers the slope failure (Lee *et al.*, 2009). Furthermore, heavy downpour may cause a perched water table with positive pore-water pressure develops in the soil slope, which will further decrease the shear strength of soil and eventually make the slope increasingly susceptible to failure. Rainfall infiltration is one of the important factors affecting the stability of a slope.

Most of the time, the main reason for slope failure occurrence is the influence of rainfall which is one of the external and triggering factors of slope instability (Ayalew *et al.*, 2004; Pentilidis, 2009; Woldearegay, 2013; Raghuvanshi *et al.*,2014; as cited by Lamessa, (2019)). The rainfall which infiltrates into the slope will increase the instability of the potential failure plane by reducing shear strength (Pentilidis, 2009; Raghuvanshi, 2017). One of the impacts of rainfall is it increase elevation of groundwater level. Groundwater in turn affects stability of the rock slope for the following reason (Wyllie and Mah, 2004).

2.5.2 Seismicity

Seismicity is another factor that causes slope stability, especially in active seismic zones (Hoek et al., 1995). According to (Kundu et al., 2018) the minimum magnitude of an earthquake that causes a slope failure is about 4–5 mm. From a safety point of view, it is recommended to consider seismic activity for critical structures such as steep slopes (Dahle *et al*., 1992).

2.5.3 Human activity

Human activities such as improper slope modification and excavation can cause slope stability. The most human activities that can cause runway failures are: Unplanned logging of slopes, steepening of slopes, inappropriate excavation at the bottom of slopes, and adding additional loads (Bayou, 2020).

2.6 Mode of slope failure

The common types of slope failures that are expected in soil slopes are translation, planar or wedge, circular, non-circular, and combinations of both circular and non-circular (Khursheed & Sharma, 2020). According to (Durrani, 2005; Dyson & Tolooiyan, 2020) translational failure occurs when shallow soil is placed on top of relatively strong material. Planar slope failure happens in soil layers or relict joints with relatively low strength, which determines the failure surface. Similar to how soil slopes fall in a circular manner, heavily fragmented rock can also fail in this manner (Sharma et al., 2019). When a slope has a heterogeneous composition, the noncircular mode of failure typically occurs.

According to geology and engineering knowledge, slope can be either natural or man-made (cutting and filling). A slope that develops naturally on a slope or as a stream bank is known as a natural slope. Long ago, ground movements and earthquakes created slopes. Unless there is construction, these slopes often remain undisturbed. These slopes may become unstable as a result of a variety of internal (natural processes) and external (forces) (human actions). A cut slope is a slope made by removing part of a natural slope's surface to make room for construction (such as road construction or tunneling).

These common four types of failure are detail described as flows:

A. **planar failure**

   A rock slope undergoes this mode of failure when combination of discontinuities in the rock mass from blocks or wedges within the rock which are free to move. The pattern of the discontinuities may be comprised linked to a single discontinuity or a pair of discontinuities that intersects each other, or a combination of multiple discontinuities that are linked together to from a failure mode. A planar failure of rock slope occurs when a mass of rock in a slope slide down along a relatively planar failure surface. The failure surface are usually structural discontinuities such as bedding planes, faults, joints or the interface between bedrock and an overlying layer of weathered rock. According to Hoek E., (2009) failures in rock slopes can be classified into four types; (a) Plane mode of failure, (b) Wedge mode of failure, (c) Circular or Rotational mode of failure, and (d) Toppling mode of failure.

- The dip direction of the planar discontinuity must be within (±20˚) of the dip direction of the slope face.
- The dip of the planar discontinuity must be less than the dip of the slope face.
- The dip of the planar discontinuity must be greater than the angle of friction on the surface.

B. Wedge failure

Wedge failure occur when two discontinuities strike obliquely across the slope face and their line of intersection daylights in the slope face. The wedge of rock resting on these discontinuities will slide down the line of intersection, provided that the inclination of this line is significantly greater than the angle of friction. Necessary structural conditions for wedge failure can be summarized as follows (Hoek & Bray, 1981):

- The trend of the line of intersection must approximate the inclination direction of the slope face.
- The plunge of the line of intersection must be less than the inclination of the slope face and thereby the line of intersection must daylight in the slope.
- The plunge of the line of intersection must be equal or greater than the angle of friction of the intersecting surfaces (discontinuities).
- When cohesion (C) equals to zero

C. Toppling failure

Toppling failure occurs when columns of rock, formed by steeply dipping discontinuities in the rock rotate about an essentially fixed point at or near the base of the slope followed by slippage between the layers. Jointed rock mass closely spaced and steeply dipping discontinuity sets dip away from the slope surface are necessary prerequisites for toppling failure.

D. Rotational (Circular) failure

The failure surface in section of rotating slips can be a circular are or non-circular curve. Circular slips are generally associated with homogeneous soil conditions, whereas non-circular slips are associated with non-homogeneous conditions. When the shape of the failure surface is altered by the presence of a neighboring stratum of significantly differing strength, translation and compound slide occur. Translational slips are most common where the next stratum is at a shallow depth below the surface and the neighboring stratum is planar and generally parallel to the slope. When the next stratum is at a larger depth, compound slips occur, with the failure surface comprising curved and planar parts. A rotating slide is the movement of material along a curved surface.

E. Rock fall

When rock blocks detach from the rock mass and fall freely under gravity it is known as rock fall. The rock blocks may role down, bounce or slide along the surface. These are characterized by movement away from existing discontinuities, such as; joints, fissures, steeply-inclined bedding planes, fault planes, etc. and within which the slope failure assisted or precipitated by the effects of water or ice pressure (Roy, 2001; as cited in Balaram Naik *et al*. 2013). Rock fall is triggering lot of problems in safety and maintenance of highways in mountainous terrains. In mountainous terrain, infrastructure such as highways, railways, and power generation facilities, as well as houses and apartment buildings, may be subject to rock fall hazards. These hazards can result in economic losses due to service interruptions, equipment damage, and loss of life (Wyllie, 2014).

2.7 Soil and rock mass failure criteria

Soil and rock mass failure criteria are used to evaluate the stability of soil and rock masses under different loading conditions. The following are some commonly used failure criteria:

1. Mohr-Coulomb Failure Criterion: This criterion is used to evaluate the shear strength of soils and rocks. It states that failure occurs when the shear stress on a plane reaches a critical value, which is a function of the normal stress on the plane and the friction angle of the material.
2. Hoek-Brown Failure Criterion: This criterion is used to evaluate the strength of rock masses. It takes into account the effect of the rock mass structure and the presence of discontinuities such as joints and faults. The criterion is based on the concept of equivalent Mohr-Coulomb strength parameters.
3. Bishop's Method: This method is used to evaluate the stability of slopes in soil and rock masses. It takes into account the shear strength of the soil or rock mass, the slope angle, and the pore water pressure in the soil.

4. Terzaghi's Method: This method is used to evaluate the stability of soil masses under different loading conditions. It takes into account the shear strength of the soil, the normal stress on the soil, and the pore water pressure in the soil.

These failure criteria are used in geotechnical engineering to evaluate the stability of soil and rock masses in various applications such as slope stability analysis, foundation design, and tunneling.

2.8 Slope stability analysis methods

Slope stability is one of the most important engineering practices, especially in large, critical projects such as: highways (roads), dams, and tunnels. There are many techniques for assessing the stability of a particular embankment. Slope stability analysis can be performed using a variety of techniques. Rock mass rating, slope mass rating, kinematic, deterministic and numerical methods (Abramson, *et al*., 2002; Raghuvanshi, 2017). Previous methods of slope stability analysis were generally based on hand performed, which simplified the calculations.

2.8.1 Discontinuity surveying

Discontinuity surveying is one of the slope stability analysis methods for discontinuous rock mass which contains discontinuities and its failure mechanism is controlled by pre-existing discontinuities (Aleumu & Abebe, 2007). The movement of intact rock blocks bounded within discontinuities and the deformation of intact rock can be addressed for both, static and dynamic conditions (Stead et al., 2006). In discontinuity surveying slope geometry, discontinuity characteristic, discontinuity shear strength and stiffness, in-situ stress and groundwater data are used as input data.

2.8.2 Rock mass classification system

The rock mass classification system is one of the empirical methods used to determine rock quality and performance based on intrinsic structural parameters (Molla, 2011). Rock classification systems were developed many years ago for underground excavation as an alternative to analytical analysis of discrete rocks. It was first proposed by (Bieniawski, 1973) for application to the design of tunnels, dams, mines and excavations. Its application to assess slope stability was subsequently introduced by (Bieniawski, 1979). To determine rock quality and analyze the stability of critical rock slopes, rock quality can be classified according to the basic rock rating system (Beiniaswski, 1989). It classifies rock mass quality using five basic rock mass classification parameters, which are intact rock strength, rating index of rock quality (RQD), discontinuity space, discontinuity condition, and groundwater conditions. The strength of a intact rock can be determined either by the uniaxial compressive strength of the rock or by the point load strength index. The uniaxial compressive strength (UCS) of rock can be determined from the point load strength index using (Broch & Franklin, 1972) an empirical relationship as follows:

UCS = 24*Is (50) …………… … ………………………………………………… eq 2.1

Where is (50) size corrected point load strength

Similarly, the rock quality index (RQD) is determined by the sum of intact rock greater than 10 cm per core total governing equation (Deere, 1989). In the area where core rock data were not available, the rock quality index (RQD) was determined using the volume interface calculation method (Palmstrom, 1982), which is the total number of discontinuities greater than 10 cm (Jv) one square meter of rock as shown in the below.

RQD = 115-3.3*JV………………………………………………………………… eq 2.2.

Here the volumetric discontinuity joints (jv) is the sum of the number of discontinuities per unit length for all discontinuity sets, which can be determined from the discontinuity set spacings within volume of the rock mass as (Palmstrom, 1982) , as the follows eq. 2.3 $\mathrm{Jv} = 1/\mathrm{s1} + 1/\mathrm{s2} + 1/\mathrm{s3} + \cdots + 1/\mathrm{sn}$ (2.3) Where s1, s2, and s3 are the mean discontinuity set spacings. Palmstrom (1982) suggests that r= 5 m be assumed. As a result, the volumetric discontinuity frequency Jv can be generalized as eq.2.4 , $\mathrm{Jv} = 1/\mathrm{s1} + 1/\mathrm{s2} + 1/\mathrm{s3} + \cdots + \mathrm{Nr}/5$ (2.4) where Nr is the number of random discontinuities.

2.8.2.1 Uniaxial compressive strength (UCS) of intact rock

The uniaxial compressive strength is a crucial parameter in rock engineering practice, as noted by (Çobanoğlu & Çelik, 2008). To determine the strength of intact rock material, rock cores are tested in the laboratory. The uniaxial compressive strength (UCS) can be estimated using the empirical formula proposed by Broch and Franklin (1972) based on the point load strength index Is (50), as well as through Schmidt hammer rebound hardness value (R) measurements in both laboratory and in situ tests, as suggested by (Kahraman, 2001). In rock mechanics, N-values obtained from Schmidt hammer hardness measurements are used to evaluate the UCS and modulus of elasticity (E) of intact rock in both laboratory and in situ tests, as highlighted by Rahim et al. (2021). Miller (1965), as cited in (Torabi-Kaveh et al., 2023b) proposed a correlation between rebound number and UCS for determining rock quality. Additionally, Barton & Choubey (1977) suggested that UCS can be calculated by multiplying the rebound number by the dry density of the rock using a specific equation below.

$log10(UCS) = 0.00088 * \gamma * R + 1.01$ ………………………………………………eq. 2.5

Where, UCS is the uniaxial compressive strength in Mpa, γ is the dry rock densities in KN/m^3 and R is the average Schmidt rebound value.

2.8.2.2 Slope mass rating

Slope Mass Rating (SMR; Romana, 1985) is calculated using correction factors of basic RMR (Bieniawski, 1989). It was initially used only for planar and toppling mode of failure. The method was later adapted by Anbalagan et al. (2008)) to include the wedge mode of failure. It was obtained from the basic rock mass rating (RMR) by adding adjustment factors derived from joint–slope relationship and factor depending on method of excavation. Later, stability class and probability of failures for rock slope can be shown in below relationship. These factors depend on the existing relationship between discontinuities affecting the rock mass and the slope, and the slope excavation method. Its obtained using expression below (equation1):

SMR = RMRb + (F1 × F2 × F3) + F4) ………………………………………………… Eq 2.6

2.8.2.3 Geological strength index (GSI)

The Geological Strength Index (GSI), one of the methods of rock mass classification develop new by Marinos et al., (2007)), offers a system for calculating the reduction in rock mass strength under various geological conditions. According to (Singh et al., 2020) the GSI value was determined by examining the weathering state of the discontinuity surface, the structure of the rock mass, and the interlocking of rock blocks at the study site. The parameters needed to define the properties of the rock mass strength are derived using the following formula after the geological strength index and mi have been estimated.

Mb = mi exp $((GIS - 100)/(28 - 14D))$ ……………………………………………… Eq 2.7

mi for intact rock is determined from lab triaxial test or the tabulated data proposed by Hoek et al., (2000) for different types of rock.

2.8.3 Kinematics analyses

Kinematic analysis is method used to identify various types of rock slopes failures (plane, wedge, topping failure) that may occur in existing or planned rock slopes, roads, identified by the presence of unaligned discontinuities along hills, and pit slopes (Aksoy & Ercanoglu, 2007; RK et al., 2011; Wyllie & Mah, 2004). It indicates the motion of an object regardless of the force that moves it Goodman (1989). Kinematic analyzes are performed to identify slopes failures in various types of rock slope failures, most commonly performed by stereographic projection. This is the first step in identifying rock slope failures types and modes H. Park & West, (2001). The analysis can be done by importing the friction angle (friction cone), and slope direction of the slope, and discontinuities into the slope software. The software then performs kinematic analysis to identify major joints, daylight envelopes, lateral boundaries, and rock slopes failures types (Goodman, 1989; Hudson and Harrison, 1997; Willy and Mah, 2004).

2.8.4 Limit equilibrium methods

The limit equilibrium analysis method is an established method and is widely used by engineering geology and engineers. The most widely applied analytical technique used in geotechnical analysis is that of limit equilibrium, whereby force or/and moment equilibrium conditions are examined on the basis of statics. These analyses require information about material strength, but not stress-strain behavior. This method primarily assesses slope stability in relation to a safety factor. To determine the safety factor for a given slope, the strength properties of the soil material in question are the main requirement and its stress-strain behavior is not considered. The limit equilibrium method only provides an estimate of slope stability and does not provide information on the extent of slope movement (Kundu et al., 2018; Loka et al., 2017). LEM was used to analyze the crushing stability of rock slopes using Rocscience slide software (Pant JR, Acharya IP. , 2021). The typical output from a limit equilibrium analysis is the “Factor of Safety”: FS = resisting forces /driving forces. FS > 1.0 represents a stable situation, FS < 1.0 denotes failure Eberhardt2003 (2017). There several number of limit equilibrium methods available therefore, only the most popular and well-known methods presented in this study. Hopkins *et al*. (1975) and Duncan (1996(*No Title*, n.d.)) presented a review on several methods. According to (Aryal *et al*., 2005) these methods are based on the method of slices and can be divided broadly into four categories, depending on the number of equilibrium equations to be satisfied.

2.8.4.1 Analytical methods of limit equilibrium

The method of slices is a widely used analytical method in geotechnical engineering for analyzing the stability of slopes and embankments. The method involves dividing the slope into a series of vertical slices and analyzing the forces acting on each slice. Here is a list of the different types of method of slices (Fredlund & Krahn, 1977):

1. Ordinary Method of Slices: This method assumes that the soil is homogeneous and isotropic, and the slices are assumed to be straight and parallel.
2. Bishop's Simplified Method of Slices: This method is an improvement over the ordinary method of slices and takes into account the variation of shear strength along the slip surface.
3. Janbu's Simplified Method of Slices: This method is similar to Bishop's method but considers the variation of pore water pressure along the slip surface.
4. Morgenstern-Price Method of Slices: This method is a more advanced method that considers the non-linear variation of shear strength along the slip surface.
5. Spencer's Method of Slices: This method is a modification of the bishop’s method and considers the effect of the pore water pressure on the stability of the slope.

In general, the method of slices involves dividing the slope into a series of vertical slices, calculating the forces acting on each slice, and determining the factor of safety for the slope. The factor of safety is the ratio of the resisting forces to the driving forces, and if it is less than 1, the slope is considered unstable. The method of slices is widely used in geotechnical engineering for analyzing the stability of slopes, embankments, and other earth structures.

2.8.5 Finite element methods

The finite element method is a powerful calculating method in engineering. This method is a method used to analyze geotechnical problems. In contrast to the limit equilibrium method, the finite element method considers the linear and nonlinear stress-strain behavior of the soil when calculating the analytical shear stress. The finite element approach causes slope failure through a zone that cannot withstand the applied shear stress. According to (Mebrahtu et al., 2022; Memon, 2018; Rodrigo Garcia Motta, Angélica Link, Viviane Aparecida Bussolaro et al., 2021; Suparyanto dan Rosad (2015, 2020) the results obtained from this analysis are considered more realistic than the limit equilibrium method . In slope stability analysis, the main advantage of the finite element method over the limit equilibrium method is that no assumptions need to be made about the shape and position of the failure surfaces, the slice side forces, and their orientation in the FEM (Liu.*et.al.* , 2014).

2.9 Remedial measure for slope instability problems

After the problems of slope stability are identified, the appropriate remedial measure for slope is selected on the basis of feasibility, stability and economy (Kazmi *et al.*, 2017). According to Pun & Urciuoli, (2008) surface protection and drainage, subsurface drainage, slope regarding, retaining structures, structural reinforcement, strengthening of slope-forming material, vegetation and bioengineering, removal of hazards and others are the remedial measures generally considered to stabilize unstable slope. Movement of soil and rock down unstable slopes due to gravity is called mass wasting; surface movement resulting from the effects of wind and water is called erosion. The remedial methods proposed by Broms and Wong are divided into three main categories.

1. **Geometrical method**

This method is simple and cheaper in cost but require sufficient space. Slope safety can be enhanced easily to convert steeper slopes into gentler ones. This method can be executed by trimming the slope or making the slope free from extra loading. Backfilling of toe also lies under this category. By changing the geometry of a steep slope to a gentler slope either flatten the slope or backfill at the toe of slope, the stability of a slope can be increased. This method is easy and most cost effective. However, it depends very much on the site condition. As there are existing building at the site, this method cannot be adopted (Kazmi, Qasim, Harahap, Baharom, et al., 2017). Adding (counter weight berm or fill) material to stability maintain area removing material from landslide driving area (light weight fill) reducing the slope angle.

2. **Drainage method**

This method usually works in combination with other methods. Drainage method is viable in those conditions where proper maintenance of surface and sub-surface drains is performed. Saturation of subsoil and pore water pressure building up are major factors causing the instability of slope. With the proper design of surface and subsurface drainage system, the chances of building up pore water pressure and saturation of subsoil can be minimized and therefore the stability of slope can be increased. However, as a long-term solution to increase the stability of slope, this method suffers greatly because the drainage systems must be maintained if they are to continue to function It is always easy to maintain the surface drains but very difficult for the subsoil drains. This method is generally used in combination with other methods (Kazmi, Qasim, Harahap, Baharom, et al., 2017). Surface drains for diversion of water (pipes and ditches) Shallow or deep trench drains having filled with free draining Geo-materials Vertical boreholes for self-draining Vertical wells for gravity draining Buttress counterforts of coarse-grained materials Sub vertical and sub horizontal boreholes Drainage tunnels, galleries drainage by siphoning.

3. **Retaining structures method**

This method is quite expensive but flexible in nature. In this method retaining structures are used to withstand against the pushing forces of the soil masses. Retaining structures have different varieties such as gravity and cantilever retaining wall, contiguous bored piles and sometimes method of soil nailing is also used to stabilize slopes. Retaining structures include gravity types of retaining wall, cantilever retaining wall, contiguous bored piles, caisson, steel sheet piles, ground anchors, soil nails etc. This method is generally more expensive as compared with the other methods. However, it is always the most commonly adopted method in remedial works due to its flexibility in a constraint site. For this scenario, the remedial work can only be carried out within the boundary, a restrained structure is inevitable in order to stabilize and reinstate the failed slope (Kazmi, Qasim, Harahap, Baharom, et al., 2017).

The remedial works proposed by (Popescu & Sasahara, 2009) carry four groups namely slope geometry, drainage, retaining structures and internal slope reinforcement. The initiatives in the category of slope geometry involve fundamental changes that include removing material from the landslide driving area and reducing the slope angle. The remedial works in the class of drainage involve different methods which include providing boreholes, wells and water removal techniques. The category of retaining structures includes provision of different types of structure to give stability to the slope while the category of internal slope reinforcement includes providing anchors, micro piles and soil-nailing. There a lot of retaining structure such as; Gravity retaining and Gabion walls, Crib-block walls Passive piles, Piers, Cessions Cast in situ reinforced concrete walls, Reinforced earth retaining structures, Buttress counterforts of coarse-grained materials, Rock fall attenuation or stopping systems and Protective rocks or concrete blocks against erosion.

Retaining walls: Constructing retaining walls at the base of the slope can help to stabilize it by providing additional support and reducing the driving forces acting on the slope.

Rockfall protection: Installing rockfall protection measures such as rockfall barriers or catch fences can help to prevent rockfall from destabilizing the slope.

It's important to note that slope instability problems can be complex and require a thorough assessment by a qualified geotechnical engineer. The remedial measures listed above are just a few examples and may not be appropriate for all situations

2.10 Slope stability analysis software

Slope stability analysis software is a type of computer program that is used to analyze the stability of slopes or embankments. These software programs use mathematical models to simulate the behavior of soil and rock materials under different conditions, such as changes in water content, loading, and seismic activity. The analysis results can be used to determine the safety of a slope or embankment and to design appropriate stabilization measures.

There are several types of slope stability analysis software available, including limit equilibrium methods, finite element methods, and numerical modeling techniques. Limit equilibrium methods are based on the assumption that the slope will fail along a specific failure surface, and the software calculates the factor of safety against failure. Finite element methods use a mesh of elements to simulate the behavior of the slope, and the software calculates the displacement and stress distribution. Numerical modeling techniques use complex algorithms to simulate the behavior of the slope, and the software can provide detailed information on the deformation and failure mechanisms.

Overall, slope stability analysis software is an important tool for geotechnical engineers and geologists to assess the stability of slopes and embankments and to design appropriate stabilization measures to ensure public safety and prevent property damage.

2.10.1 Plaxis software

The PLAXIS software was first developed in 1987 at Delft University of Technology, with the support of the Dutch Ministry of Public Works and Water Management. The initial goal was to create a 2D finite element code that could easily analyze river embankments on the soft soils of the Netherlands. Over time, PLAXIS expanded to cover many other areas of geotechnical engineering. In 1993, the PLAXIS company was formed due to the growing demand for the software. The primary PLAXIS 2D deformation and stress analysis program for Windows was released in 1998. The finite element technique is used to solve differential equations problems in engineering and science. PLAXIS 2D is specifically designed to investigate stability in geotechnical design, and can analyze both natural and manmade slopes (Bayou, 2020). The software uses the Ø/c reduction approach to determine the factor of safety, where the strength parameters and cohesion of soil are gradually reduced until the structure fails. During a safety calculation, additional displacements are generated in PLAXIS 2D analysis. The total incremental displacements at the final step indicate the likely failure mechanism. PLAXIS uses finite element analysis techniques to model and solve complex geotechnical problems.

2.10.2 Phase software

As a tool for the design and study of tunnel surface excavation, Phase2 Software was created by Ro science Inc. in Toronto, Canada. It is a 2D finite element program that can be used to analyze the stability of slopes, excavations, and underground structures. The software is widely used in the geotechnical engineering industry for designing and analyzing slopes and excavations in rock and soil. It contains a computer software called Limit Equilibrium in Two Dimensions (LEM) that evaluates the stability of circular or noncircular failure surfaces (Ro science 2004, slide 6). modeling in the software Slide for many researches was possible for external loading, groundwater, and force like surcharge and pseudo-static earthquakes.

The examination of soil and rock slope stability is also based on the finite element approach. In addition to four primary sub-procedures, this software includes many FEM models. These steps include of calculations, outputs, curve charts, and inputs. The strength 30 parameters are gradually decreased until the final computation yields a fully established failure mechanism. For a variety of geotechnical applications, deformation and stability assessments are performed using this (Maula & Zhang, 2011).

The Phase2 software uses a finite element method to model the behavior of soil and rock materials under different loading conditions. The software can simulate the effects of changes in water content, seismic activity, and other factors on the stability of slopes and excavations. It can also be used to design and evaluate stabilization measures, such as retaining walls, anchors, and soil nails. One of the key features of Phase2 software is its ability to model complex geometries and material properties. The software can handle non-linear material behavior, such as strain-softening and strain-hardening, and can model the effects of anisotropy and heterogeneity in the soil and rock materials. It also includes a range of analysis options, such as stress analysis, deformation analysis, and safety factor analysis.

The Phase2 software includes a user-friendly interface that allows engineers and geologists to create and analyze models quickly and efficiently. It also includes a range of visualization tools, such as contour plots, cross-sections, and animations, to help users understand the behavior of the slope or excavation under different loading conditions.

Overall, Phase2 software is a powerful tool for slope stability analysis and design. It is widely used in the geotechnical engineering industry to ensure the safety and stability of slopes and excavations in rock and soil.

2.10.3 Slide software

Slide is a software program developed by Ro science Inc. in Toronto, Canada for slope stability analysis. It is widely used in the geotechnical engineering industry for analyzing the stability of slopes, embankments, earth dams, and other geotechnical structures.

Slide uses the limit equilibrium method to analyze the stability of slopes. This method involves dividing the slope into a number of slices and calculating the forces acting on each slice. The software then determines whether the slope is stable or not based on the factor of safety (FS) calculated for each slice (https://www.rocscience.com/software/slide).

Some of the key features of Slide include (Azarafza *et al.*, 2021):

1. User-friendly interface: Slide has a user-friendly interface that allows users to easily input data and analyze slope stability.
2. Advanced analysis capabilities: Slide can perform a range of advanced analyses, including probabilistic analysis, seismic analysis, and dynamic analysis.
3. Customizable output: Slide allows users to customize the output of their analysis, including generating graphs, tables, and reports.
4. Integration with other software: Slide can be integrated with other Rocscience software programs, such as RS2 and Dips, to provide a more comprehensive analysis of slope stability.

Overall, Slide is a powerful software program that can help geotechnical engineers and researchers analyze the stability of slopes and other geotechnical structures

2.10.4 Slope/w software

Slope/W is a software program developed by Rocscience for slope stability analysis. It is types of software developed based on the theories and principles of the limit equilibrium method. The software was developed by GEO-SLOPE International Canada for both rock and soil slope stability analysis in terms of safety factor. It can determine safety factor for all slip surface shape using different limit equilibrium techniques such as Fellenius, Janbu, Bishop, Morgenstern-Price and Spencer method and widely used in the geotechnical engineering industry for analyzing the stability of slopes, embankments, earth dams, and other geotechnical structures.

Slope/W uses the limit equilibrium method to analyze the stability of slopes. This method involves dividing the slope into a number of finite elements and calculating the forces acting on each element. The software then determines whether the slope is stable or not based on the factor of safety (FS) calculated for each element.

Some of the key features of Slope/W include (Satyanarayana *et al*., 2021):

1. User-friendly interface: Slope/W has a user-friendly interface that allows users to easily input data and analyze slope stability.
2. Advanced analysis capabilities: Slope/W can perform a range of advanced analyses, including probabilistic analysis, seismic analysis, and dynamic analysis.
3. Customizable output: Slope/W allows users to customize the output of their analysis, including generating graphs, tables, and reports.

CHAPTER THREE

3. METHODS AND MATERIALS

3.1 METHOD

To accomplish the overall and specific goals of this study effectively, various systematic approaches and materials were utilized through the following methodology. This chapter focuses on the overall process and methodology that were implemented for the detailed field survey, laboratory testing, data processing, and analysis. Secondary data was collected from various organizations after conducting a systematic literature review. In addition, representative and fresh rock samples were collected during a detailed field investigation for laboratory testing. These samples from critical surface are chosen based on several factors, including the presence of weak or loose materials and structures, the slope of the site, and the presence of water in the surrounding area. Soil samples were also collected from test pits. The rock and soil samples were then tested in the laboratory to determine the point load strength of rock, direct shear strength of soil, specify gravity of soils, hydrometer and sieve analysis, Atterberg limit, standard proctor and the unit weight of both soil and rock.

3.1.1 Desk study

The research involves conducting a literature review on the various types, causes, and impacts of slope stability issues that occur globally, as well as in Ethiopia and the specific study area. This includes analyzing published and unpublished geological maps, reviews, and theories used to assess slope stability in different fields such as highways, mines, and dams. Using the information gathered from the literature review, a conceptual framework and a general methodological flowchart are being developed.

3.1.2 Secondary data collection

Various data related to and essential for analyzing the stability of the slope were collected from different organizations such as the National Meteorological Service Agency and Geological Survey of Ethiopia. The data collected during this stage included meteorological data, geological and topographic maps, and reports on the regional geology of the area. Based on the knowledge obtained from the review, the methodology was designed, and detailed fieldwork for data acquisition was planned.

3.1.3 Detailed field survey and sampling

After conducting a reconnaissance survey and thorough literature review, a detailed field survey was carried out to investigate slope stability in the study area. Prior to the investigation, a sampling plan was developed and sampling locations were identified to minimize errors. The investigation included geological structure analysis, lithology identification, geological mapping, discontinuity surveying, in-situ strength testing, and soil and rock sampling to determine the strength, saturation, and groundwater conditions of the slopes. Eight critical slope sections were selected for slope stability analysis, including six rock slopes, two of which were structurally controlled and four were non-structurally controlled. Two of the rock slopes were heterogeneous with soil at the bottom, while the other two were either heterogeneous or homogeneous. The remaining critical surfaces were soil slopes, specifically residual soil. Various geological structures, such as minor faults, fractures, angular unconformity, and dikes, were observed during the investigation. Fresh rock samples were collected from the field to determine their geotechnical properties, including strength parameters and unit weight. Additionally, disturbed soil samples weighing 25kg were taken from four pits with depths ranging from 1-3.5m to determine their geotechnical properties. To preserve their natural moisture content, both rock and soil samples were placed in plastic containers immediately after sampling and transported to the laboratory. For structurally controlled slopes, the dip and strike of joints were measured, and the critical benching system was observed in the field, with measurements taken of the bench width and slope height. The benching system is crucial for stabilizing the road and preventing landslides. GPS coordinates were taken for each lithology, and the dip and strike of geological structures were measured and observed using a Bruno compass to prepare the geological map.

It is important to note that collecting data on geology, rock strength, and groundwater conditions is a general rule that applies to rock slope design and stability analyses (Hoek & Bray, 1981).

3.1.3.1 In situ strength test

he Uniaxial Compressive Strength (UCS) of intact rock near failure surfaces is crucial in determining shear strength parameters. This study used a Schmidt hammer to measure the UCS of intact rock near the failure surface in the field. The Schmidt hammer strength test is simple, suitable, and reliable, as it can handle practically unlimited sample sizes. Therefore, this study directly determined the UCS of intact rocks in the study area using the Schmidt hammer in the field Habtamu et al., (2022). The guideline for the Schmidt hammer strength test was given by

ISRM (1978) and ASTM (2018) in which the former recommended the use of L-Schmidt hammer type while the latter did not specify the hammer type. Aydin, (2014) suggested that N-type hammers are less sensitive to surface irregularities and are preferred for field surveys, while L-type hammers are more sensitive to lower ranges and give better results for weak, weathered, and porous rocks. Due to the geological complexity of the study area and the highly weathered rock material, the test was conducted using Schmidt hammers (L-type) in accordance with the standards suggested by Barton & Choubey (1977); Bieniawski & Hawkes (1978) and UCS calculated using equation 2.5.

Figure 3. 1: In-situ strength test using Schmidt hammer A) Smoothing the rock and make square B) Taking the rebound value (R)

3.1.4 Observed critical slope section

During field survey along the study area different slope section was identified within various formation. Due to the study area in the southeastern plateau most of the observed rock were tertiary volcanic with pyroclastic formation. And also, the aphanitic basalt was cover most of the area with different degree of weathering. The residual soil also identified which cover upper part of the study from Agarfa to before Oda Chefo area along the road to Wabe river bridge.

Figure 3. 2: Critical slope sections a) Heterogenous critical slope (welded scoria-colluvial material-aphanitic basalts) **R1SS** and b) Heterogenous critical slope two (aphanitic basalts-vascular basalts- scoria) **R2SS1** which are filled by soil due to erosion problems

Figure 3. 3: Critical soil slope section and its sample (black cotton soil, **SS1**)

Figure 3. 4: Residual soil affects by erosion with at top basaltic rock

Figure 3. 5: Non-homogenous critical slope section **R3SS1** a) soil sample (SS2) (silt clay soil from side slope section at top by aphanitic basalts)

Figure 3. 6: A) Slope section of soil sample (**SS3**) and B) Circular failure of highly weathered basalts from bench two

Figure 3. 7: Circular failure of welded scorious with at top moderately basalt

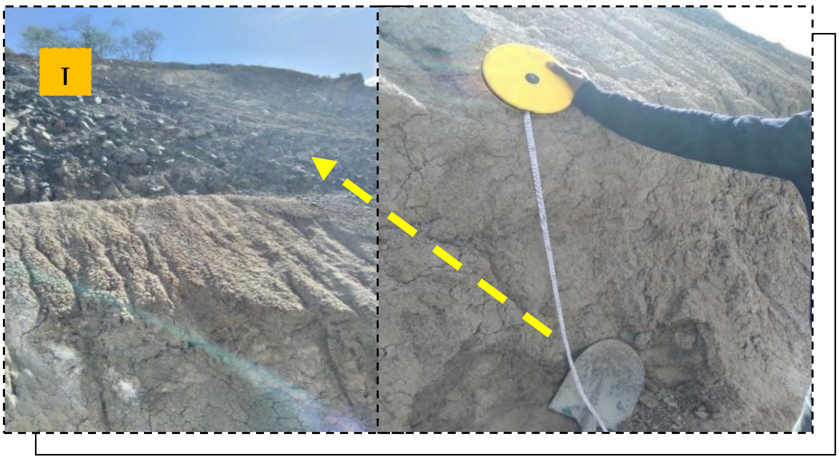

Figure 3. 8: Non-homogenous critical slope section R5SS2 a) soil sample (SS4), silt sand with highly disturbed alkali olivine basalts

3.4 Rock and soil laboratory tests

In slope stability analysis, the determination of strength parameters of materials is typically carried out in a laboratory. The purpose of this test was to determine the index and engineering properties of soil and rocks. Various laboratory tests are conducted for soils and rocks to determine their strength parameters. In the case of soils, these tests include particle size distribution, hydrometer analysis, water content determination, compaction, direct shear test, natural moisture content and specific gravity. Unit weight and direct shear test was conducted on remolded soil sample according to ASTM 3080 standard. Furthermore, the soil was subjected to sieve and hydrometric analyses to obtain a broad classification of the soil based on ASTM D 422 standards. These all tests conducted for test pits. For rock point load, dry and saturated density and intact Schmidt hammer was tested.

3.4.1 Laboratory testing on rock sample

This laboratory test was conducted on rock sample including point load and unit weight test. Each of these is discussed as follows.

3.4.1.2 Compressive strength test

The compressive strength test is a commonly used laboratory test to determine the strength of a material when subjected to compressive forces. It is widely used in the construction and engineering industries to assess the quality and suitability of materials for various applications. The strength of rock materials is a crucial factor in the design of civil and mining engineering projects, but obtaining this information is challenging and requires laboratory tests and specialized equipment such as loading machines, core drilling, and sampling techniques. However, the Point Load test is an alternative method that can be used to predict the uniaxial compressive strength of rock materials using portable and simpler equipment. Although the Schmidt Hammer Rebound test is also used for this purpose, its results are more variable and can be affected by testing methods. During the compressive strength test, a steady load is applied until failure occurs, and the crushed load pressure is recorded. The standard reference used for this test was BS 1881: PART 116. This method requires the rock to be in a near-concrete shape. Therefore, before crushing the rock, it should be made into a concrete form, and the average width and length of the rock must be measured.

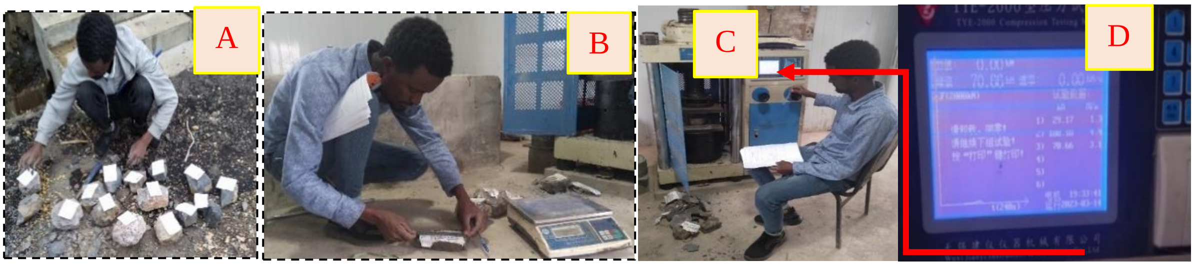

Figure 3. 9: Compressive strength test for soils A) Sample preparation for compressive strength test B) weighing the prepared sample and measuring the width and length of the prepared sample C) Operating the machine by pressing on /off D) The machine part which can show crushing load

Table 3. 1. summary of laboratory tests for rocks

Types of tests	Numbers of test	Standards of tests
Compressive strength	16	BS 1818 part 116
Unit weight	10	ISRM (1978)

3.4.1.2 Determination of dry density of rock sample

This test is used to calculate the dry density of rock. The procedure for this test is as follows: first, weigh the rock collected from the critical slope section (M1) and oven-dry it for 18 to 24 hours. Then, weigh the oven-dried rock sample (M2). Take a cylindrical material with a visible measuring (ml) value and read the initial volume (V1). Put the oven-dried sample into the known volume cylinder and take the volume (V2). The ratio between the mass of the dried rock sample and the volume change gives the density of the rock.

$\Delta V = V2 - V1$……………………………………………………………………eq.3.1

$\rho d = \frac{M2}{\Delta V}$ ……………………...……………………………………………….... eq. 3.2

$\gamma d = \rho d * g$ ………………………………………………………………………. eq. 3.3

Where, ρd- dry density of rock in g/cm^3, M2- mass of oven-dried rock sample in (g), ΔV-the difference between volume before oven-dried sample placed into cylinder and the volume after rock sample placed in cylinder, γd - dry unit weight of rock sample in KN/m^3, g- gravitational acceleration).

3.4.2 Soil laboratory tests

Soil samples were analysed in the laboratory to assess the strength and index properties of the soil in the study area. The laboratory tests conducted on the soil samples comprised of grain size analyses (sieve and hydrometer analyses), specific gravity tests, natural moisture contents, Atterberg limit tests (liquid and plastic limit), as well as compaction and shear strength tests (cohesion and angle of internal friction).

3.4.2.1 Grain Size Analysis (Sieve and Hydrometer Analysis)

Mechanical analysis is the determination of the size range of particles present in a soil, expressed as a percentage of the total dry weight. Two methods generally are used to find the particle-size distribution of soil: (1) sieve analysis for particle sizes larger than 0.075 mm in diameter, and (2) hydrometer analysis or particle sizes smaller than 0.075 mm in diameter.

A) Sieve analysis

To analyze the particle-size distribution, the ASTM D 422 procedures were employed. The slope and road sections were composed of soil, and grain size analyses were conducted to identify the type of soil present. Seven soil samples were collected from the field by digging test pits, and mechanical analyses were performed on particles larger than 0.075mm diameter (No. 200 Sieve). For particles smaller than 0.075mm diameter (No. 200 Sieve), hydrometer analyses were conducted on all soil samples taken from the seven test pits at the slope section to determine the soil with a particle diameter less than 0.075mm. The procedure involved performing wet sieve, and hydrometer analyses on disturbed samples, and plotting the graph using soil particle size in millimeters on a semi-log scale against the percentage finer. This curve was used to determine the proportion and type of soil particles.

B) Hydrometer

The hydrometer analysis is utilized to determine the distribution of fine particles with a diameter smaller than 75µm. The test was conducted in accordance with the ASTM D422 (1998) standard test. The laboratory test was performed as follows: first, 50g of fine-grain soil retained on the pan was weighed and placed in a beaker with water. Then, a mixture of 125ml of dispersing agent (sodium hexametaphosphate) was added to the soil. The soil slurry was then transferred to an empty sedimentation cylinder and distilled water was added up to the mark. The soaking soil added 125ml of the dispersing agent to the control cylinder and filled it with distilled water.

Figure 3. 10: Hydrometer

3.4.2.2 Atterberg limits

The moisture content, in percent, at which the transition from solid to semisolid state takes place is defined as the shrinkage limit. The moisture content at the point of transition from semisolid to plastic state is the plastic limit, and from plastic to liquid state is the liquid limit. These parameters are also known as Atterberg limits.

A) Liquid limit (LL)

Under this research work, the Casagrande method was used to determine the Atterberg limit values of air-dried and oven-dried soil samples, following the procedures given in AASHTO T 89 and T 90 standards, by passing a 0.425mm sieve sample. The liquid limit is the moisture content at which the groove, formed by a standard tool into the sample of soil taken in the standard cup, closes for 13 mm after being given 25 blows in a standard manner. This method was performed for three numbers of blows: the first number of blows was greater than 25 but less than 32 blows, the second was much closer to 25 blows, and the third was less than 25 blows. After collecting the sample that closed to the groove, the sample was placed into a can and inserted into an oven dry machine for the determination of moisture content. The moisture content is the average of the three samples.

B) **Plastic limit (PL)**

This test was conducted on a sample taken from the first blows of the liquid limit test, which was performed according to the standard AASHTO T89 and T90. The plastic limit of soil is the moisture content at which the soil begins to behave as a plastic material. At this water content (plastic limit), the soil will crumble when rolled into threads of 3.2mm (1/8in) in diameter. The plastic limit is the lower limit of the plastic stage of soil. The plastic limit test is simple and is performed by repeatedly rolling an ellipsoidal-sized soil mass by hand on a ground glass plate. The crumbled sample is collected in a can and entered into an oven for 24 hours for the determination of water content."

A) Plasticity index

The plasticity index (PI) is a measure of the plasticity of a soil. The plasticity index is the size of the range of water contents where the soil exhibits plastic properties. The PI is the difference between the liquid limit and the plastic limit (PI = LL-PL). Soils with a high PI tend to be clay, those with a lower PI tend to be silt, and those with a PI of 0 (non-plastic) tend to have little or no silt or clay.

Figure 3. 11: Atterberg limit test for soils A) Liquid limit (LL) B) Plastic limit (PL) C) Moisture cans for both LL and PL

3.4.2.3 Natural moisture contents tests

The in-situ natural moisture content of soil is indicative of its field condition and provides valuable information. Moisture content is a critical factor that affects the engineering behaviour of soil, especially cohesive soils (Rasti et al., 2020). The test was performed on fresh soil samples according to ASTM D 2216 (1998) standard using the oven drying technique. Additionally, another test was conducted on representative soil samples collected from four critical slope sections. These samples were put in plastic bags to preserve their natural moisture content. The wet mass (Mw) of the soil samples was determined by weighing them using a digital balance. To obtain their dry mass, the samples were oven-dried for 24 hours at 105°C (Md). Finally, the natural moisture content was calculated using equation (3.1)

$$W = \frac{(Mw - Md)}{Md} * 100\% \qquad \text{eq. 3.4}$$

Where w is natural moisture content in (%), Mw is the mass of wet soil sample in (g) and Md is the mass of oven-dried soil sample in (g).

3.1.4.3 Specific Gravity of soil

The specific gravity of the soil was determined using oven-dry techniques in accordance with the ASTM D854 (1998) standard procedures. Before beginning the test, the empty, clean, and dry pycnometer (W1) was weighed using a digital balance. Then, 10g of an oven-dried soil sample that had passed through sieve #10 was added to the pycnometer, and its weight was recorded as (M2). The pycnometer was filled with distilled water to a level slightly above the soil sample, and the sample was immersed for 10 minutes to release any entrapped air using the boiling method. After that, the pycnometer was filled to the mark with distilled water, and the weight of the pycnometer containing soil and water (W3) was recorded. The pycnometer was then drained, cleaned, and refilled with distilled water to the mark, and the weight of the pycnometer and distilled water was recorded (W4). Finally, the specific gravity was calculated using an equation 3.2.

$$Gs = \frac{W2-W1}{(W4-W1-(W3-W2))} \text{...} \text{ eq. 3.5}$$

Where, W1 is the weight of clean and dry pycnometer, W2 is the weight of oven-dried soil and pycnometer, W3 is the weight of the pycnometer filled with water and W4 is the weight of a pycnometer filled with water and soil.

Figure 3. 12: specific gravity for soils A) Soil sample with digital balance B) Pycnometer filled with water and soil

3.4.2.4 Compaction tests

Compaction is a process that determines the maximum density and optimal moisture content of soil used in shear strength tests. Proctor tests are utilized to determine how soil compaction changes with moisture content. In accordance with ASTM D698 (1998), tests were conducted on four soil samples taken from the critical slope section of the study area. The laboratory test was conducted as follows: 5kg of soil sample passing through the No.# 4 sieve (4.75mm) was taken, and a measured amount of water was added to the soil and mixed thoroughly. The weight of the compaction molds within the base (M1) was determined. The soil sample was then filled into the cylinder mold in three layers, with 25 blows for each layer (Fig.3.4c). The collar was removed, and excess compacted soil beyond the rim of the mold was trimmed and the weight of the compacted soil within its molds and base was recorded (M2). The soil compacted from the molds was removed using a mechanical extruder. The soil sample was then split using a knife, and a sample from the bottom and top of the moisture cans was taken and placed in an oven at 105 ° C for 24 hours. The bulk density and dry density of the soil were determined using equations 3.4 and 3.5, respectively.

$$\Upsilon b = \frac{M2-M1}{V} \text{ ....} \text{eq. 3.6}$$

Where, Ɣb- the bulk density of the soil, M2- the mass soil after being compacted with mold, M1- the mass of the mold and V- is the volume of the mold.

The equation of dry density of soil

$$\Upsilon\text{d} = \frac{\Upsilon b}{(1+\frac{w}{100})} \text{...} \text{eq. 3.7}$$

Where, Υd is dry unit weight, Υb is the bulk unit weight, W is the moisture contents of soils

Figure 3. 13 : Compacted test of soil from critical slope section of my study area, A) Soil sample preparation for compaction B) Fixing the molds.

3.4.2.5 Direct shear tests

Is the maximum resistance to shearing stresses which a specimen or element of soil can withstand before failure occurs. It is considered one of the most crucial engineering properties of soil. In this study, the direct shear strength test was used to determine the shear strength parameters, including cohesion and angle of internal friction, in the failed slope sections that were selected. There are a few grammatical errors in your sentence. The test was performed on four soil samples, each measuring 60 x 60 x 25 mm, that were remolded at their natural moisture contents compacted and compacted using ASTM D 698 standards at the Geotechnical Laboratory of Addis Ababa Science and Technology University. The samples were subjected to three different shear loads: 100 kPa, 200 kPa, and 300 kPa.

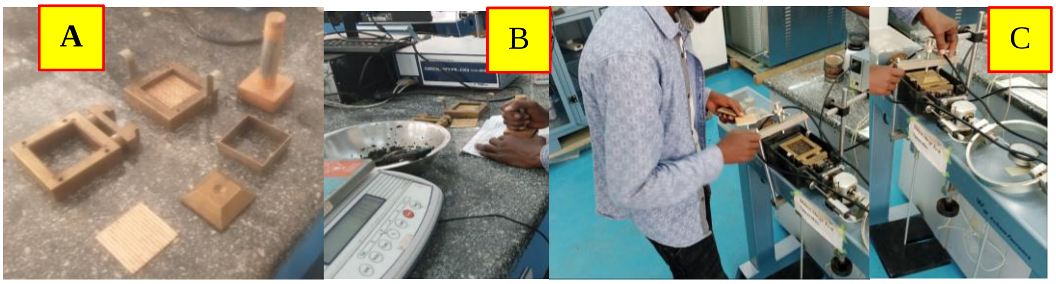

Figure 3. 14: Direct shear test

3.4.2.6 Unit weight of soil

The stability of soil slopes is evaluated using various input parameters, including the unit weight of the soil. In this study, both the saturated and dry unit weights of soil were determined from laboratory test results of soil samples collected from critical slope sections. The in-situ unit weights of soil were calculated by multiplying the corresponding density with the acceleration of gravity. Four soil samples were collected for this study, and their unit weights were determined using the bulk and dry density results. The unit weight of the soil samples was calculated by multiplying the bulk density and dry density with the acceleration of gravity. The test was conducted by the ASTM D 2937-00 standards.

Table 3. 2. A summary of soil laboratory tests

Tests types	Numbers of tests	Standard
Atterberg limit	4	AASHTO T89, T90
Wet sieve analysis	4	ASTM D 422
Hydrometer	4	ASTM D 422
Unit weight	4	ASTM D 2937- 00
Direct shear	4	ASTM D 854
Specific gravity	4	ASTM D 854
Natural moisture content	4	ASTM D 42216
Compaction	4	ASTM D 698

3.5 Data processing and analysis

The information gathered from various sources, including desk study reconnaissance, field surveys, laboratory tests, and literature reviews, was organized and analyzed in a manner that allowed for easy access during future slope stability evaluations. Once all the necessary data was collected and processed, the slope stability assessment was conducted using Rocsciences software such as rocdata, Slide6.00, Rockplane 6.00, Geos studio 2012 (SLOPE / W), phase 2 and Plaxis 2D.

3.5.1 Rock mass classification

Rock mass classification systems are commonly used in the design and construction of rock engineering (Salmanfarsi et al., 2020). This method is an important tool for engineers and geologists to evaluate the engineering properties of rock masses and to design safe and efficient structures in rock. The rock mass rating (RMR) is undoubtedly a helpful tool for rock mass characterization commonly used for planning and design in engineering applications introduced by (Bieniawski, 1974) later modified many times over the years. The applicability of RMRb has certain limitation address the engineering geology problems. Therefore, the combination of geological strength index (GSI) and RMRb is necessary to understand the behaviour of fracture/ jointed rock mass. The rock quality des is one of the most important parameter to assess the RMRb as well as (Zhang, 2016). In the study area, the Rock Quality Designation (RQD) was determined by evaluating the volumetric jointing of the rock mass, as described by Palmstrom in 1974. To estimate the strength of the rock mass, the method primarily relied on assessing the interlocking of rock blocks and their surfaces, which is based on the approach developed by Kumar et al. (2022). This method is commonly used to evaluate the strength and stability of rock masses in geotechnical engineering. The quality of the rock mass was evaluated using five fundamental parameters for rock mass rating. These parameters include the uniaxial compressive strength of the intact rock, the Rock Quality Designation (RQD), the spacing of discontinuities, the condition of the discontinuities (infilling material, aperture, roughness, persistence and the groundwater conditions (saturation condition) was identified in field. Based on these parameters, the quality of the rock mass was classified. To determines the spacing of the discontinuities, the distance between consecutive discontinuities was measured and the average value was calculated. Similarly, the aperture and persistence of the discontinuities were estimated by measuring these parameters for some discontinuities and then taking the average value. The condition of the discontinuities and water saturation were visually assessed in the field. The strength of the intact rock can be determined using various methods such as point load strength, uniaxial compressive strength, and Schmidt hammer rebound value. In this study, the strength of the intact rock was determined using these two methods on an irregular rock sample and rock mass in the field. These two methods have almost the same value but for analysis the Schmidt hammer rebound value was preferable since the reading of rebound value taken within the discontinuities of rock (rock mass). Due to the rock fail with discontinuities.

The rock mass quality was evaluated using five fundamental parameters of rock mass rating. These parameters include the uniaxial compressive strength of the intact rock, rock quality designation (RQD), spacing of discontinuities, condition of the discontinuities, and groundwater conditions. To measure the uniaxial compressive strength of the intact rock, an irregular rock sample was subjected to a point load strength test during the study. Measuring the distance between adjacent spacing and calculating the average value is a crucial factor in determining the classification of rock mass based on discontinuity spacing. This parameter was measured in the field. Additionally, the conditions of discontinuities, including persistence, aperture, roughness, infilling, and weathering condition of the wall rock, were also estimated in the field. According to (Pantelidis, 2009) the condition of groundwater was visually assessed in the field by observing the flow of water from a slope or the presence of water stains on the slope face.

The RQD and Jv are calculated by the equation (2.2) and (2.3) respectively. The basic rock mass (RMR_b) was to classify the rocks mass of the study area according to (Bieniawski,1989) as cited in Bekele (2022) as shown in eq. 3.9 below.

$$\mathrm{RMR}_b = R_1 + R_2 + R_3 + R_4 + R_5 \qquad \text{eq. 3.8}$$

Where, (R_1, R_2, R_3, R_4, R_5) are represents Uniaxial compressive strength of intact rocks, rock quality designation, discontinuity spacing, condition of discontinuity, and the condition of groundwater respectively.

3.5.2 Shear strength parameter

The shear parameter of the rock was calculated using Rocdata software, while the shear strength of the soil was determined in the laboratory through a direct shear test. The input parameters used to calculate the cohesion and friction angle of the soil in Excel included the recorded horizontal displacement, the area of the shear box, the shear load, and the shear stress.

3.6 Methods of slope stability analysis

3.6.1 Limit equilibrium methods

The safety factor is determined by comparing the shear strength adjacent to the sliding surface with the force required to maintain the slope's equilibrium, using the limiting equilibrium approach Ullah et al. (2020). To analyze the stability of rock and soil slope failures, a limiting equilibrium method was employed with the Ro science slide software (Raji Pant, 2021). The deterministic method was used to calculate the safety factor and evaluate the stability analysis for the mode of rock and soil slope failures Park et al. (2005). In this study, the most vigorous LE methods, for example Janbu generalized (JG), Morgenstern-Price (M-P), Spencer's, general limit equilibrium (GLE) and slide software procedure were selected for analyses of both soil and rock slope section. The Morgenstern-Price method, which considers force and moment equilibrium, is suitable for analyzing potential failure surfaces on both circular and noncircular surfaces Kadakci Koca & Koca (2020). To calculate the safety factor, the method requires input parameters such as cohesion, friction angle, unit weight of the rock or soil, and slope geometry. The safety factor is computed for each dry and wet condition, as well as static and dynamic conditions, to determine the impact of these parameters on the slope section. The analysis included both homogenous and heterogenous slopes.

3.6.2 Finite element methods

In finite element (FE) slope stability analysis, the use of the strength reduction method with advanced soil models leads to a behavior similar to the Mohr–Coulomb model since stress-dependent stiffness behavior and hardening effects are excluded from the analysis. As cited in Bushira et al. (2018) there are many FE methods, among those methods, gravity increase method (Swan and Seo 1999) and strength reduction method (Matsui and San 1992) is considered the most widely used methods. The safety factor of a slope was calculated using the Phase 2D software. This software uses the finite element method to determine the factor of safety. The analyses were conducted under various anticipated conditions, including static saturated and static dry conditions, as well as varying slope height. The method utilized input data such as cohesion, friction angle, unit weight, Young's modulus, Poisson's ratio and slope geometry to determine the safety factor. These input parameters determine in laboratory test and by empirical formula. The poison's ratio of rock was determine by empirical formula suggested by proposed by (Lógó & Vásárhelyi, 2019) as show in equation 3.10. And also, the young's modulus of rocks mass determined using Hoek -Brow criteria and Rocdata software. and soils were obtained from Prior to inputting data into the strength reduction method, designing the slope geometry was a crucial step.

$V = -0.002GSI + 0.003mi + 0.457$ ……………………………………………………3.9

where: - ν is the Poisson's ratio of the rock mass, mi is the material constant, which is a parameter that reflects the degree of rock mass fracturing and ranges from 0.5 to 1.0, GSI is the geological strength index, which is a measure of the overall strength and deformation characteristics of the rock mass and ranges from 0 to 100.

The soil's elasticity modulus (E) and Poisson's ratio (v) are important parameters used in numerical modelling to analysed soil deformation. Suitable values for these parameters were determined based on a combination of numerical correlations and a review of literature. The standard penetration test (SPT) has been widely used to correlate various soil parameters, such as unit weight (γ), angle of internal friction (φ), and undrained compressive strength (qu), for estimating the stress-strain modulus of elasticity and Poisson's ratio of soil. This study calculated the corrected standard penetration test N value to an average energy ratio of N60 using equation (3.11) proposed by (Shahien, 1998). The Poisson's ratio of soil calculated by equation (3.10) as suggested by (Dhar, 1996)

The soil's modulus of elasticity was determined by utilizing the SPT N60 value, as suggested (Chopra & Arboleda-Monsalve, 2020) . This calculation was performed using equation 3.12 in the following manner:

$V = 0.1 + 0.3\frac{(\phi-25)}{20}$ for $\phi < 45°$ …………………………………………...3.10

$\gamma sat = 16.8 + 0.15N60$ (KN/m3) ……………………………………………… 3.11

$Es = 1200\,(N+6)$ KN/m2 for $N < 15$

$Es = 4000 + 1200(N-6)$ KN/m2 for $N > 15$ ………………………………………3.12

3.6.3 Kinematics analysis

Kinematic analysis is a technique used to identify potential failure modes and failure zones in jointed rock slopes. The orientation of rock discontinuities was measured using the Burno compass. Based on visual observations in the field, two slope sections were found to exhibit a structurally controlled failure mode. These slopes were located in the western and northeast part of the study area and were composed of aphanitic and alkali olivine basaltic rock. The analysis was used by the dip 6.008 software. The failure type observed in these slopes was toppling and wedge.

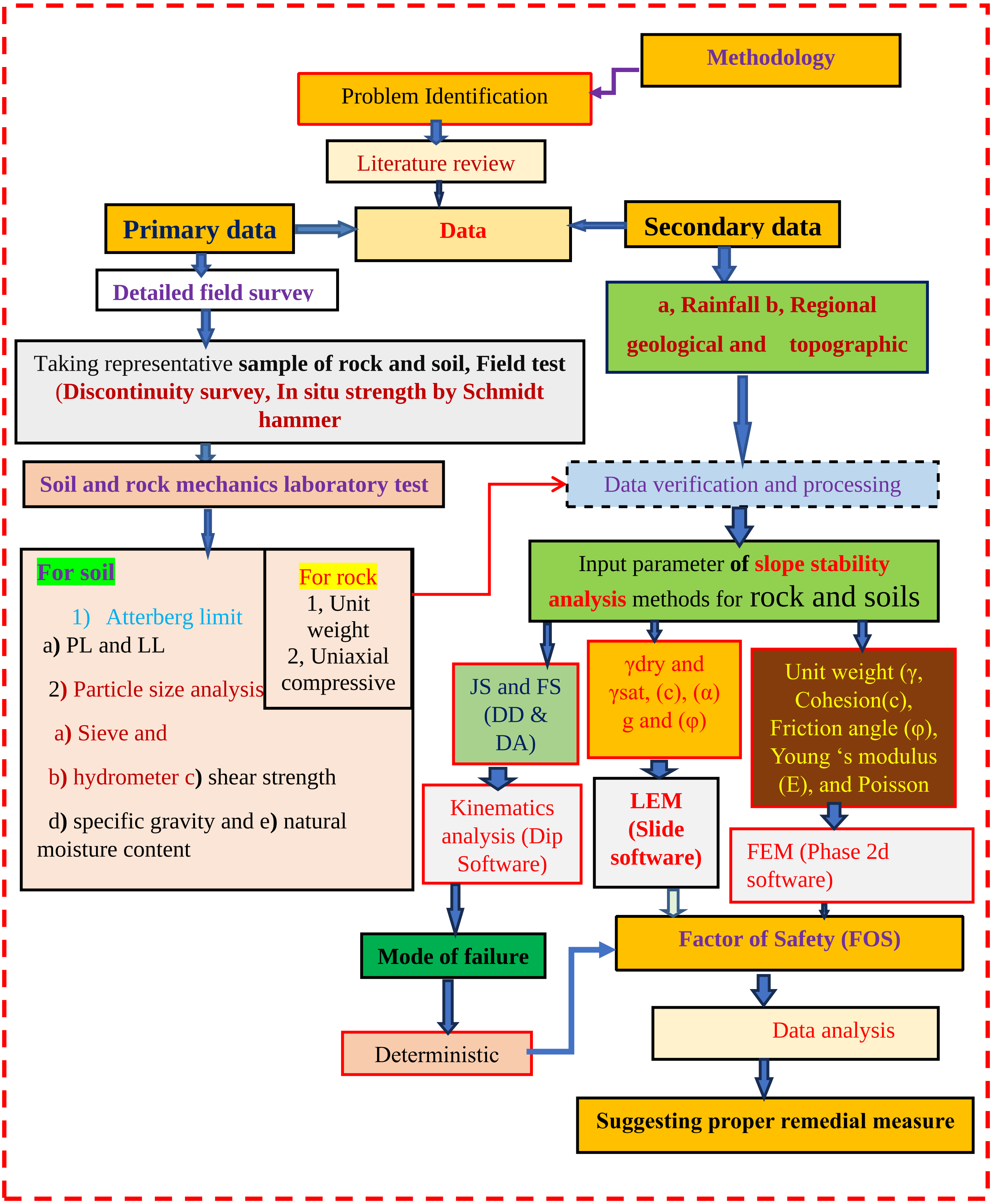

Figure 3. 15. Methodology flow chart

CHAPTER FOUR

4. GEOLOGY OF THE STUDY AREA

4.1 INTRODUCTION

Ethiopia is characterized by a wide variety of landscapes and landforms. They were generated by a complex of tectonic, erosive, and depositional processes acting on rocks with different characteristics. The geological evolution of Ethiopia, with alternating phases of orogenesis, peneplanation, crustal up doming, faulting, emplacement of huge amounts of lava, and deep fluvial dissection has imprinted the geomorphological landscapes of the country with specific characteristics, in places unique on Earth.

The Ethiopian landmass consists of a large, high elevated plateau bisected by the Rift Valley into the northwestern and the southeastern highlands, each with associated lowlands. The contrast in relief is remarkable as land elevation ranges between −155 m of Asal Lake in the Afar depression (the lowest point in Africa) to the peak of Mt. Ras Dejen at 4,620 m a.s.l. in the Simen Mountains. The plateau stands between 1,500 and 3,000 m a.s.l. and it is strewn with a number of volcanoes making up high mountain ranges, the highest of which are the Simen in the north and the Bale mountains in the south (Billi, 2015).

Ethiopia can be divided into four major physiographic regions these are:

1. Western Plateau: This region is located in the western part of Ethiopia and is characterized by highlands and plateaus with elevations ranging from 1,500 to 4,620 meters above sea level. It is the source of many of Ethiopia's major rivers.
2. Southeastern Plateau: This region is located in the southeastern part of Ethiopia and is characterized by rugged terrain and high plateaus with elevations ranging from 1,500 to 3,000 meters above sea level. It is home to many of Ethiopia's national parks and wildlife reserves.
3. Main Ethiopian Rift: This region is located in the central part of Ethiopia and is characterized by a series of interconnected valleys and lakes that run from the Red Sea to Lake Turkana in Kenya. It is a major geological feature of East Africa and is home to many unique plant and animal species.
4. Afar Depression: This region is located in the northeastern part of Ethiopia and is characterized by a low-lying desert basin that lies below sea level. It is one of the hottest and driest places on earth and is home to many unique geological features, including active volcanoes and hot springs.

According Haro *et al.* (2020) the Ethiopian plateau is a highland region that covers much of Ethiopia and is believed to have formed as a result of tectonic activity associated with the Afro-Arabian Shield. The Precambrian rocks of the Afro-Arabian Shield are important because they provide clues about the geological history of the region and the processes that have shaped it over millions of years.

After the formation of the Main Ethiopian Rift, which down-faulted the upper pyroclasts and early formed lava flows, localized younger central type eruption formed the highlands of Arsi and Bale areas. These first erupted basalt lava, followed by trachytes. These are previously mapped as Chilalo formation (Mengesha Tefera & Haro, 1996). Mountain peaks such as Chilalo, Galema, Kaka, Berole, and the top part of Bale mountains were mapped as Chilalo Formation. The Chilalo Formation is Pliocene in age. The Bale mountains within the map area covered by highland basalt, is pierced with multiple trachytic dike swarms. These dike swarms seem to be the root source of the trachyte there. On the plateau of Bale, Quaternary basaltic fissure eruptions occur. These are previously known as Ginir Formation. Locally both the plateau of Arsi and Bale, are pierced with scoria fall Haro *et al*. (2020).

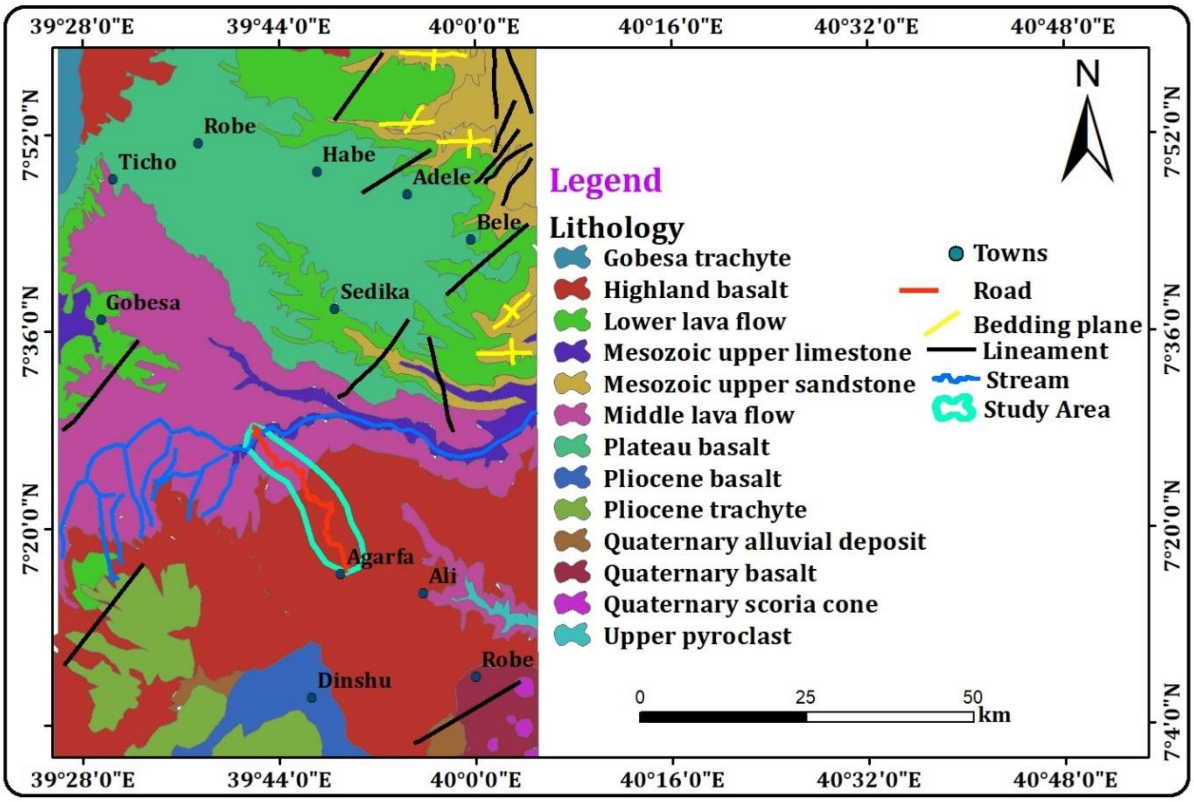

Figure 4. 1 Regional geology of study area along road, (Haro et al., 2010)

4.2 Description of the study area

4.2.1 Location and Accessibility

The present study area is in Agarfa woreda, Bale zone in Oromia Regional State in southeastern Ethiopia. It's part of southeastern Ethiopian plateau between Agarfa town and Wabe River Bridge, in the northwest corner of the Bale Zone of the Oromia Region. It is bordered on the south by Sinanana, Dinsho on the west by west Arsi, on the north by the Wabe River which separates it from the Arsi Zone, and on the east by Gaserana Gololcha. The area can be can be accessed by travelling 440km from Addis Ababa on the Addis Ababa - Asella - Bekoji - Dodola – Robe – Ali - Agarfa town – Wabe River bridge Asphalt Road. Its boundaries are 39° 49' 21" to 39° 41' 40" E longitude and 07° 17' 03" to 07° 28' 26"N latitude.

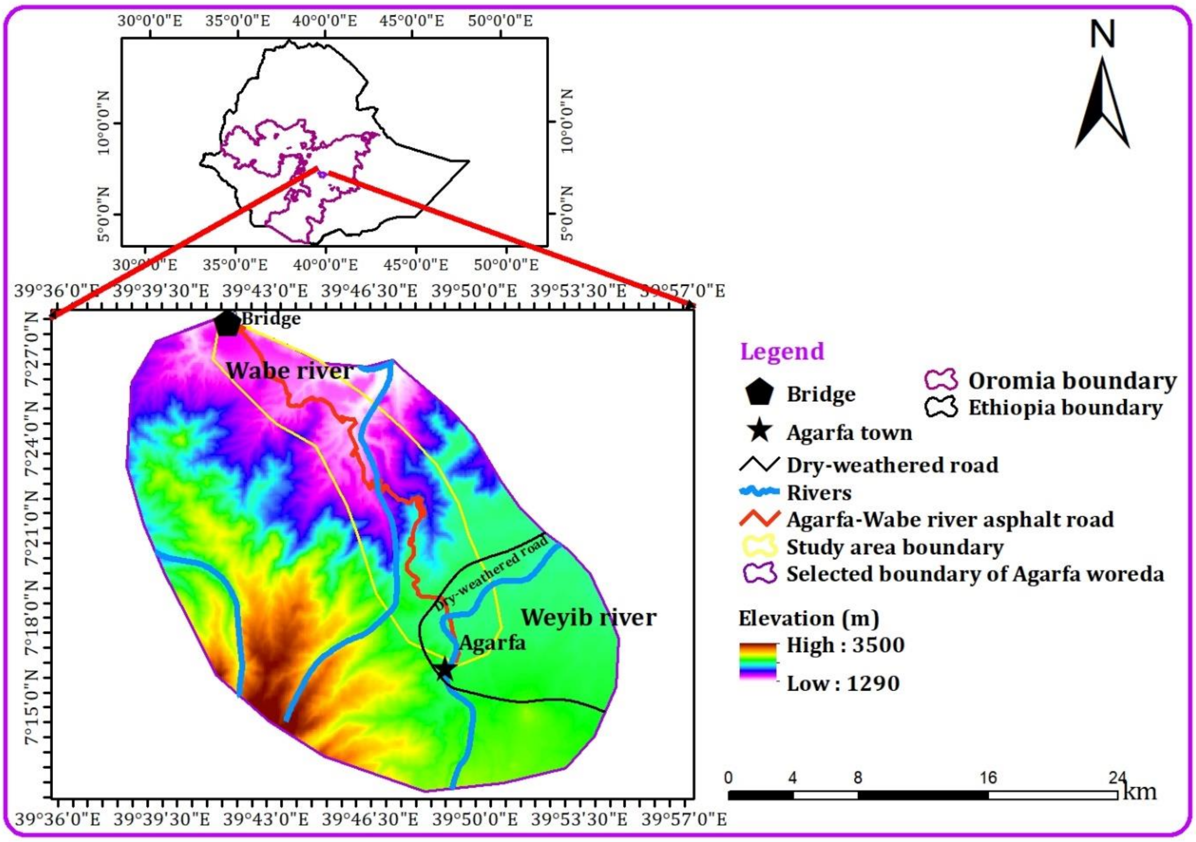

Figure 4. 2. Location and accessibility map of the study area

4.2.2 Physiography

According to (Zewdie & Asmare, 2023) physiography is strongly related to the geological setting and geomorphological history of rock. The study area is part of southeastern highland plateau of Ethiopia. The study area is undulated landform with elevation ranging from 1350 to 2450m above sea level. The topographical features are represented by plateau, valleys, cliff, hill and flat area with slope gradient varying from steep to gentle slope. The flat land from Agarfa town to Sire village densely populated and cultivated mainly by white. The hill plateau to gentle along the road to Wabe bridge cultivated by sugarcane and sorghum at the side of river exposure and some of flat area on the plateau.

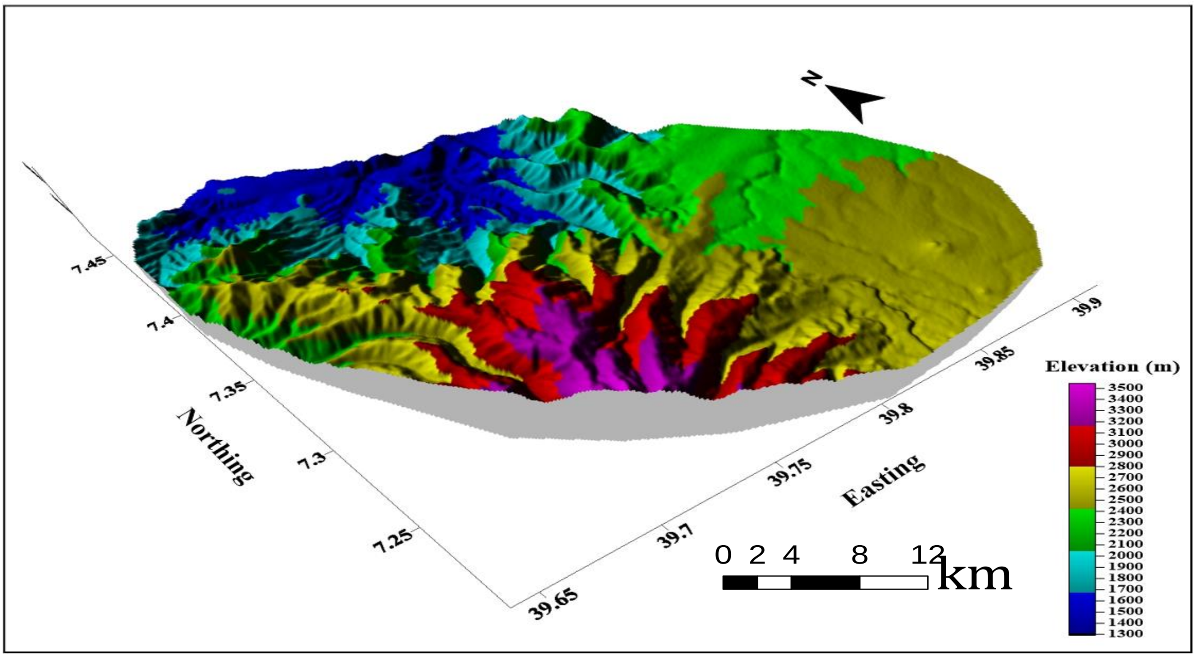

Figure 4. 3 Physiographic maps of the study area

4.2.3 Drainage pattern

The study area is located on the Southeastern Ethiopian plateau which contains the major rivers such as; Wabe and Weyib and their tributaries. Several small tributary streams run through the study area and intersect at various points and drain to Wabe and Weyib River. The road pass through the steep to gentle slope and the drainages are flow easily from the escarpment to the rivers in the lowland area. The area has a combination of basaltic rock and steep slopes, it can further influence by the drainage.

Steep slopes can enhance the erosive power of water, leading to the formation of deep valleys and narrow channels. In such areas, the drainage pattern may exhibit a more dendritic or radial pattern, where streams flow in a branching or radial manner from a central high point or ridge.

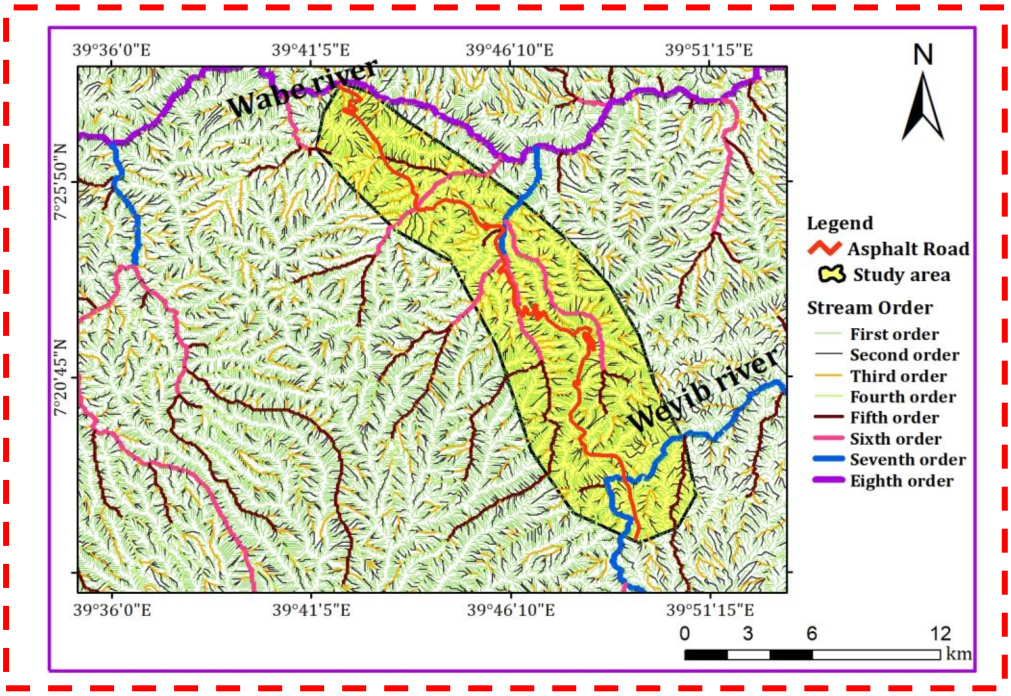

Figure 4. 4 Drainage pattern and stream order of the study area

4.2.4. Seismicity of the study area

Seismic activity is one of the factors that contribute to slope instability, particularly in active seismic zones (Hoek & Bray, 1981). The seismic risk map of Ethiopia for a hundred-year return period and 0.99 probability according to the report Asfaw (1986) showed that the present study falls in the area of low seismic intensity which show no damage occur as shown in fig. 1.3. Thus, there is a low probability of slope instability issues occurring in the study area, which could potentially be caused by seismic activity. The study area shown in the Ethiopia seismic map (Figure 4.5) below.

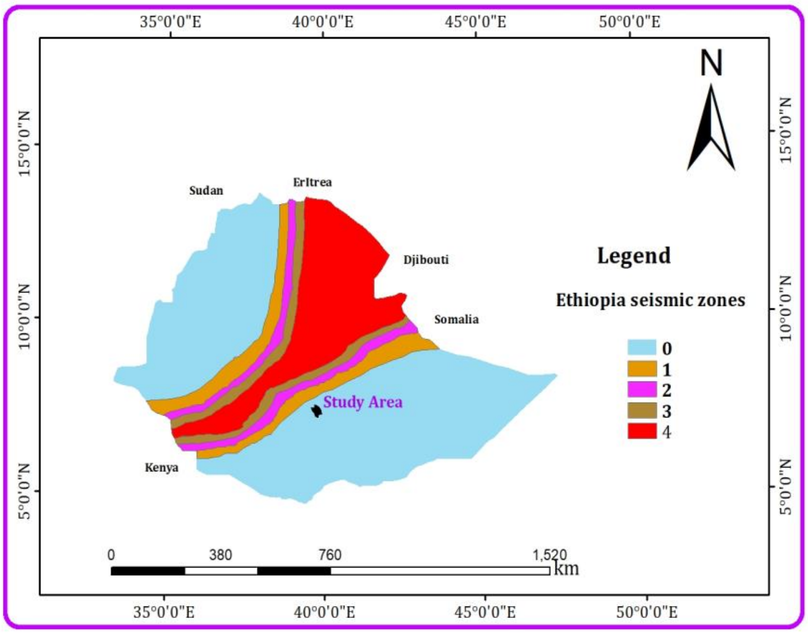

Figure 4. 5. Seismic risk map of Ethiopia 100-year return period 0.99 probability (Modified after Asfaw & Woldeyes (1986).

4.2.5. Rainfall data of the study area

According to Yokota & Iwamatsu, (2000) the primary cause of slope instability is the presence of an adequate amount of water during precipitation events. Erener & Düzgün (2010), also state that rainfall is the most common factor that triggers landslides in many parts of the world. The distribution of pore water pressures within the soil during heavy rainfall can vary greatly depending on factors such as hydraulic conductivity, topography, degree of weathering, and soil fracturing. According to Liang (2020), an increase in pore-water pressure can be caused by either the infiltration and percolation of rainfall or the accumulation of a perched or groundwater table. The permeability of the material plays a significant role in determining its response. According to Giannecchini et al., (2007) suggest that in soils with high permeability, the accumulation and release of positive pore pressures during heavy rainfall can occur quickly. In such cases, slope instabilities are triggered by intense rainfall, and previous rainfall has little impact on the occurrence of instability of slope (Bogaard & Greco, 2016). The present study was conducted in a tropical and subtropical region along the road from Agarfa town to Wabe river bridge. Rainfall data was collected from two stations, namely the station in Agarfa woreda and the station in Sirka woreda (Gobesa), which are located at a reasonable distance from each other and connected by the road.

Based on field observations, it has been noted that slope instability in the area being studied is more common during the summer months of June, July, and August, as well as in May.

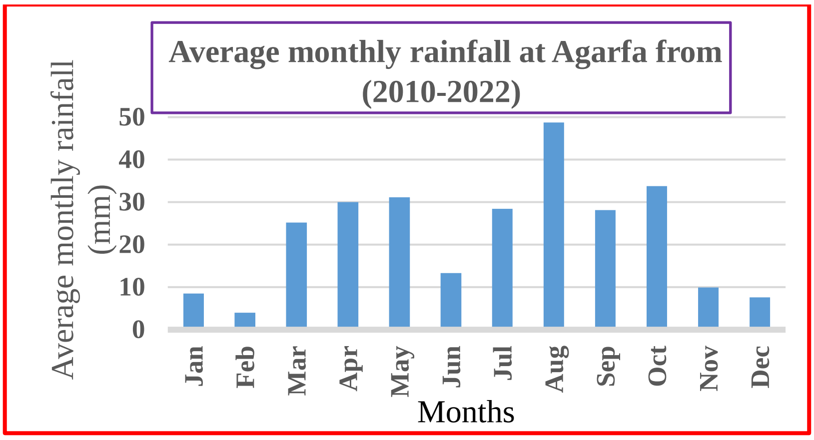

Figure 4. 6 Average monthly Rainfall data of the study area (2010-2022)

B)

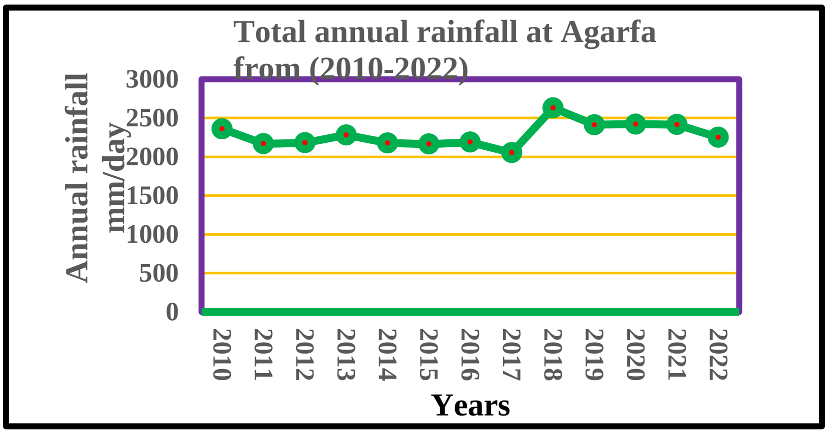

Figure 4. 7 Annual Rainfall data of the study area (2010-2022) at Agarfa station

(Source: National Meteorological Agency of Ethiopia)

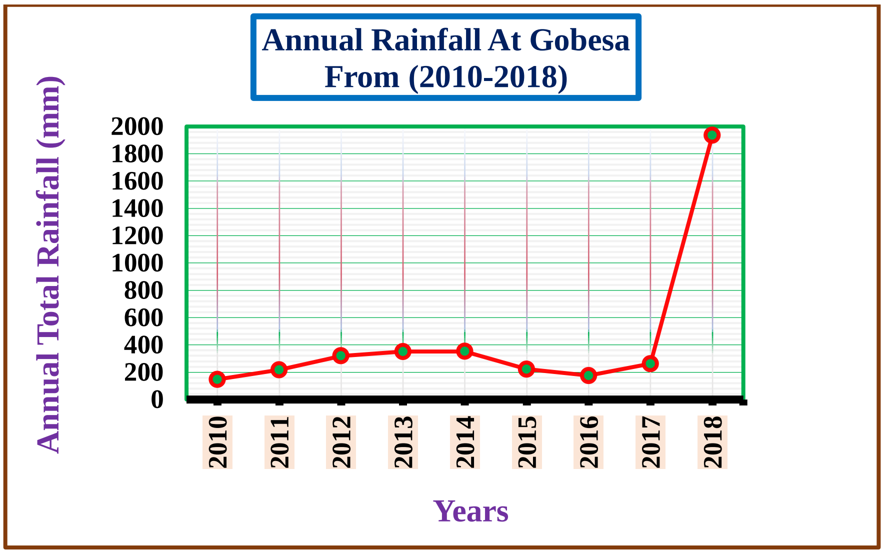

Figure 4. 8 Annual Rainfall data of the study area (2010-2018) at Gobesa station

(Source: National Meteorological Agency of Ethiopia)

4.3 Local geology

The study area covered by outcropped of Aphanitic and vascular basalts, Ignimbrite, scorious basalt, Alkali olivine basalt and unwelded tuff. According to DH (2021) most parts of the Agarfa woreda are underlain by Tertiary volcanic rocks of plateau, highland and lower basalts

4.3.1 The lower lava flows

This formation is exposed in the southeastern part of the study area, from Agarfa town to the Weyib river and Sire area. This unit contains dominantly basalts, with minor amount of lower pyroclastic rocks. Compositionally, they are aphanitic basalts, fine to medium, coriaceous basalt, olivine- plagioclase phyric basalt (Haro *et al.*, 2020). The aphanitic basaltic is slightly to moderately weathered and it's also change color from black to slightly grey to white. As the elevation of my study decrease this unit become more weathered. It's also occurred by columnar joint with the thickness average of five to ten meters. The contact between each lava layer is usually sharp. But at places unconformity is recorded containing paleosol.

Figure 4. 9. A) Moderately weathered aphanitic basalt of columnar joint B) slightly weathered aphanitic basalt

4.3.2 Scoria

The scoria is rather loose, or unconsolidated, but are gently stratified and forms cone. The material is composed of gravely fall deposit of scoria pieces, but also occur sandy or minor sizes which are either grey or pinkish to reddish in color. This unit exposed along road section at the Ija Doke and Sire area.

Figure 4. 10. Observed scoria unit with intercalation of basalts and tuff along road section A) welded scoria with highly weathered basalt at the top B) Unwelded scoria with tuff

4.3.3 The middle lava flows

This unit is exposed in various localities lying above the lower lava flows with distinct unconformity, marked by paleosoil. They are thin relative to lower lava flows, and are continuous over wide geographic areas. They are relatively thinner, and these are also horizontally stratified relatively hard and compact dark grey basalts. This hardness and compact feature of the flows protect the area from further degradation and they form plateau scarp. These rocks are cliff forming on the plateau scarp east of Chafo kebele.

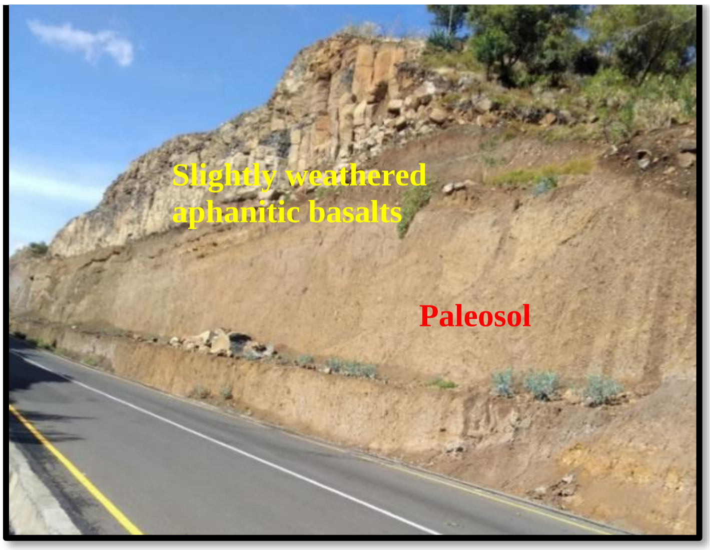

Figure 4. 11. Aphanitic basalts underline by paleosol

4.3.4 The upper pyroclasts

This exposure continues to occur before Oda Chefo kebele, from Agarfa town to Wabe river bridge. In some literature, these pyroclasts are reported as young Quaternary lacustrine deposits (Haro *et al.*, 2020). These pyroclasts includes ash-fall tuffs, gravelly ash, ash-fall deposits, volcanic breccias, & normal tuff. The rock is usually massive with minor fractures in most places, except at places major joints or faults cut this rock unit. There are few columnar joints developed in this unit.

4.3.5 Pyroclastic materials

This units mainly composed of normal ash, gravel to unwelded tuff, and ash-fall its cover most of my study area from Oda Chefo to Buro kebele. The units occurred at the gentle slope of my study area.

Figure 4. 12. Pyroclastic material along road section of my study A) unwelded tuff to gravel with boulder B) Ash-fall with sand material

4.3.6 Residual soil

Residual soils refer to soils that have formed in place by the weathering of underlying rock. These soils are typically found in areas where the underlying rock is relatively stable and has not been transported by erosion or other geological processes. Residual soils can vary in composition and properties depending on the type of rock from which they were formed and the environmental conditions in which they developed. They are often characterized by a high degree of cohesion and low permeability, which can make them suitable for certain engineering application.

This soil is occurred around Weyib river along road section of my study from Agarfa two Wabe river

Figure 4. 13. Black cotton soil along road section of my study area

4.5 Geological structures

In the study area, several structures such as micro fault, dykes, fractures and columnar joints commonly associated with basaltic unit.

4.5.1 Dykes

Dykes are tabular bodies of igneous rock that are formed when magma is injected into a vertical or near-vertical crack in the host rock and then solidifies.

Figure 4. 14. Dykes, Trachyte's intrusion in the lower lava flow

4.5.2 Minor fault

A geologic fault in which the hanging wall has moved upward relative to the footwall. Reverse faults occur where two blocks of rock are forced together by compression. This unit visualized along exposed road section around Ija Doke area, left side of road from Agarfa to Wabe bridge. It's also orientation is NE and nearly the same to strike direction. Figure 4.9 shows minor fault of scoria flows with intercalation of moderately weathered of aphanitic basalts.

Figure 4. 15. Observed minor faults in the study area A) minor reverse fault along exposed road section

4.5.3 Joint

This structure are the most common features in the study area with varying geometry and orientation and mainly on the aphanitic basalt and other units. These are mostly vertical columnar joints and other structure were also observed at some places of the basaltic and ignimbrite rock unit. This structure indicates vertically crystallized units. Figure 4.10 a, b are shows moderately to slightly weathered aphanitic basalt respectively. Both joints are slightly rough surface with joint spacing 0.06 to 1.2m. In present study area the observed joints are show the strike direction SE, and NEE-SW.

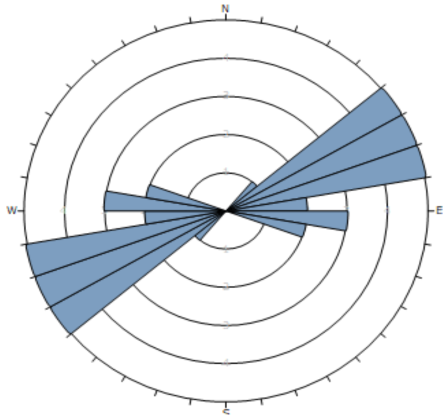

Figure 4. 16. Rosset plotted diagram which indicate the joint orientation along the road sections

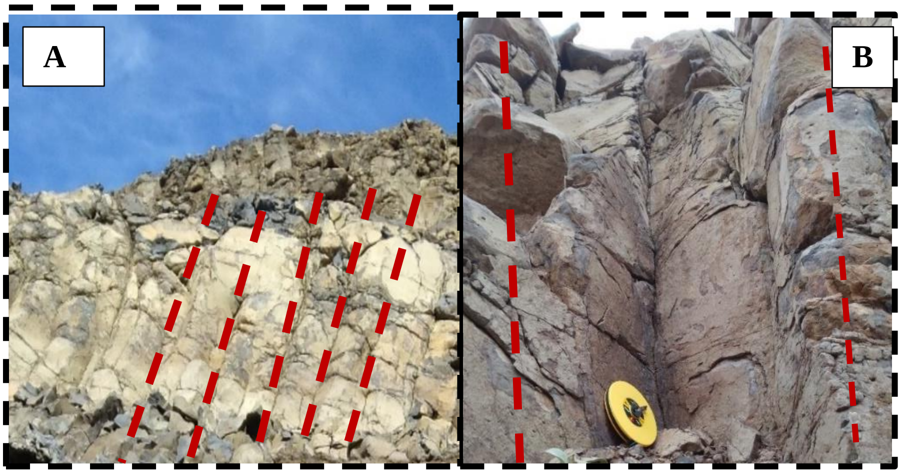

Figure 4. 17. Visualized joints in the study area A) columnar joint in moderately weathered basaltic rock B) columnar joint with slightly rough and weathered aphanitic basalt

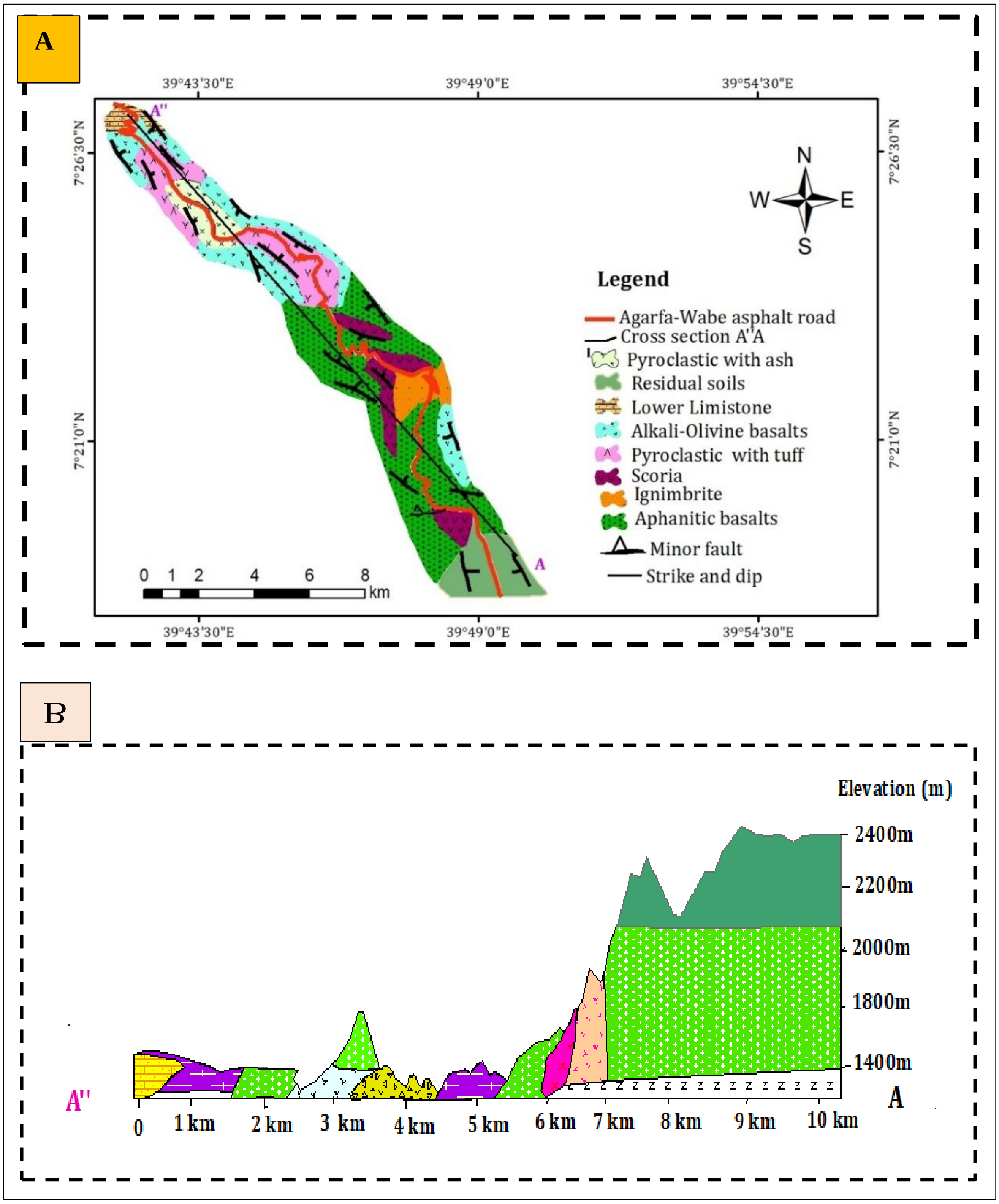

Figure 4. 18: Local geological map of the study area and its cross section

CHAPTER FIVE

5. RESULTS AND DISCUSSION

5.1 INTRODUCTION

In order to evaluate the stability of the critical soil and rock slope sections, a series of laboratory tests and field surveying were conducted. The soil laboratory tests comprised of sieve, hydrometer, compaction, direct shear, Atterberg limit, specific gravity, and water content tests. On the other hand, the rock sample properties were determined using dry and saturated density, compressive strength, and Schmidt hammer tests.

To determine the factors of safety and mode of failure of the critical slope section, different methods were employed. The finite element and limit equilibrium methods were used to calculate the factors of safety. Additionally, kinematics analysis was used to determine the mode of failure of the critical slope section.

5.2 Engineering properties of rock mass

For the present study, a comprehensive field evaluation was carried out to determine the unstable slope areas along the road section and to characterize the geological composition of the soils and rocks. The study area's rock type, weathering, fracturing and ground water condition were identified through a thorough visual inspection during the field survey. The survey revealed two critical rock slope sections which are structurally control, four non-structurally slope section and two soil slope failures. Additionally, the discontinuity conditions observed in the field indicated that the joint roughness ranged from rough to smooth, with some joints filled with none to soft materials.

5.2.1 Discontinuity surveys

The rock mass in the study area's road section was characterized through a discontinuity survey conducted in accordance with the International Society of Rock Mechanics (ISRM, 1978) standard. The discontinuity parameters obtained from the survey, such as joint orientation, joint spacing, joint filling, aperture, joint roughness, groundwater, and weathering condition, are crucial for analyzing the stability of critical rock slopes (structurally control) section.

Table 5. 1. summary of discontinuity parameter for structurally controlled rock slope

<table>
<tr><td colspan="2"></td><td colspan="2">Critical slope sections</td></tr>
<tr><td colspan="2">Discontinuity parameter</td><td>R1SS1</td><td>R3SS2</td></tr>
<tr><td colspan="2">Joint spacing(cm)</td><td>60-100</td><td>50-80</td></tr>
<tr><td rowspan="5">Condition of discontinuity</td><td>Persistence (m)</td><td>0.3-1.0</td><td>2-5</td></tr>
<tr><td>Joint aperture (cm)</td><td>0.05-0.1</td><td>0.1-1.5</td></tr>
<tr><td>Filling materials</td><td>Soft filling>5mm</td><td>None</td></tr>
<tr><td>Roughness</td><td>Moderately rough</td><td>Slightly rough</td></tr>
<tr><td>Degree of Weathering</td><td>Slightly weathered</td><td>Slightly weathered</td></tr>
<tr><td colspan="2">Groundwater condition</td><td>Dry</td><td>Dry</td></tr>
<tr><td colspan="4">RSS- Road slope section</td></tr>
</table>

5.2.2 In-situ strength of rock

In this study, the uniaxial compressive strength (UCS) of the intact rock in the critical slope section was determined using the Schmidt hammer strength test conducted in the field, following the method proposed by Barton & Choubey (1977). The test was carried out in accordance with ASTM D5873 (2001) to obtain rebound values, which were then converted into UCS values using empirical equations (eq. 2.5) suggested by Barton and Choubey Barton & Choubey (1977). The Schmidt hammer (L-type) was used to determine the lowest and highest strength of the rock, which ranged from 16.14 MPa to 146.89 MPa for slope sections R2SS1 and R1SS2, respectively, as presented in Table 5.2.

Table 5. 2. Data of rock mass strength tested by Schmidt hammer (L-type)

Slope sections		Schmidt hammer rebound value from each critical slope sections	Average of (R)	UCS (MPa)	According to ISRM (1981)
R_1SS_2	SW-B	36, 42, 42.5, 43.5, 46, 48, 48.5, 51.5, 52, 53	46.3	146.89	Strong
R_2SS_1	MW-B	28, 29, 31.2, 32, 32.5, 33, 34.5, 35.9, 36, 38	33.01	56.67	medium
	SC	11.25, 12, 13, 13.5, 14, 15.5, 16, 17.35, 18.5, 21	15.21	16.14	weak
R_3SS_1	SW-B	11.25, 12, 13, 13.5, 14, 15.5, 16, 17.35, 18.5, 21	42.13	76.28	medium
R_3SS_2	W-SC	24, 25, 26, 29, 32, 33, 34.5, 39, 40, 41	32.35	19.09	weak
	SW-B	32, 32.5, 34, 34.5, 36, 36.5, 38, 41.5, 46, 52	38.3	82.08	medium
R_4SS_1	SW-IG	41.5, 42, 42.2, 46, 46.5, 48, 48.5, 51.75, 52, 53	47.13	84.75	medium
R_5SS_2	SW-AOB	36, 42, 42.5, 43.5, 45, 46.6, 48, 48.5, 50, 51.5	45.36	92.86	medium
R-Rebound value					

5.2.3 Rock quality destination (RQD)

In the present study, the classification of rock mass was determined by volumetric joint count (JV) for the rock mass that was exposed at critical slope sections along the study area, as suggested by (Palmstrom, 1982). The volumetric joint count was measured on rock surfaces that were exposed along the critical slope sections of the road in the study area. After measurements were conducted on the rock slope section, the volumetric joint count was calculated from the average spacing of joints using equation 2.2. This classification was performed on two rock slope sections because they were structurally controlled. In general, RQD is a measure of the degree of jointing or fracturing in rock mass. The higher the RQD value, the better the rock quality and the more suitable it is for construction purposes.

Table 5. 3. The Rock Quality Designation (RQD) index determined from the volumetric joint count.

Slope section	JV (Av)/1m*m	RQD%	According to Deere (1988)
R1SS2	14	68.8	Good rock quality
R3SS2	12.35	74.25	Good rock quality

5.3 Laboratory results of rock sample taken from critical slope section

The laboratory conducted tests such as point load and unit weight to characterize the rocks. Seven rock types were identified from four non-structurally and two structurally controlled critical slope sections for this study.

5.3.1 Compressive strength test

The tests were conducted on sixteen rock samples, with a minimum of two samples taken from six critical slope sections, and the average strength was calculated. The BS 1881:PART116 was used to determine the strength of these intact rocks. Before inserting the sample into the load-crushing area, the machine required the rock to be in a near-concrete shape. Therefore, the sample was fixed to a shape similar to that of concrete. Finally, the average corrected point load strength was converted to the corresponding uniaxial compressive strength (UCS) using equation (2.1). From the calculated value the table 5.4 was papered.

Table 5. 4. laboratory results of compressive strength tests

Critical slope sections	Sample ID	IS (50) Mpa	UCS (Mpa)	According to ISRM (1981)
R_1SS_2	Slightly weathered basalts	5.1	122.4	Strong
R_2SS_1	Moderately weathered basalts	4.7	112.8	Strong
	Moderately weathered vascular basalts	4.0	96	Medium
R_3SS_1	Moderately weathered aphanitic basalts	4.6	110.4	Strong
	Moderately weathered aphanitic basalts	4.5	108	Strong
R_4SS_1	Slightly weathered basalts	3.8	91.2	Medium
R_5SS_2	Slightly weathered -Akali olivine basalts	5.0	120	Strong
R1SS2 = Road one slope section two (Day one slope section two)				

5.3.2 Dry and saturated unit weight of rock sample

The unit weight of rock is an important parameter in slope stability analyses. To determine the density of the rock, buoyancy techniques were used on irregular rock samples following the (Bieniawski & Hawkes, 1978) standard, specifically using equation 3.8. The study area included six critical rock slope sections from which representative rock samples were collected. The observed rock samples were slightly and moderately weathered aphanitic basalts (SW and MW-A. B), slightly weathered basalts (SW-B), moderately weathered vascular basalts (MW-V. B) slightly weathered basalt (SW-B), welded scoria (W-SC), and alkali olivine basalts (AOB). The unit weight of these samples was estimated. The results, as shown in **Appendix**

F and **G**, indicate that the dry unit weights range from 13.5 to 28.4 KN/m3, while the saturated unit weights range from 21.13 to 29.95 KN/m3.

5.4 Rock mass classification

Rock mass classification is a system used to categorize rock masses based on their physical and mechanical properties. It takes into account factors such as rock strength, joint spacing and orientation, weathering, and other characteristics that affect the behavior of the rock mass. The classification system is used to assess the stability of rock slopes, and to design appropriate support systems. There are several different rock mass classification systems in use, including the Rock Mass Rating (RMR) system, the Q-system, and the Geological Strength Index (GSI) system. In this present study, the RMR and GSI data were determined from the field discontinuity surveys and visual observed respectively.

5.4.1 Rock mass rating (RMR)

In this study, two of the rock slope section identified as structural control were selected for this method since, most of my study area was non-structural slope section. RMR Values calculated based on measured the discontinuity parameter rock slope section as shown in Table 5.5 below and using equation 3.9.

Table 5. 5 summarized parameter of structural controlled slope section

Slope section	Rock types	Rating of five basic RMR values					RMR	Class	Description of rock quality according to Bieniawski, Z.T. (1976)
		USC	RQD	SP. D (mm)	CON.D	GW.C			
R1SS2	SW-B	12	13	15	25	15	80	II	Good
R3SS2	MW-B	7	13	15	25	15	75	II	Good
USC=Uniaxial compressive strength, RQD = Rock quality designation. SP. D = Spacing of discontinuity, CON. D = Condition of discontinuity and GW.C =Ground water conditions, SW = slightly weathered and MW = moderately weathered									

5.4.2 Geological strength index

Geological Strength Index (GSI) is a rock mass classification system used in engineering geology to evaluate the strength and stability of rock masses for design purposes. The system was developed by Hoek and Brown in 1980 and is based on the Geological Strength Index (GSI) which is a measure of the strength of the rock mass. It’s determined by assessing the rock mass characteristics such as the rock type, structure, and discontinuities, and assigning a value between 0 and 100 based on the quality of the rock mass. A higher GSI value indicates a stronger and more stable rock mass. The GSI value is used to calculate the shear strength of the rock mass, which is an important parameter in slope stability analysis and rock engineering design. It is an important tool for evaluating the strength and stability of rock masses and for designing safe and efficient infrastructure. In present study, the GSI of the critical slope section were visual observed in the field depend on the rock surface conditions as shown in **Appendix: E.**

5.5 Engineering characterization of soils

In order to determine the stability of the slope section, various geotechnical properties of the soil were examined from four different test pits at varying depths. Soil samples were collected from a depth of 2.5m, 1m, 2m, and 1.5m for test pit 1, test pit 2, test pit 3, and test pit 4, respectively. The specific gravity of the soil samples obtained from these test pits were 2.71, 2.63, 2.70, and 2.60. All of the soil samples collected from the test pits were identified as medium to high plasticity clay soil. The liquid limit values for test pit 1, test pit 2, test pit 3, and test pit 4 were 73.5, 68.9, 52.2, and 54.1, respectively. The plastic limit values for the same test pits were 36, 33, 37.1, and 20.7, respectively.

Based on the AASHTO classification, the soil was classified as clay silt soil with a water content of 39.4%, 37.45%, 25.13%, and 30.314% for test pit 1, test pit 2, test pit 3, and test pit 4, respectively. To determine the shear strength parameters of the soil, a direct shear test was conducted. The cohesion parameters calculated for the soil samples were 45.31 KN/m2, 38.68 KN/m2, 18.47 KN/m2, and 17.65 KN/m2, while the frictional angles were calculated to be 19.16°, 19.22°, 23.21°, and 24.88° for test pit 1, test pit 2, test pit 3, and test pit 4, respectively.

5.5.1 Particle size distribution curve

Grain size analyses were conducted on the soil along critical slope section for classifying the types of soil and identify the mechanical property of the problematic area of the soil mass. mechanical tests (sieve and hydrometer) were conduct on four critical slope section. From these two of the soil samples (S1 and S3) are taken at the homogeneous slope section and the other two were taken heterogenous side of the slope section.

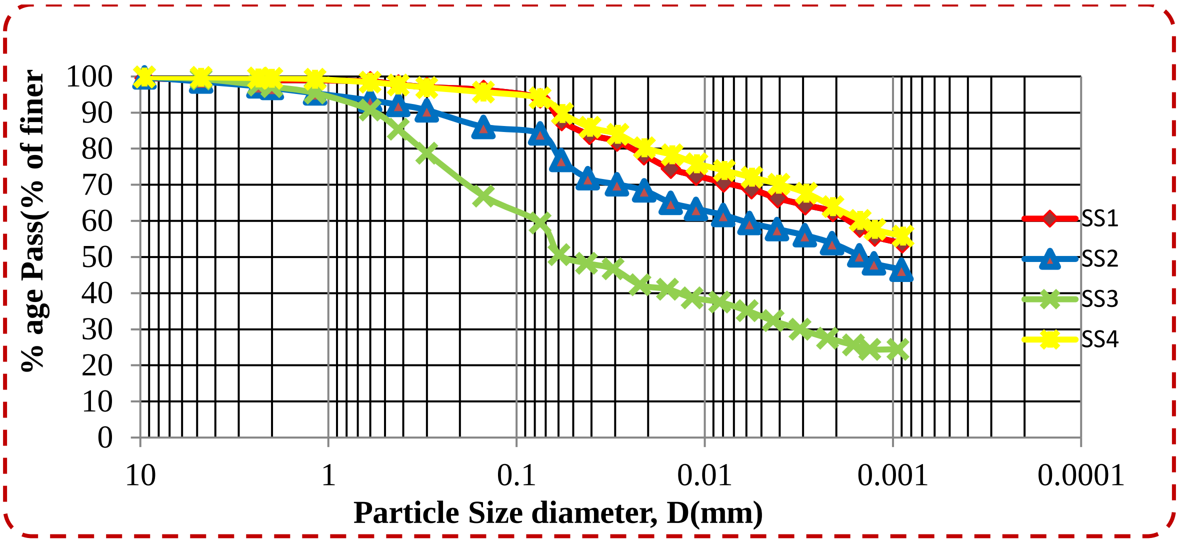

Figure 5. 1. particle size gradation curve

Table 5. 6. Summary of the combined data of sieve and hydrometer analysis of all soil samples.

NO.		SS1	SS2	SS3	SS4
1	Particles larger than (4.75mm) (%)	0.94	1.40	0.22	0.70
2	Coarse Sand (4.75mm-0.425mm) (%)	1.29	5.20	1.38	13.90
3	Fine Sand (0.425mm - 0.075mm) (%)	3.83	7.33	2.73	25.95
4	Silt (0.075-0.002mm)	31.44	35.07	34.91	40.55
5	Clay smaller than (0.002mm) (%)	62.50	51.01	60.76	18.90

SS- soil samples

5.5.2 Atterberg limit

After mechanical test (sieve analysis) were conducted, Atterberg limit (Casagrande) test such liquid limit, plastic limit and plastic index tests was determined in the laboratory and a liquidity curve or a flow curve is plotted on a semi-logarithmic graph representing water content on the arithmetical scale and the number of drops on logarithmic scale. This graph used to identify the maximum water content at the 25 numbers of blows.

Table 5. 7. Laboratory results of Atterberg limit in my study area

Sample location	Liquid limit (LL)	Plastic Limit (Pl)	Plastic Index (PI)
SS1	73.5	36	37.5
SS2	68.9	33	35.9
SS3	52.2	37.1	15.1
SS4	54.1	20.7	33.4

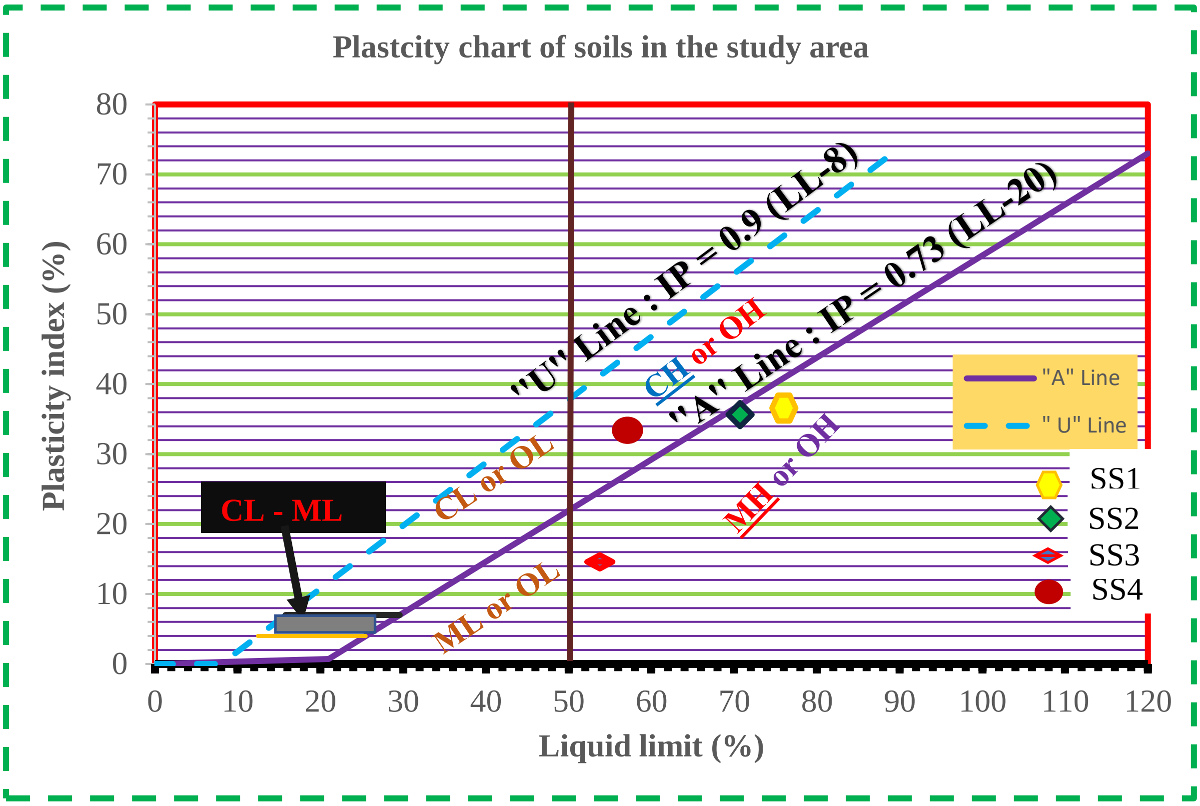

Figure 5. 2. plasticity chart

5.5.3 Soil classification

Based on the results of the sieve and Atterberg limit tests (Table 5.1 and 5.2), the soil samples (SS1, SS2, SS3, SS4) are classified as A-7-6 in the AASHTO classification system. In the USCS system, the soil samples from the critical slope section (SS1, SS2, and SS3) in my study area are classified as MH, while soil sample SS4 falls under the CH soil type. This indicates that the soils in the critical slope section are clay to silty clay soils respectively (Fig. 5.2)

Table 5. 8. classification of my study soil by AASHTO and USCS

Sample ID	Sieve opening (mm) with % of passing			Atterberg limit		Classification		
	2.0	0.425	0.075	LL	PI	AASHTO	USCS	
							Group symbol	Group name
SS1	98.9	97.1	92.0	73.5	37.6	A-7-6	MH	Inorganic silt of high plasticity
SS2	96.8	92.2	84.2	68.9	35.9	A-7-6	MH	
SS3	97.2	95.4	59.5	52.2	15.1	A-7-5	MH	
SS4	99.5	97.7	94.1	54.1	33.4	A-7-6	CH	Inorganic clay of high plasticity

5.5.4 Compaction test

The compaction test was a laboratory test used to determine the maximum dry density and optimum moisture content of a soil sample. This test was conducted for all of the soil sample from critical slope section.

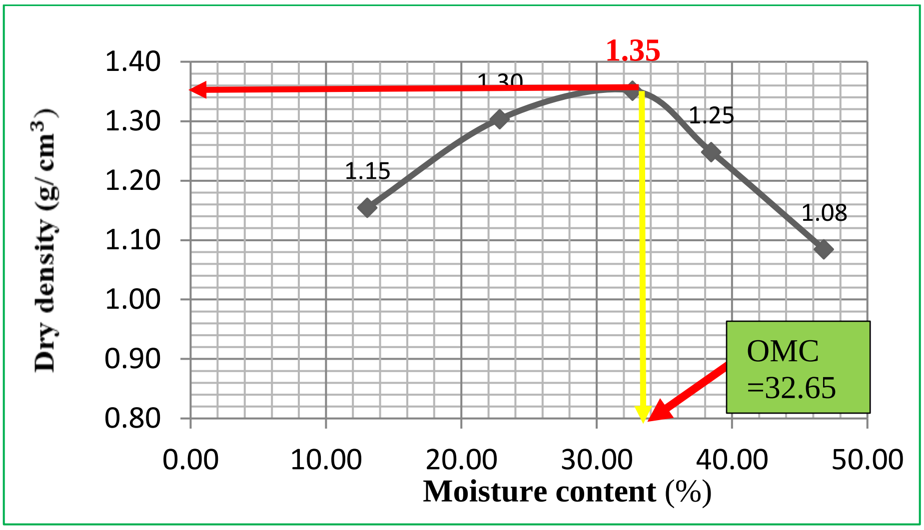

Figure 5. 3 *Moisture content to dry density relation* SS_1

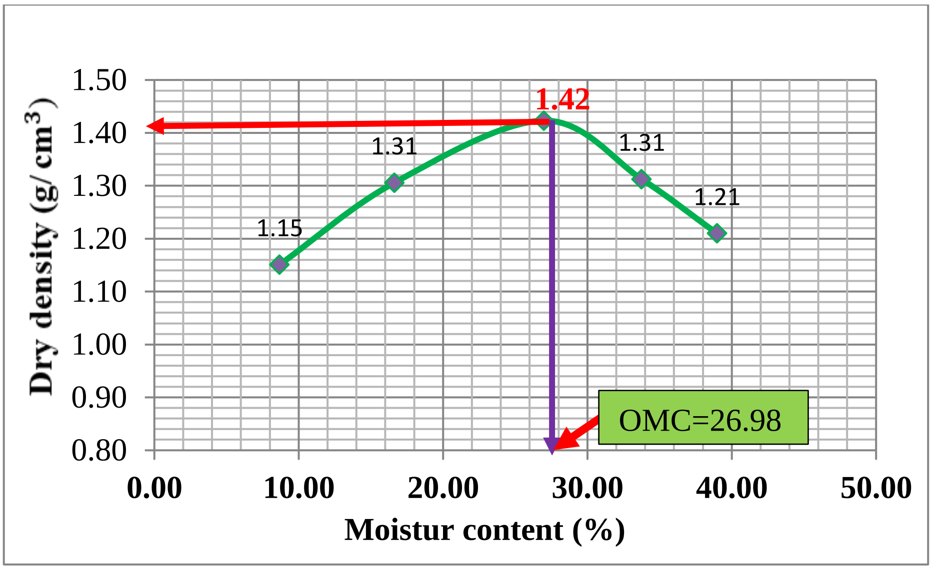

Figure 5. 4 *Moisture content to dry density relation* SS_2

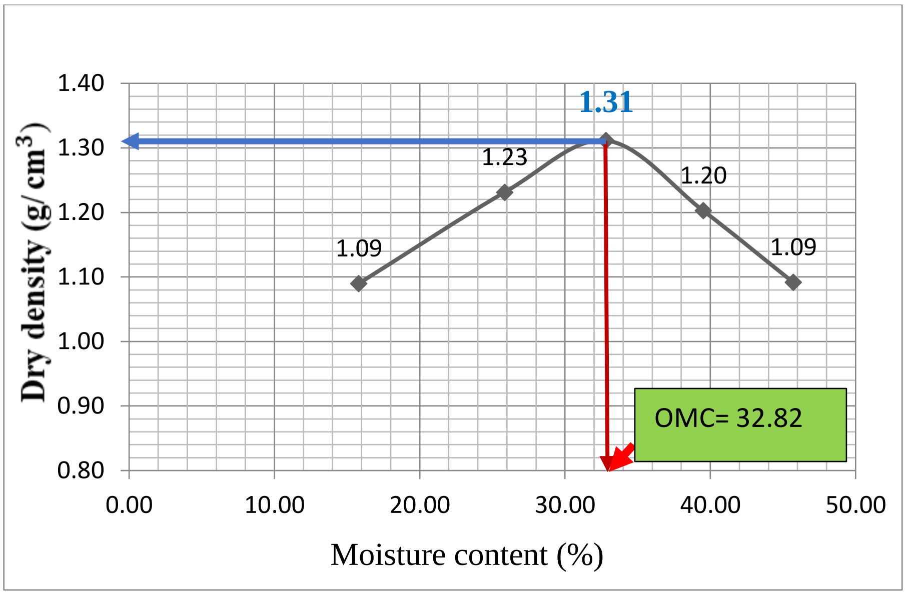

Figure 5. 5. Moisture content to dry density relation SS3

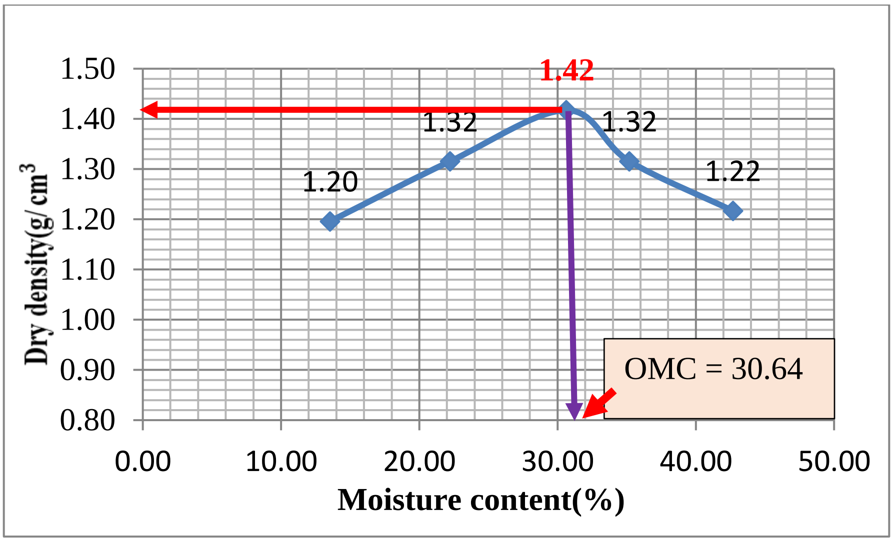

Figure 5. 6. Moisture content to dry density relation SS4

5.5.5 Shear strength of soils

The shear strength of the soils (cohesion and frictional angle) was determined by direct shear test. These input parameters play a crucial role in the stability analysis of selected critical slopes, along with the unit weight of soils (dry and wet). The cohesion and frictional angle of the soil samples obtained from direct shear tests for SS1, SS2, SS3 and SS4 were 45.31 KN/m^2, 38.68 KN/m^2, 18.47 KN/m^2, 17.65 KN/m^2, and 19.16°, 19.22°, 23.21°, and 24.88°, respectively.

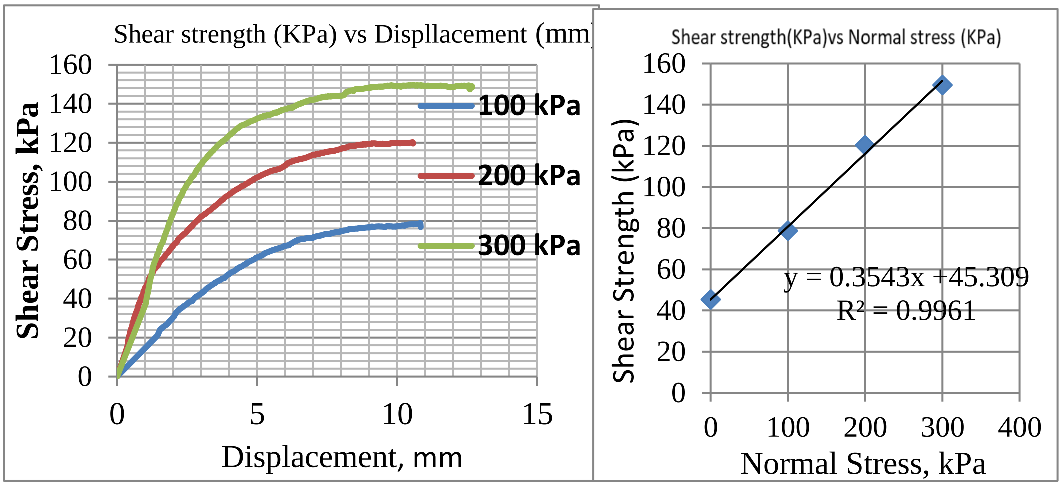

Figure 5. 7. Direct shear test for test pit (SS1)

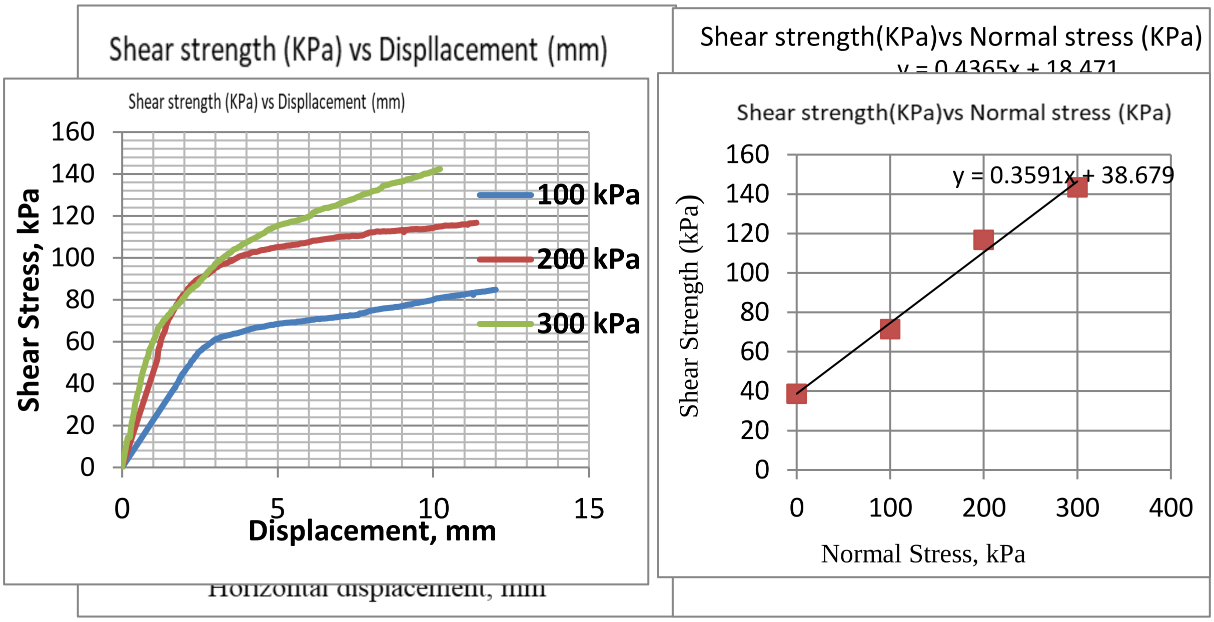

Figure 5. 8. Direct shear tests for test pit (SS2)

Figure 5. 9. Direct shear tests for test pit (SS3)

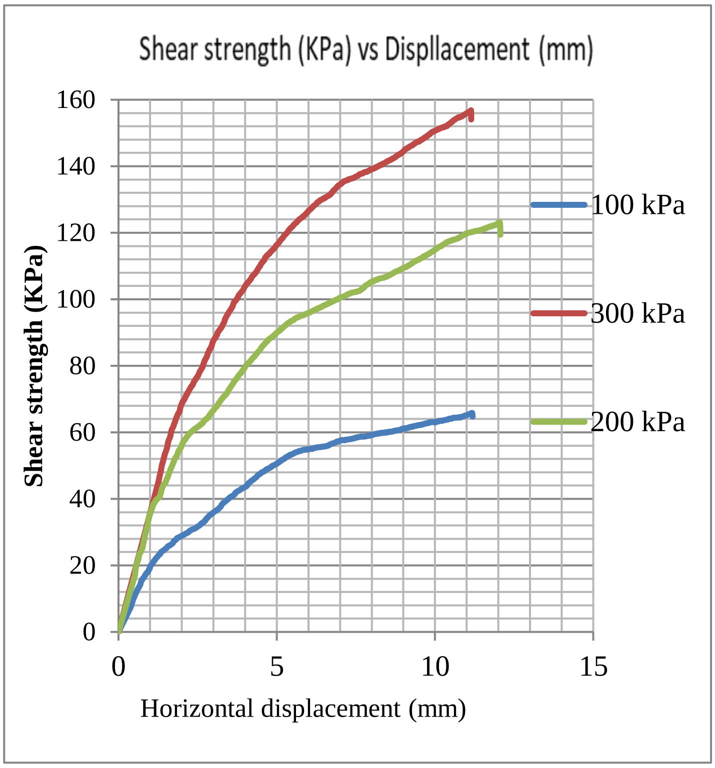

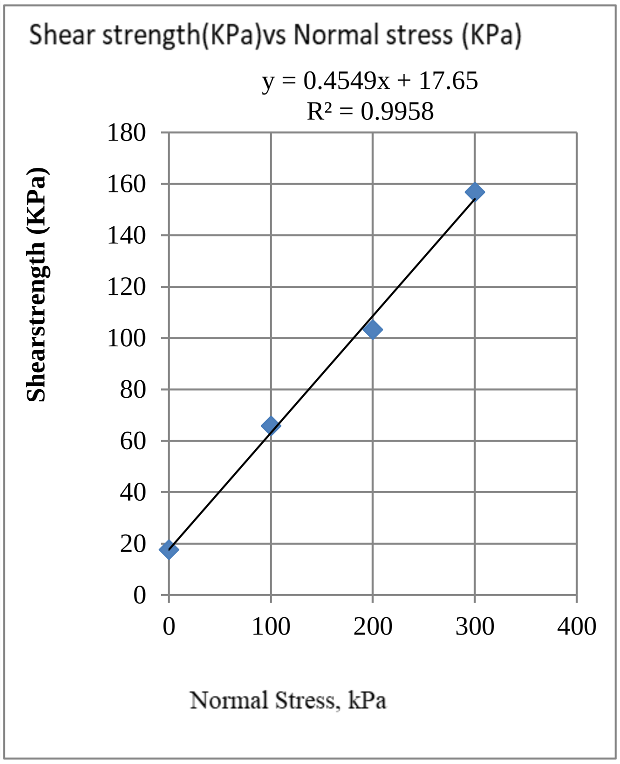

Figure 5. 10. Direct shear test for test pit SS4

Table 5. 9. summary of laboratory results of shear strength parameter, unit weight and water content of soils in study area

Critical slope section (CSS)	Soil types	Shear strength parameters		γ of soils (KN/m^3)		Water content (%)
		Cohesion (c)	Frictional angle (ϕ)	γdry	γsat.	
SS1	Clayey silt	45.31 (KN/m^2)	19.16 º	12.20	17.00	39.4
SS2	Clayey silt	38.68 (KN/m^2)	19.22 º	13.03	17.91	37.5
SS3	Silt	18.47 (KN/m^2)	23.21 º	12.12	16.890	30.3
SS4	Silt clayey	17.65 (KN/m^2)	24.88º	13.51	16.90	25.1

Table 5. 10. Laboratory soil tests and its depth

Test summary		SS1	SS2	SS3	SS4
Depth of test pit		3.5	1.5	2	1.5
Specific Gravity		2.71	2.63	2.70	2.60
Natural moisture content		39.4	37.5	30.3	25.1
Direct shear	Cohesion (c)	45.31 (KN/m^2)	38.68 (KN/m^2)	18.47 (KN/m^2)	17.65 (KN/m^2)
	Frictional angle (ϕ)	19.16 º	19.22 º	23.21 º	24.88º
Atterberg limit	Liquid limit	73.5	68.9	52.2	54.1
	Plastic limit	36	33	37.1	20.7
	Plastic index	37.5	35.9	15.1	33.4
Moisture- Density relationship	Maximum dry density (MDD)	1.35 g/cm^3	1.31 g/cm^3	1.42 g/cm^3	1.42 g/cm^3
	Optimum moisture content (OMC)	32.65 %	32.82 %	26.98 %	30.64 %

5.6 Kinematic analysis

For this analysis, two rock slope sections that were structurally controlled were chosen. These sections were located before the Weyib River (7° 18' 00″ to 39° 49' 03″) and in the Sire area (7° 21' 02″ to 39° 47' 57″) along the road from Agarfa to the Wabe River bridge, and were slightly weathered basalt. To conduct the analysis, various parameters such as slope face orientations and joint set orientations were measured in the field, and the frictional angle was taken from rocdata software. Different modes of rock slope failure were observed in the two slope sections, R1SS2 and R3SS1. At R1SS2, two planar failures occurred due to joints J3 and J4, as well as two wedge failure due to the intersection of joints J1 and J4, J2 and J4. The second rock slope section, R3SS1, also exhibited two modes of failure: planar failure at joint J1 and flexural failure due to the pole of joint J1, respectively.

Table 5. 11. Input parameters required for conducting a kinematic analysis using dips software

Types of slope section	Slope face orientations (D/DD)	Joint set orientations (Dips and Dip direction)				
	D/DD, (°)	J_1	J_2	J_3	J_4	Frictional angle
R_1SS2	75/195°	58°/165°	73°/170°	45°/182°	65°/184°	48°
R_3SS2	81.5°/145°	73°/340°	52°/330°	72°/170°	-------	49°

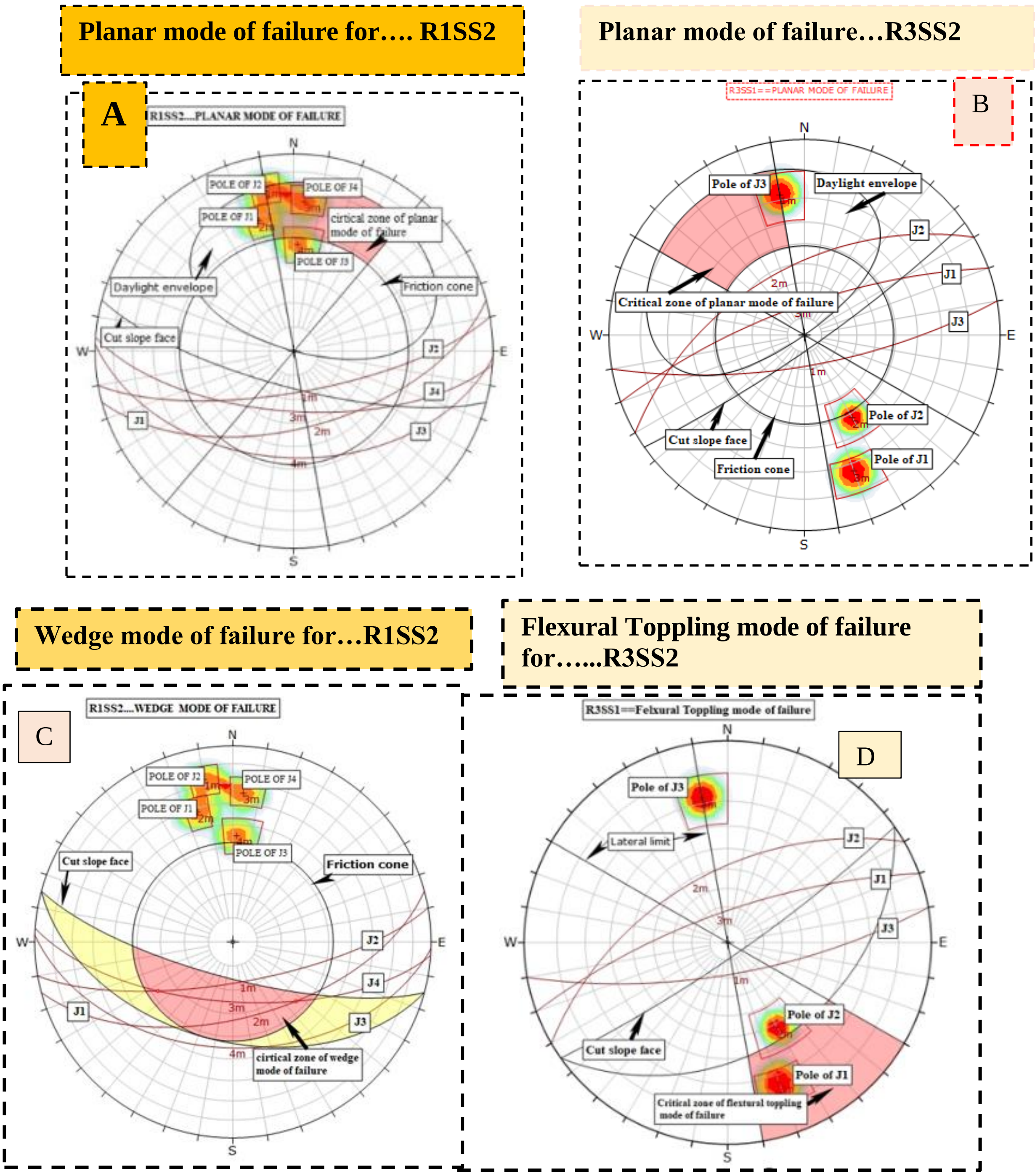

Figure 5. 11. Kinematic analyses for different mode of rock slope failure at slope section (R1SS2 and R3SS1): A and B) planar failure for both slope section respectively and C) wedge failure at R2SS1 slope section and D) flexural failure at slope section R3SS1

5.7 Deterministic stability analysis of rock slope section

The deterministic slope stability analysis was conducted on two different rock slope sections, which showed different modes of failure. The first section (R1SS2) exhibited planar and two wedge modes of failure, while the second section (R3SS1) showed planar and toppling modes of failure. This analysis conducted after kinematic analysis methods, the structurally controlled slope sections. For the analysis, Rocplane and Swedge software was selected and conducted under different conditions such as static dry, static saturated, dynamic dry, and dynamic saturated. The input parameters for the software are shown in Table 5.12.

Table 5. 12. Input parameter used in Rocplane software for planar mode of failure occurred in the R1SS2 and **R3SS2**

SCSS	Joint sets	Slope geometry		Failure plane				Shear strength parameter		Forces	
		Dip (°)	H (m)	Dip (°)	Wv	γ_r (t/m^3)	USA (°)	C(t/m^2)	Φ, (°)	γw (t/m^3)	α
R1SS2	J2	75	30	58	6	2.9	0	4.3	46.62	1	0.03
	J4			65				6	49	1	0.03
R3SS2	J3	82	35	72	4	2.83		3.3	43.54	1	0.03
SCSS = Structural controlled slope section											

5.7.1 Deterministic stability analysis at rock slope section R1SS2

The slope section was characterized as slightly weathered aphanitic basalts with slope angle 75 degree. Its show two planar mode of failure at an angle 58 and 65 degree respectively for J2 and J4. This slopes section analyzed under four different conditions by Rocplane software for planar mode of failure of slope section (R1SS2). The results of analysis show that the factor of safety decrease from static to dynamic dry and static saturated to dynamic saturated condition. The FOS for joint two (J2) and joint four (J4) were 0.99, 0.94, 0.67, 0.58 and 1.43, 1,38, 0.95,0.90 for two joints from static dry to dynamic saturated conditions which as shown the results of rock plane software in table 5.12 and 5.13 respectively.

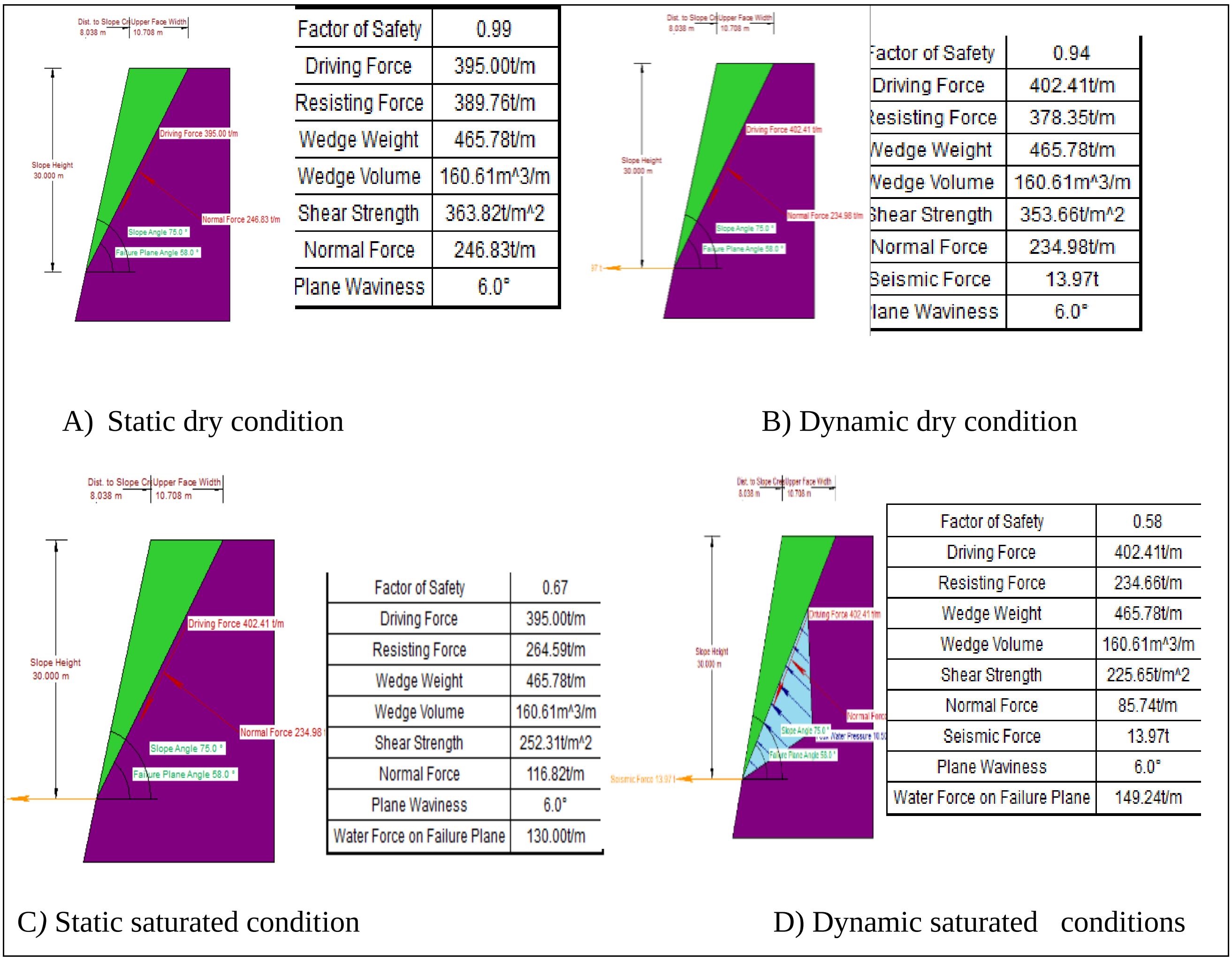

Factor of Safety	0.99
Driving Force	395.00t/m
Resisting Force	389.76t/m
Wedge Weight	465.78t/m
Wedge Volume	160.61m^3/m
Shear Strength	363.82t/m^2
Normal Force	246.83t/m
Plane Waviness	6.0°

A) Static dry condition

actor of Safety	0.94
Driving Force	402.41t/m
esisting Force	378.35t/m
Vedge Weight	465.78t/m
Vedge Volume	160.61m^3/m
hear Strength	353.66t/m^2
Normal Force	234.98t/m
eismic Force	13.97t
lane Waviness	6.0°

B) Dynamic dry condition

Factor of Safety	0.67
Driving Force	395.00t/m
Resisting Force	264.59t/m
Wedge Weight	465.78t/m
Wedge Volume	160.61m^3/m
Shear Strength	252.31t/m^2
Normal Force	116.82t/m
Plane Waviness	6.0°
Water Force on Failure Plane	130.00t/m

C) Static saturated condition

Factor of Safety	0.58
Driving Force	402.41t/m
Resisting Force	234.66t/m
Wedge Weight	465.78t/m
Wedge Volume	160.61m^3/m
Shear Strength	225.65t/m^2
Normal Force	85.74t/m
Seismic Force	13.97t
Plane Waviness	6.0°
Water Force on Failure Plane	149.24t/m

D) Dynamic saturated conditions

Figure 5. 12. shows the slope stability modelling of the planar mode of failure for the R2SS1 rock slope section on joint four (J2) using Rocplane software.

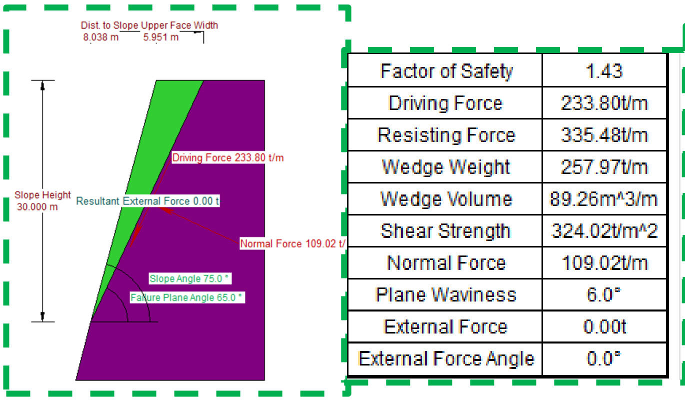

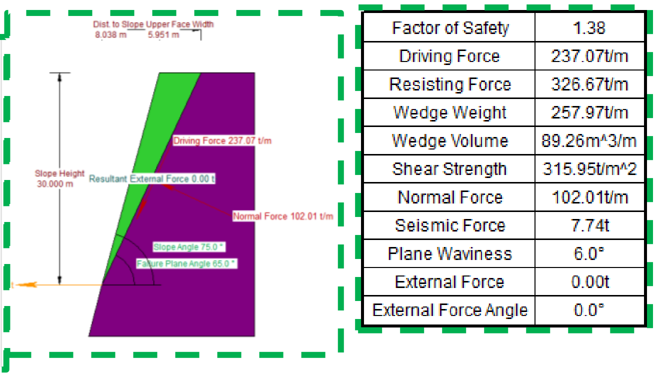

A) Static dry condition

B) Dynamic dry condition

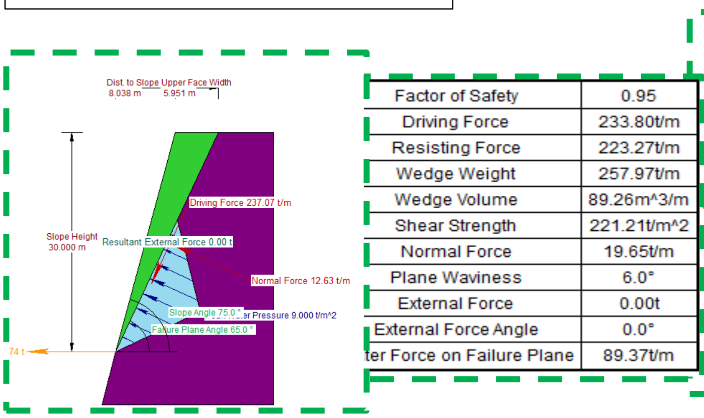

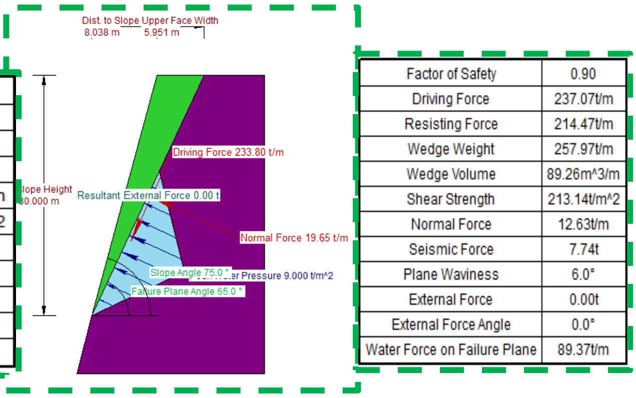

c) Static dry condition

d) dynamic saturated condition

Figure 5. 13. shows the slope stability modelling of the planar mode of failure for the R2SS1 rock slope section on joint four (J4) using Rocplane software

Table 5. 13. Summary of the modelling of joint two (J2) and four (J4) from the R_1SS_2 slope section

		Static saturated (Filled water pressure by %)		Dynamic saturated (Filled water pressure by %)		Static dry	Dynamic dry
		>35	< 35	>25	<25		
Joint ID	J2	Unstable	Stable	Unstable	Stable		
	J4	> 60	< 60	> 55	< 55	Stable	stable
		Unstable	Stable	Unstable	Stable		

5.7.2 Deterministic stability analysis at rock slope section R3SS2

The kinematic analysis results indicate that the planar mode of failure occurs in rock slope section R3SS2 along joint three (J3), which has a dip angle of 72 degrees and a slope angle of 82 degrees. The slope section is composed of moderately weathered basaltic rock and has a height of 35 meters. Table 5.14 above summarizes the parameters used in the Rocplane software analysis.

Table 5. 14. Summary of the modelling of joint three (J3) from the R3SS2 slope section

		Static saturated (Filled water pressure by %)		Dynamic saturated (Filled water pressure by %)		Static dry	Dynamic dry
	J3	> 55	< 55	> 45	< 45	Stable	stable
		Unstable	Stable	Unstable	Stable		

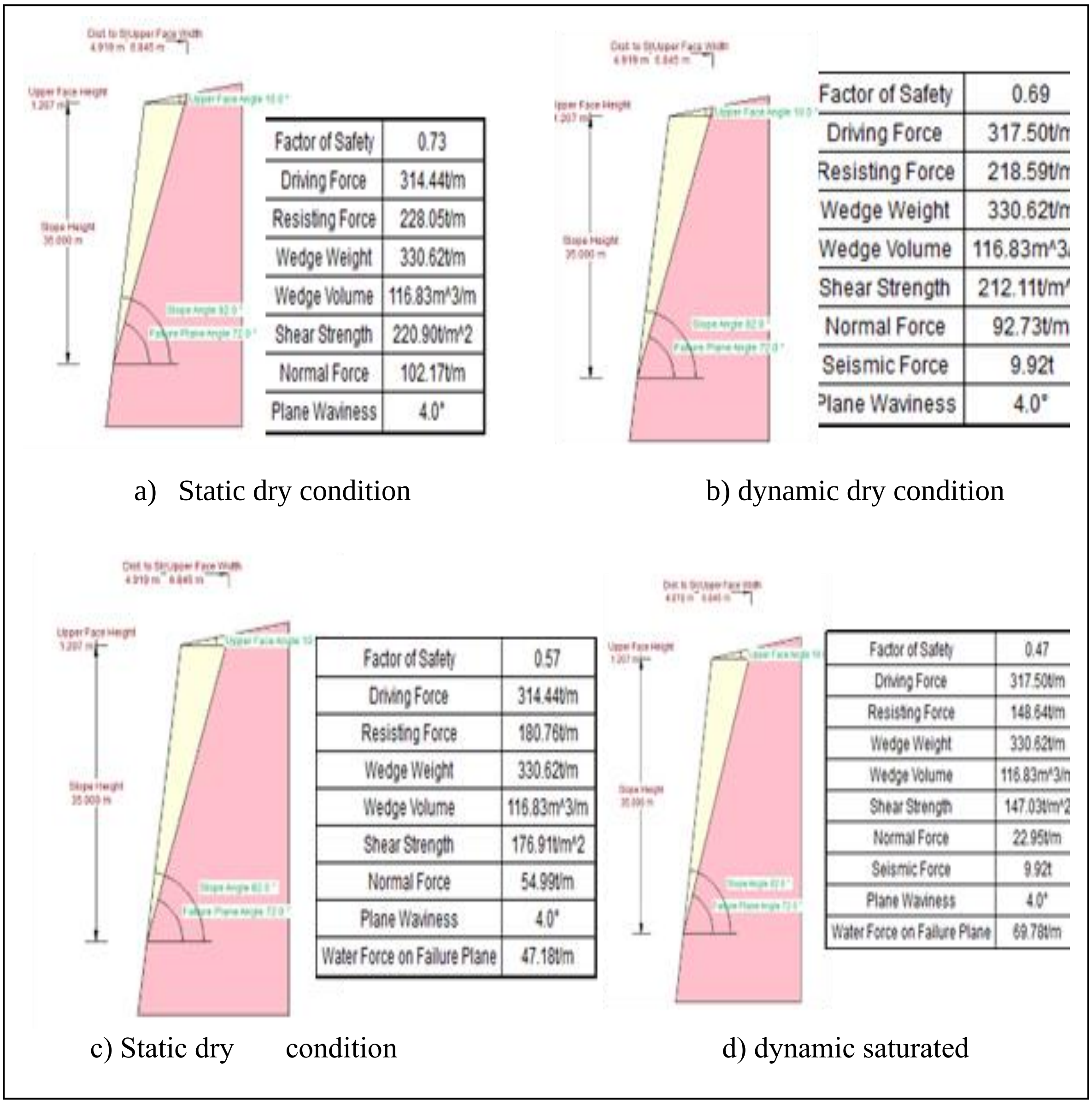

a) Static dry condition

b) dynamic dry condition

c) Static dry condition

d) dynamic saturated

Figure 5. 14. shows the slope stability modelling of the planar mode of failure for the R3SS2 rock slope section on joint three(J3) using Rocplane software

The results from the stereographic projection show that the slope along joint three is unstable in all conditions, indicating that its Factor of Safety (FOS) is below one.

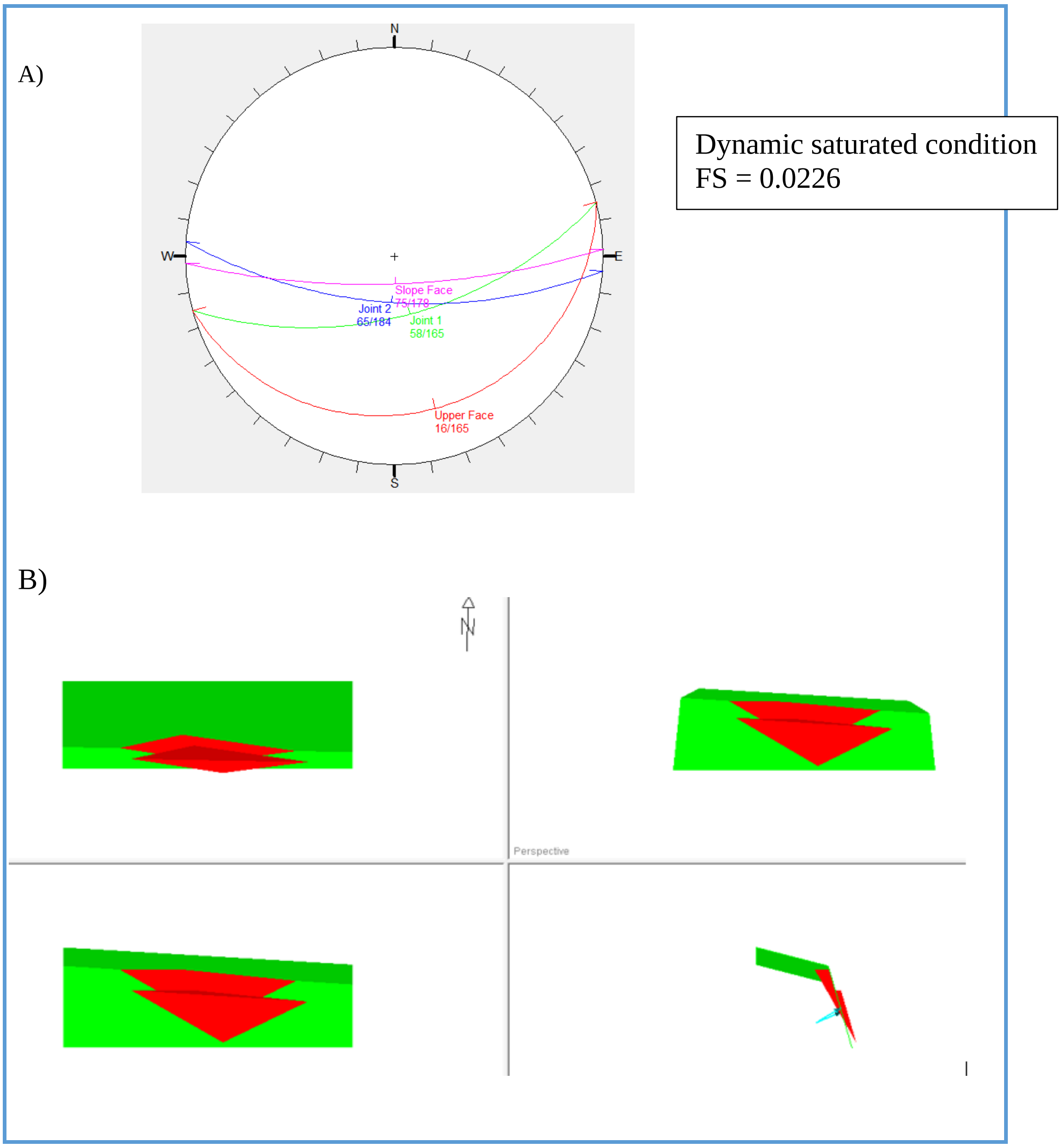

Figure 5. 15 Stereographic projection and wedge failure at rock slope section of R1SS2

5.8 Stability analysis of homogenous rock slope (R4SS2) using limit equilibrium methods (Slide software)

This rock slope section (R4SS2) was slightly weathered and highly disturbed by blasting method during the earth work for road constructing. Its slope dip angles and heights of the was 72 degrees and 30 meters. The rock slope section was analyzed by two geometrical profile one above bench two and the other above bench one these with dip amount of 70 and 48 degree with three and five bench width. Modelling of slope was conducted by slide software under four different limit equilibrium methods such as Bishop's, Janbu simplified, spencer and Mongerstern-price. The results of analysis from these four methods show that the slope section was unstable in all anticipated condition. The FOS for four conditions were shown in the figure 5.15 below.

Table 5. 15. Input parameter for Ignimbrite rock slope stability analysis using slide software (R4SS2)

Slope sections	Rock types	Strength model	Parameter used for analysis				Horizontal seismic acceleration (α)g
			Cohesion (c)	Friction angle (ϕ)	Unit weight (KN/m^3)		
					γ Dry	γ sat.	
R4SSI	SW-IG	Mohr- coulomb	0.347	51.55	22.03	28.89	0.03

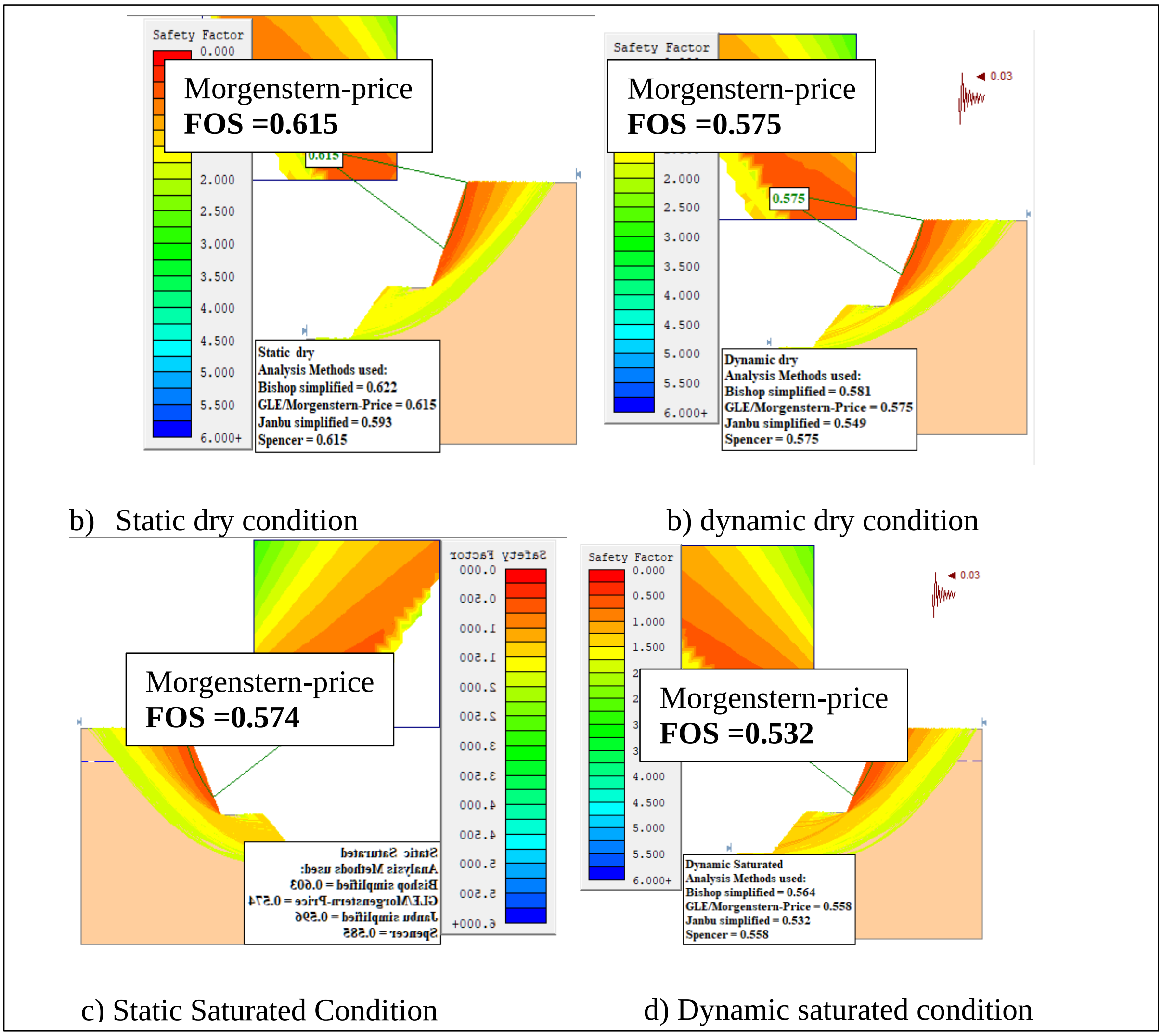

Figure 5. 16. Limit equilibrium analysis for homogenous slope (Ignimbrite) for a different condition

5.9 Non-homogenous rock slope stability analysis using limit equilibrium methods (slide software)

For this study, slope stability analysis was performed on three slope sections using Slide software and various methods. Two of the sections, R3SS1 and R5SS2, were heterogeneous at the base with soils, while R2SS1 was a heterogeneous rock slope consisting of aphanitic-vesicular basalts to scoria. The slope angles and heights were 75° and 35 m for R3SS1, 65° and 30 m for R2SS1, and 58° and 22 m for R5SS2. Four limit equilibrium methods were used for these critical slope sections: Morgenstern-Price, Spencer, Janbu simplified, and Bishop simplified, with the Mohr-Coulomb model. The shear strength parameters were obtained from Rocdata software using the Hoek-Brown failure criteria, and the unit weight of rock was determined in the laboratory. The input parameters for the software are summarized in Table 5.12. The results of the analysis showed that the factor of safety (FOS) for slope sections R2SS1, R3SS1, and R5SS2, as determined by GLE/Morgenstern-Price, ranged from 0.569 to 1.031, 0.769 to 1.038, and 0.981 to 1.43, respectively.

Table 5. 16. Input parameter for non-homogenous slope used for slide software (Limit equilibrium methods)

Slope sections	Rock types and soils	Strength model	Parameter used for analysis				Horizontal seismic acceleration (α)g
			Cohesion (c) (Mpa)	Friction angle(ϕ) (°)	Unit weight (KN/m^2)		
					γ Dry	γ sat.	
R2SS1	SC	Mohr's coulomb	0.073	34.96	14.78	21.13	0.03
	MW-V. B		0.345	55.32	24.48	26.91	0.03
	MW-A. B		0.405	58.15	25.61	29.21	0.03
R3SS1	SW-B		0.515	57.86	23.62	30.71	0.03
	SS2		0.0387	19.22	13.51	16.90	0.03
R5SS2	AOB		0.399	60.73	25	29.95	0.03
	SS4		0.0185	24.88	13.51	16.90	0.03
AOB = Alkali olivine basalts							

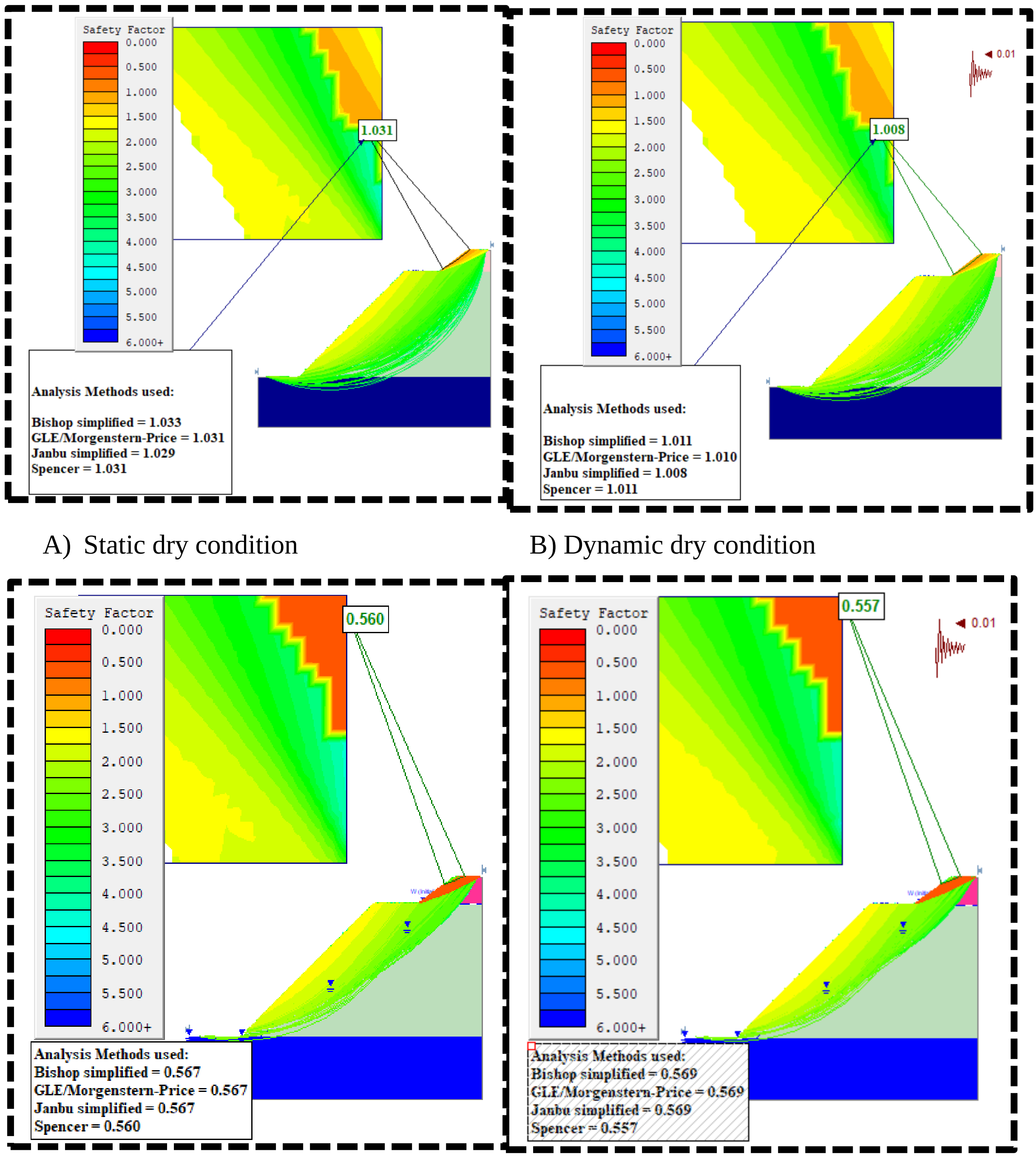

C) Static saturated condition

D) Dynamic saturated condition

Figure 5. 17. Limit equilibrium analysis for heterogenous rock slope (aphanitic - vascular basalts to scoria) for a different condition

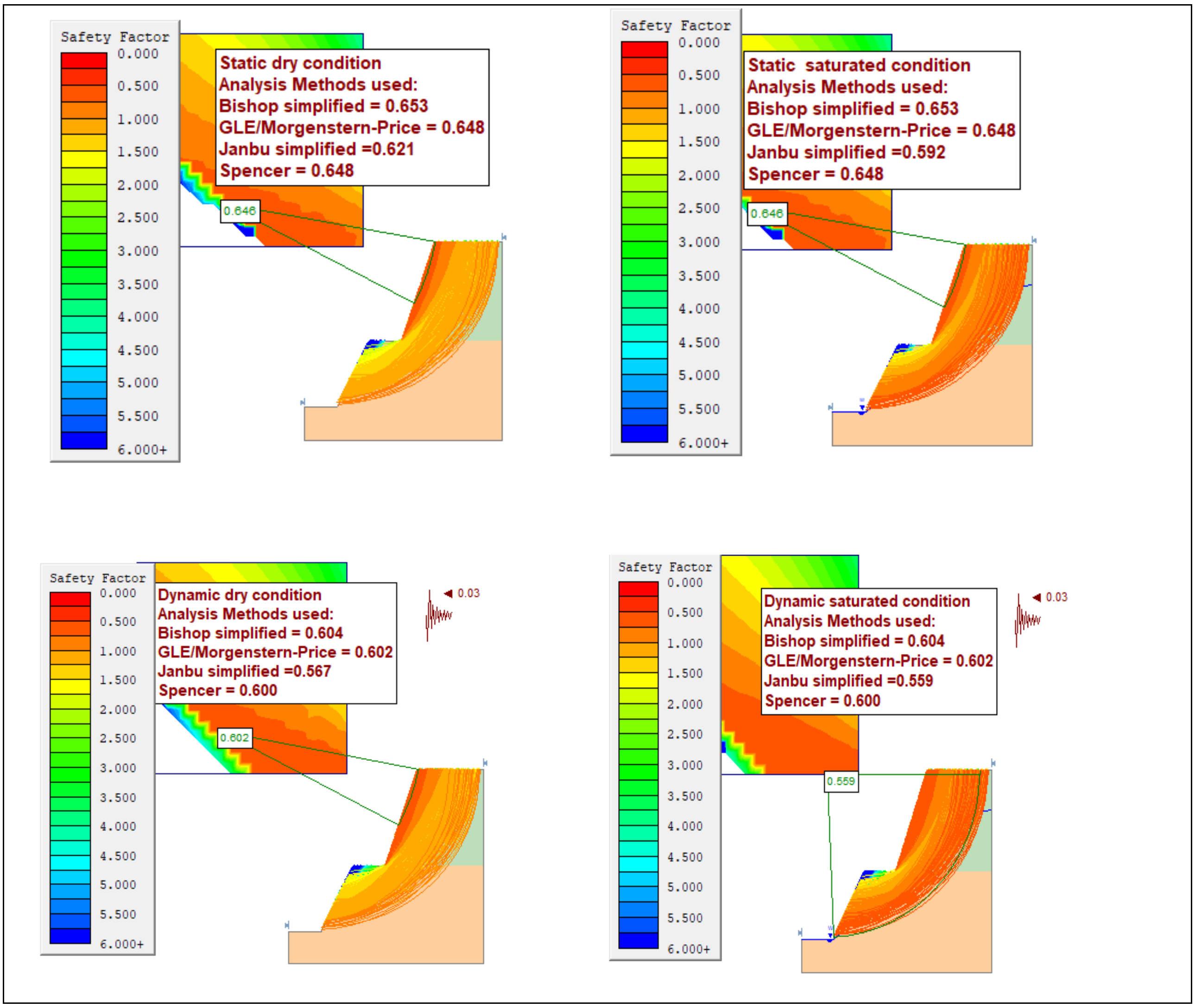

Figure 5. 18. Limit equilibrium analysis for heterogenous rock slope R3SS1(Soils - basalts) for a different condition

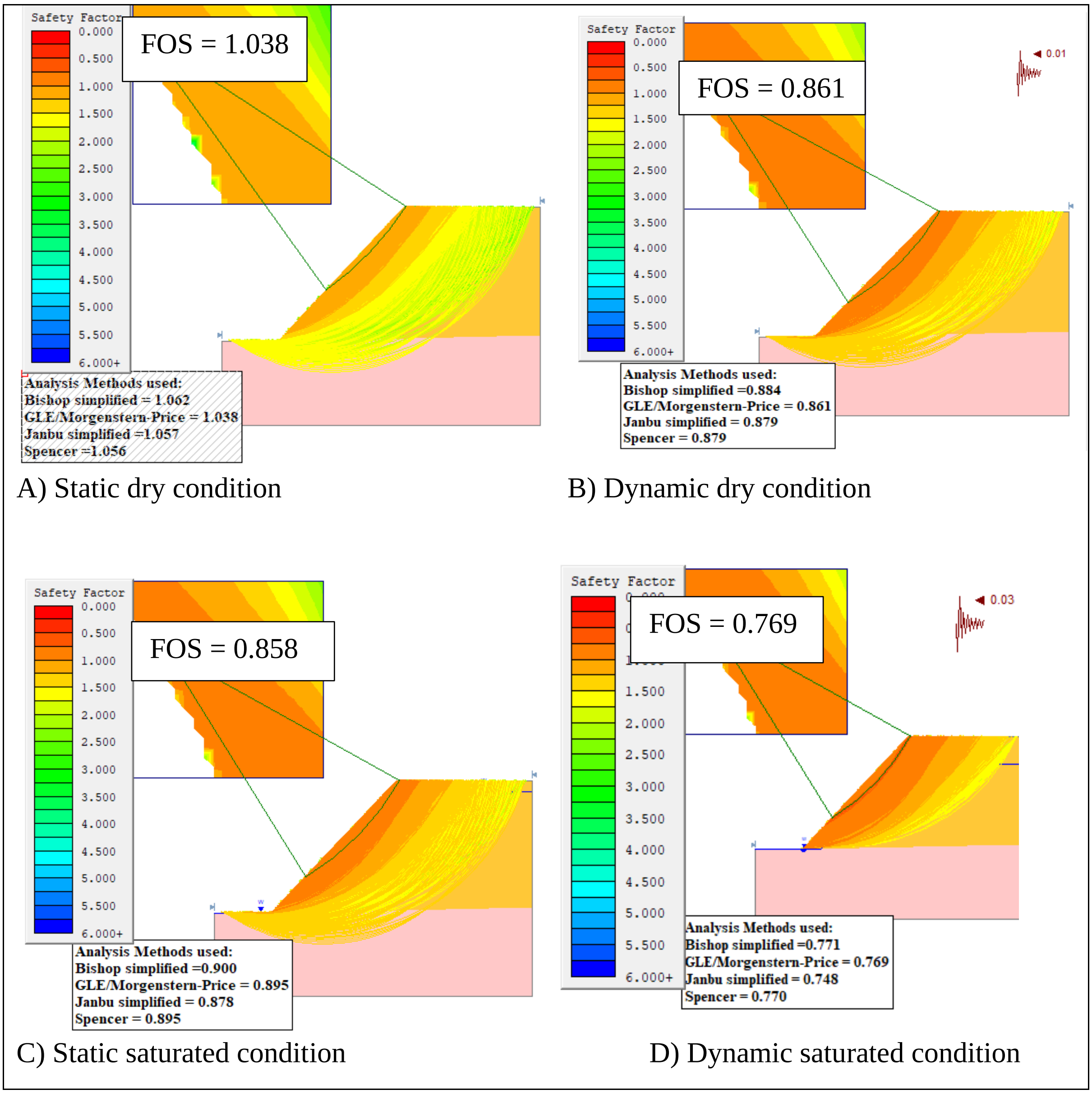

Figure 5. 19. Limit equilibrium analysis for heterogenous rock slope R5SS2 (silt sand soils – Alkali-olivine basalts) for a different condition

5.10 Homogenous soils slope section modelling using limit equilibrium methods

From field observations and surveys, two soils were identified as homogenous. These three slope sections were modeled using Slide software. The slope angles and heights of the two-slope section 58 degrees and 35 meters, and 65 degrees and 25 meters for SS1 and SS3, respectively. The model was conducted using four limit equilibrium methods. However, for the soil slope sections (SS1 and SS3), GEL/ Mongerstern-Price and Janbu simplified was selected respectively.

The two homogeneous soil slope section analysis results showed that the slopes were stable under static and dynamic dry conditions, but unstable under dynamic saturated conditions. The input parameter of these two homogeneous slope sections (rock and soils) were summarized in the Table 5.17.

Table 5. 17. The input parameter for soil slope stability analysis

Slope section ID	Types of soils	Shear strength parameter		Unit weight (KN/m^{3})	
		Cohesion (KN/m^{2})	Angle of internal friction (°)	γdry	γsat.
SS**1**	Silt clay	45.31	19.16	12.20	17.00
SS**3**	Silt clay	17.65	24.88	13.51	16.90

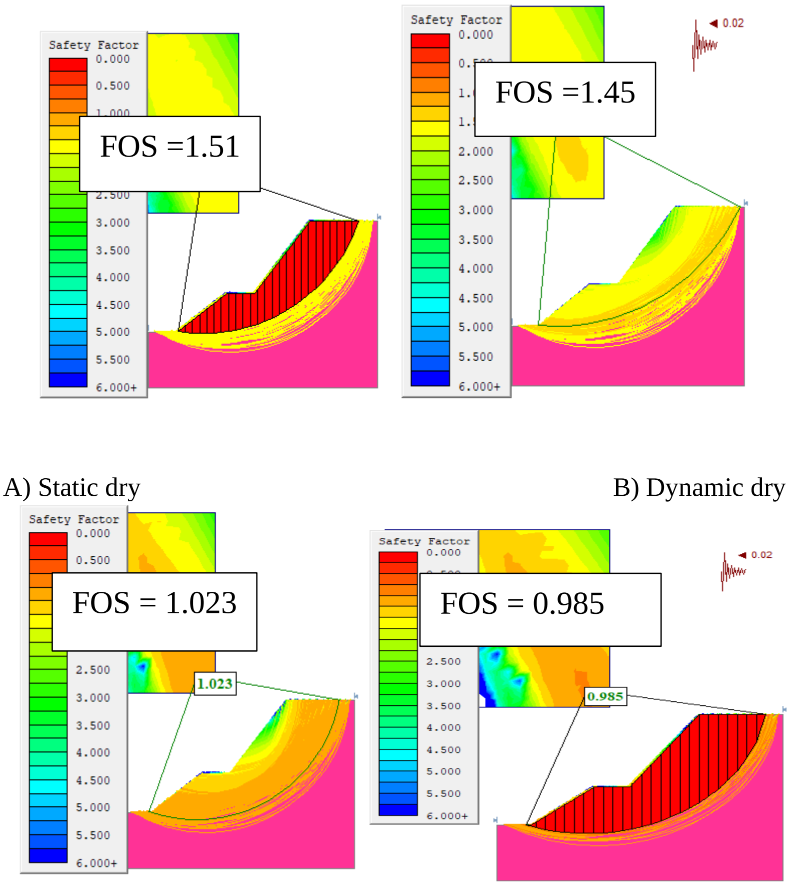

A) Static dry B) Dynamic dry

C) Static saturated condition D) Dynamic saturated condition

Figure 5. 20 Limit equilibrium analysis for homogenous soils slope SS1 (clay soils) for a different condition

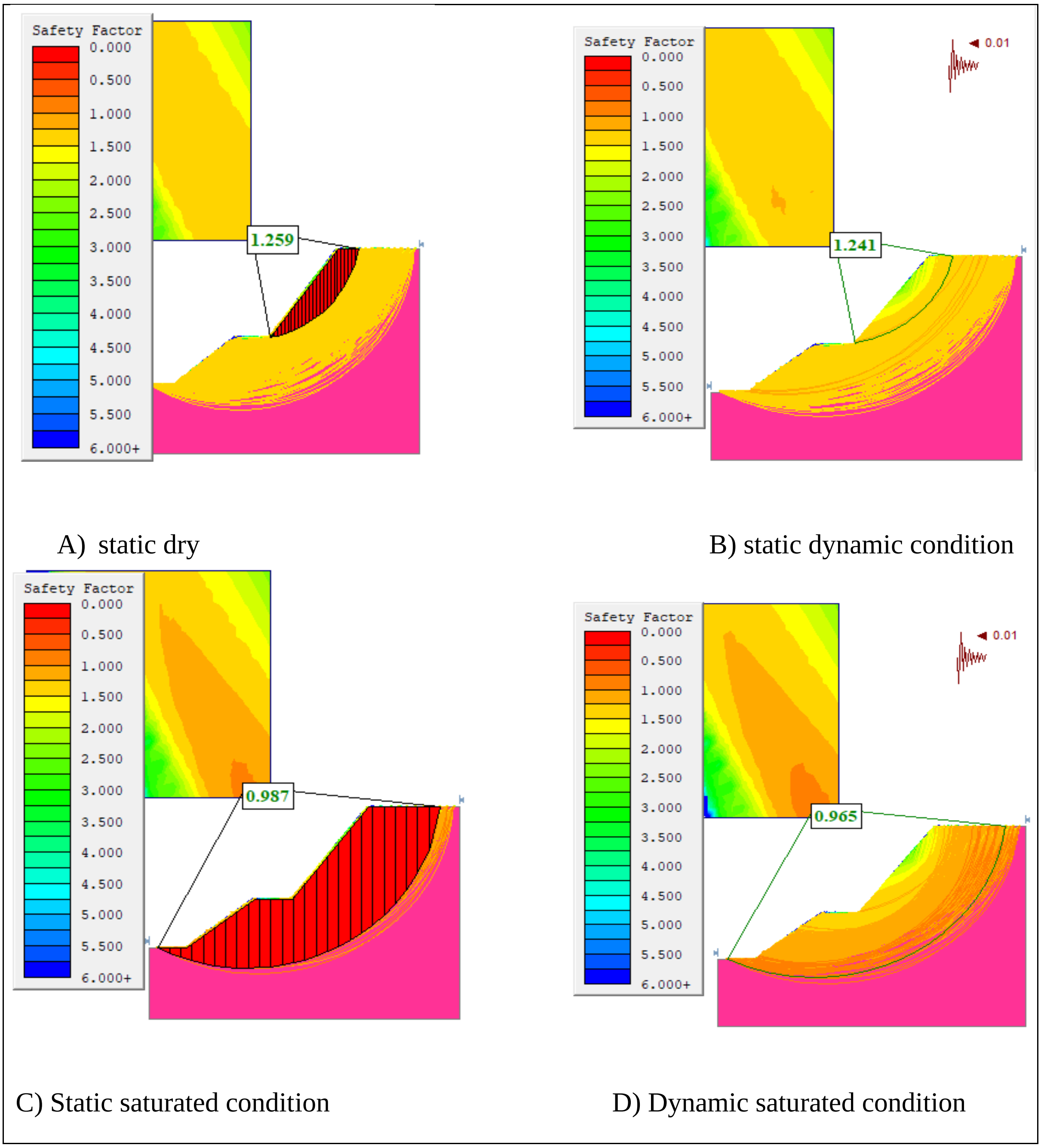

A) static dry

B) static dynamic condition

C) Static saturated condition

D) Dynamic saturated condition

Figure 5. 21. Limit equilibrium analysis for homogenous soils slope SS3 (Silt clay soils) for a different condition

5.11 Heterogenous and homogenous rock slope stability analysis using finite element methods

This modelling conducted on three different no-homogenous rock slope section and the homogenous rock slope section R4SS21 and the other slope section were soils slope section.

Table 5. 18. Input parameter for heterogenous rock slope stability analysis using finite element methods

Slope section ID	Materials types	c (MPa)	ϕ (°)	Erm (MPa)	V (μ)	Unit weight (KN/m^3)		α (g)
						γdry	γsat	
R_2SS_1	SC	0.073	34.96	1101.2	0.36	14.78	21.13	0.03
	MW-V. B	0.345	55.32	5469.1	0.288	24.48	26.91	0.03
	MW-A. B	0.405	58.15	4893.2	0.282	25.61	29.21	0.03
R_3SS_1	SW-B	0.515	57.86	7570.4	0.272	23.62	30.71	0.03
	Silt clay soils	0.0387	19.22	16	0.013	13.51	17.90	0.03
R_4SS_1	SW-IG	0.347	51.55	4487.3	0.321	22.03	28.89	0.03
R_5SS_2	SW-AOB	0.399	60.73	6776	0.28	25	29.95	0.03
	silt clayey soils	0.0185	24.88	8	0.098	13.51	16.90	0.03

5.11.1 Homogenous ignimbrite slope section (R4SS2)

This slope section was characterized as ignimbrite rock slope section with slope angle 78° with height 35m and 65° angle for the it profile. The analysis conducted in four different anticipated condition. The results of analysis shown that slope was unstable condition under all anticipated condition.

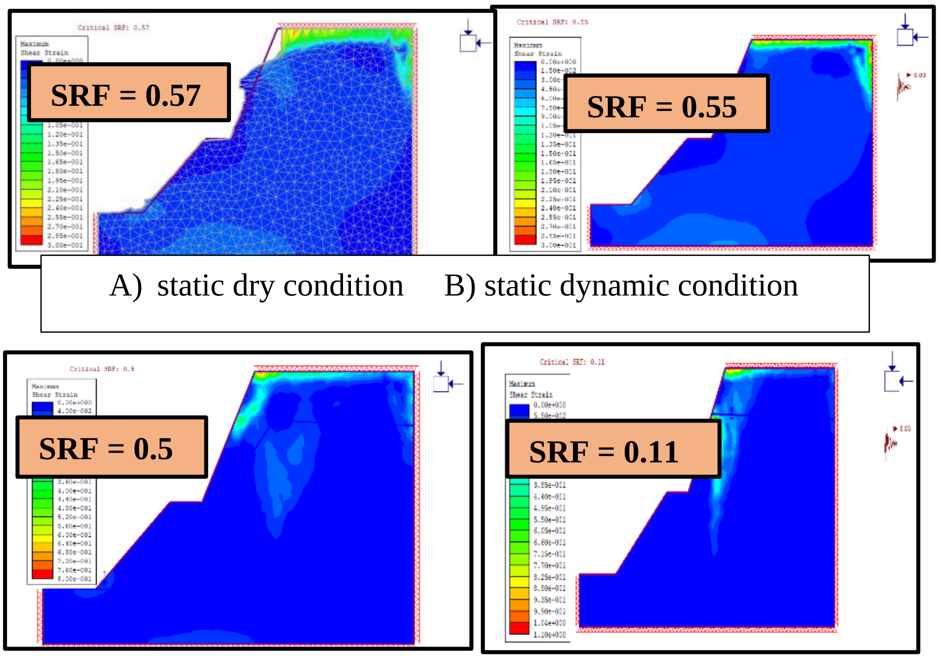

A) static dry condition B) static dynamic condition

C) Static saturated condition D) Dynamic saturated condition

Figure 5. 22. Factor of safety (Stress reduction factor) obtained for soil sample one (R3SS$_1$) by four different conditions using phase 2d software

5.11.2 Heterogeneous rock slope section with the soil base R2SS1

This rock slope section was heterogeneous and composed of different rock formations. The formations on this rock slope section, from bottom to top, were moderately aphanitic basalt, vesicular basalt, and scoria at the top. The slope angle was 65° and the height was 30m. There were two profiles with two benches and a gradient of 1H:1V. The results of the analysis showed that the slope was unstable in all anticipated conditions.

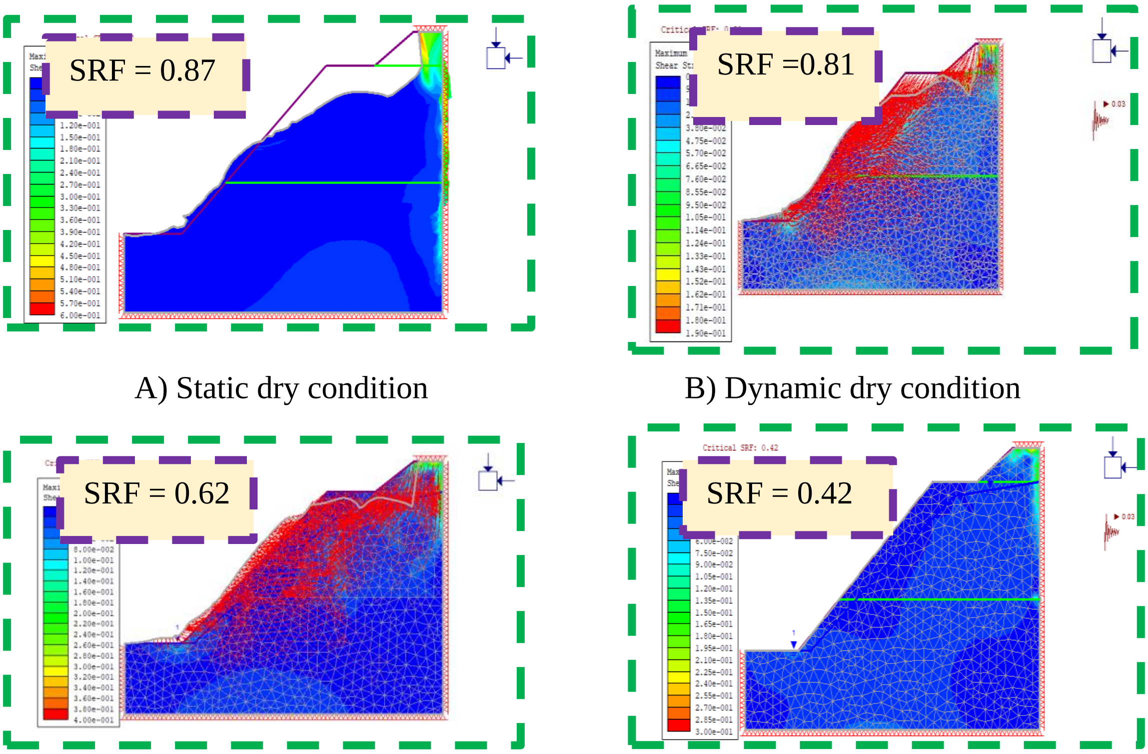

A) Static dry condition

B) Dynamic dry condition

C) Static saturated condition

D) Dynamic saturated condition

Figure 5. 23. Factor of safety (Stress reduction factor) obtained for soil sample one (R2SS1) by four different conditions using phase 2d software

5.11.3 Heterogeneous aphanitic basalts with soils layer at bottom of the slope section (R3SS1)

The slope heterogenous in formation slightly weathered aphanitic basalt with silt clay soils at bottom. The analysis results much lower SRF in all condition due that the slope unstable. The SRF 0.27, 0.23, 0.19 and 0.13 for static dry, dynamic dry, static saturated and dynamic saturated condition respectively.

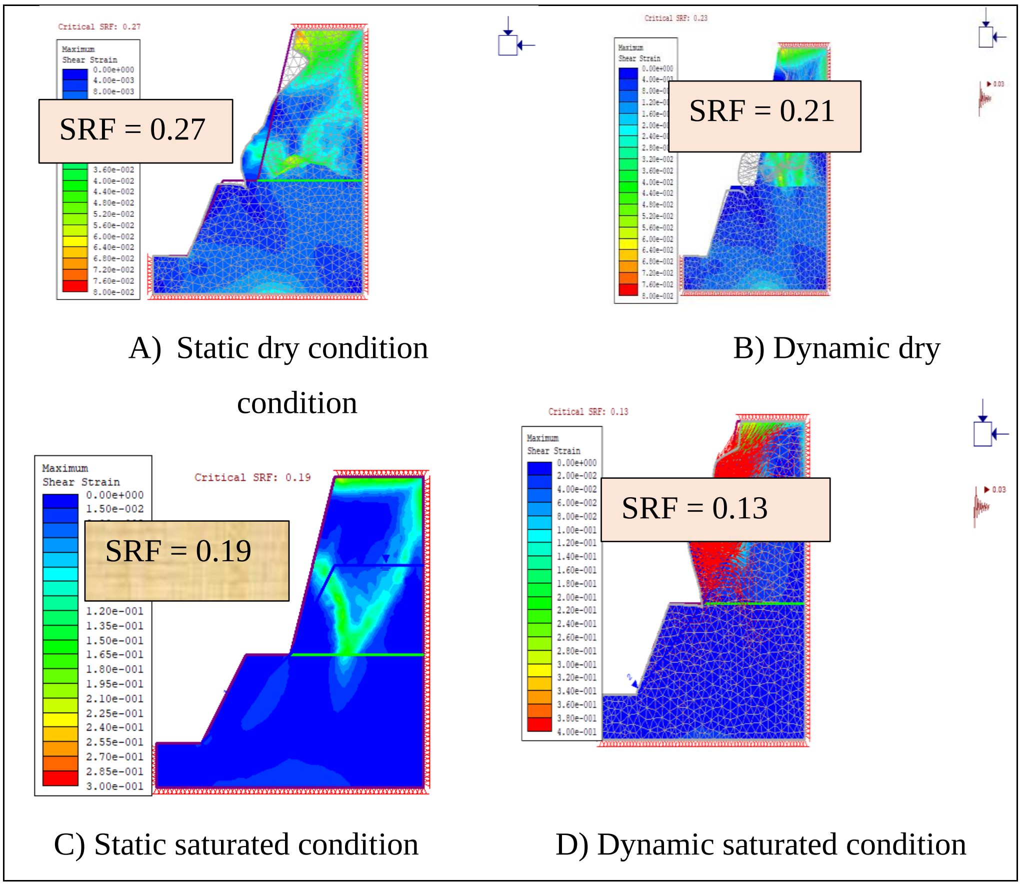

Figure 5. 24. Factor of safety (Stress reduction factor) obtained for soil sample one ($R3SS_1$) by four different conditions using phase 2d software

5.12 Homogenous soils slope stability analysis using finite element methods

In this study, four soil samples were collected. Two of them were from a homogeneous slope section, while the other two were from a slope section with a rock layer, making the soil properties heterogeneous. Additionally, the homogeneous soils were soil samples one and three, which were taken from moderately to high slope sections with slope angles of 65° and 68°, respectively. The summarized finite element methods input parameter of these two soil were showed in the Table 5.20 below. These parameter taken from laboratory test and emprical fromula. The shear parameter were determined by direct shear test in the laboratory and the poisson's ratio using equation

Table 5. 19. Input parameter for homogenous soils slope stability analysis using finite element methods

Slope section ID	Materials types	c (MPa)	ϕ (°)	Erm (MPa)	V (μ)	Unit weight (KN/m^3)		α (g)
						γdry	γsat	
SS1	Clay soils	0.045	19.16	8.8	0.013	12.20	17.00	0.03
SS3	Silt clay soils	0.018	24.88	7.92	0.073	13.51	16.890	0.03

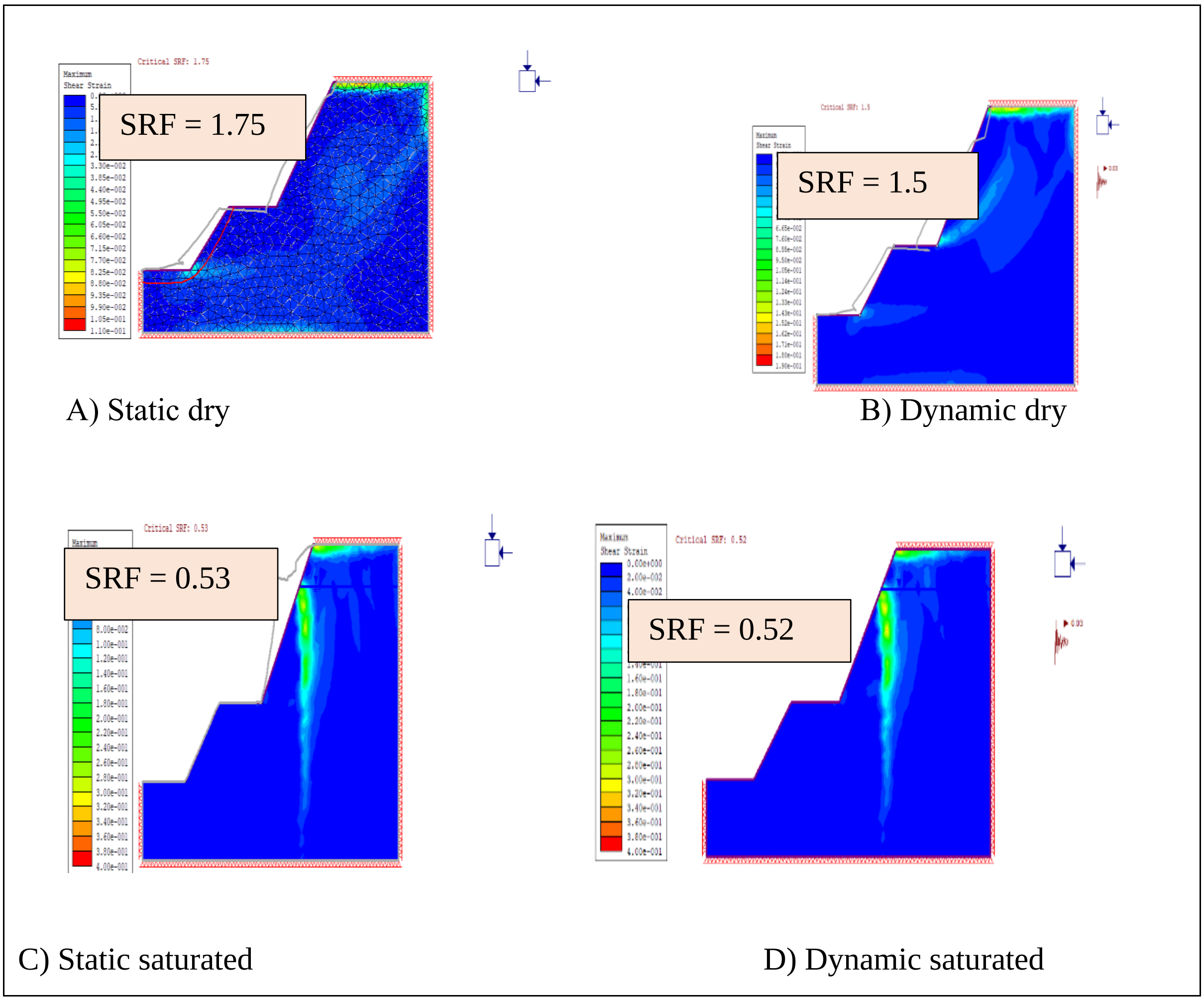

Figure 5. 25. Factor of safety (Stress reduction factor) obtained for soil sample one (SS_1) by four different conditions using phase 2d software

The analysis results indicate that the slope was stable under the first two conditions, namely static and dynamic dry. However, it was found to be unstable under the second two conditions, static and dynamic saturated, as shown in figures 5.23 a, b, c, and d. The minimum stress reduction factor for all conditions, including static dry, dynamic dry, static saturated, and dynamic saturated, were 1.75, 1.5, 0.53, and 0.52, respectively. The results show that the factors of safety obtained by static saturated and dynamic saturated were similar, as the effects of horizontal acceleration were low. The analysis revealed that when the slope is in a static saturated and dynamic saturated state, the critical SRF or FOS is less than one, indicating that the slope is unstable (Torabi-Kaveh et al., 2023b).

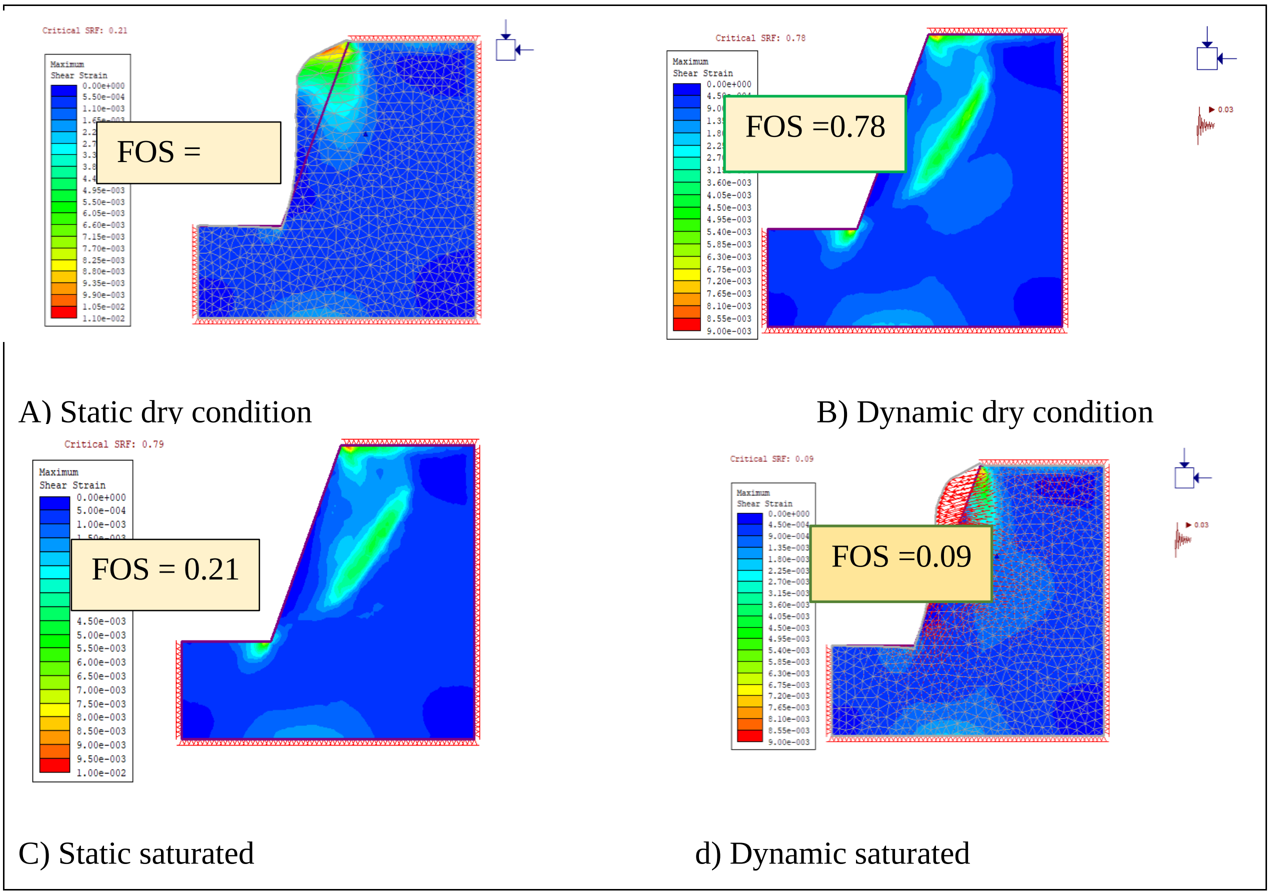

Figure 5. 26. Factor of safety (Stress reduction factor) obtained for soil sample one (SS2) by four different conditions using phase 2D software

Based on the analysis results, the soil slope showed an SRF value of less than one in all anticipated conditions, including static and dynamic dry conditions, as well as static and dynamic saturated conditions. The slope gradient was 1H:1V with an angle of 68°, and the SRF values for all conditions were 0.79, 0.78, 0.21, and 0.09. This revealed that the slope section under unstable condition

5.13 Comparison of LEM and FEM

The comparison of these two methods conduct depends on the results of analysis under four different condition viz. static and dynamic dry, static and dynamic saturated condition. The values of analysis results show that the slope section (R4SS2) was unstable in all condition except static dry condition. The dynamic saturated condition was less SRF for finite element methods. Similarly for analysis the FOS vs SRF decrease from static dry to dynamic saturated condition.

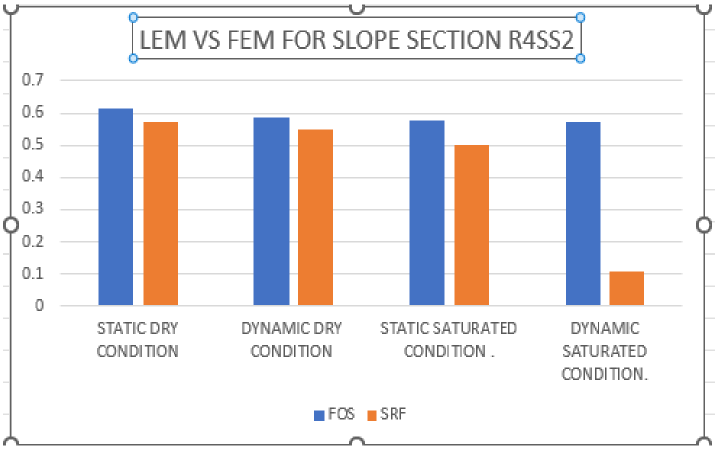

FOS	SRF
1.031	0.57
0.588	0.55
0.575	0.5
0.574	0.11

Figure 5. 27. Graphical comparison of LEM and FEM for R4SS2

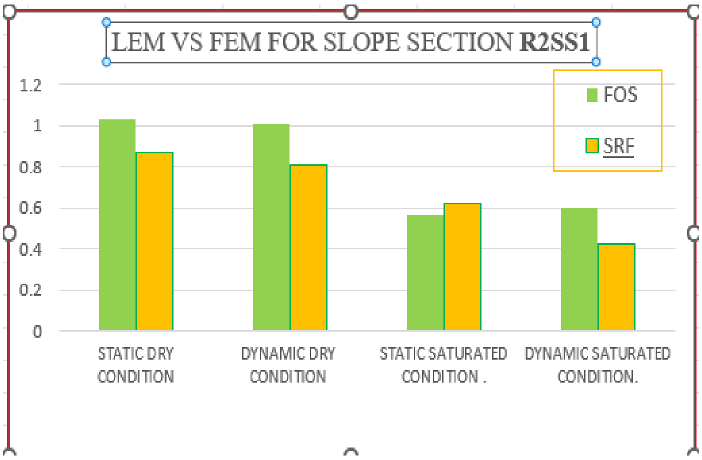

FOS	SRF
1.031	0.87
1.01	0.81
0.56	0.62
0.6	0.42

Figure 5. 28. Graphical comparison of LEM and FEM for R2SS1

FOS	SRF
0.643	0.27
0.635	0.21
0.593	0.19
0.59	0.13

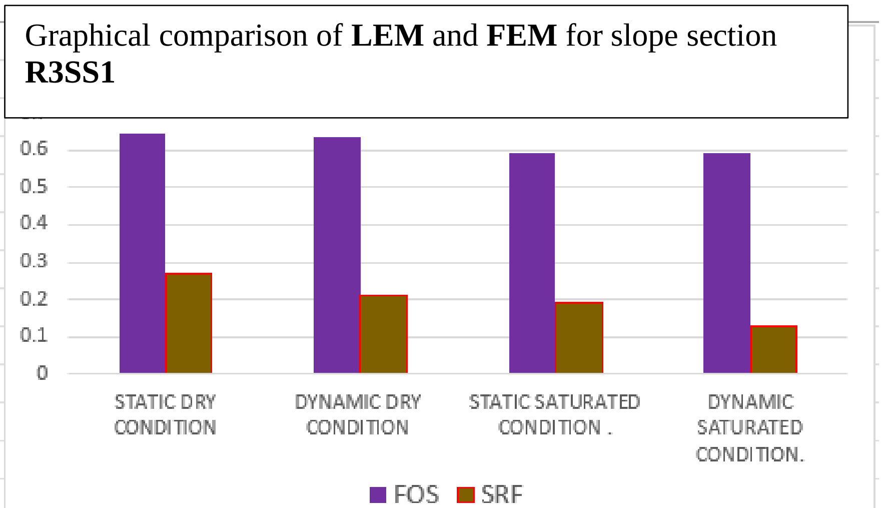

Figure 5. 29. Graphical comparison of LEM and FEM for R3SS1

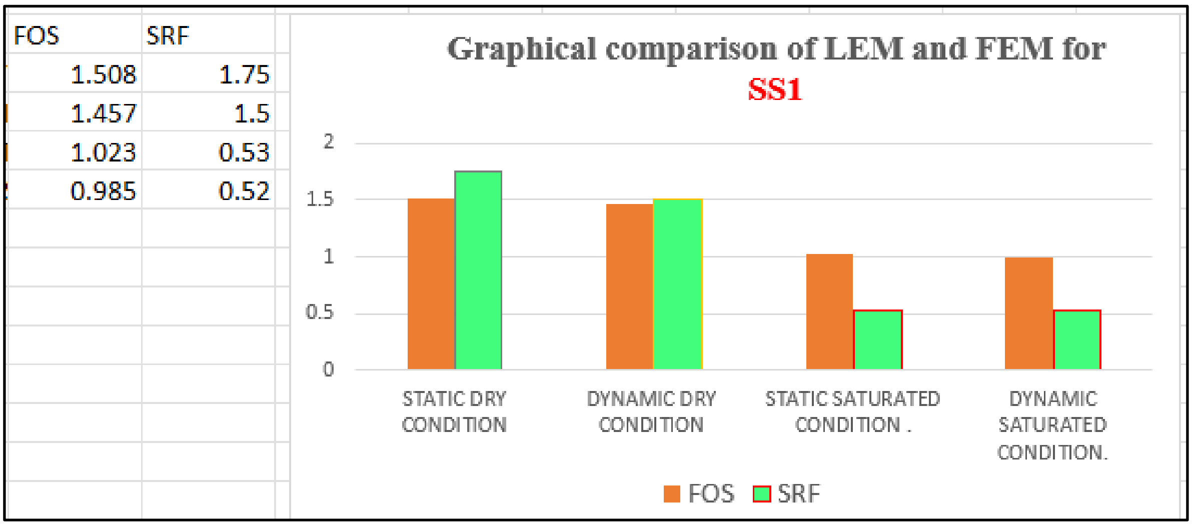

Figure 5. 30. Graphical comparison of LEM and FEM for SS1

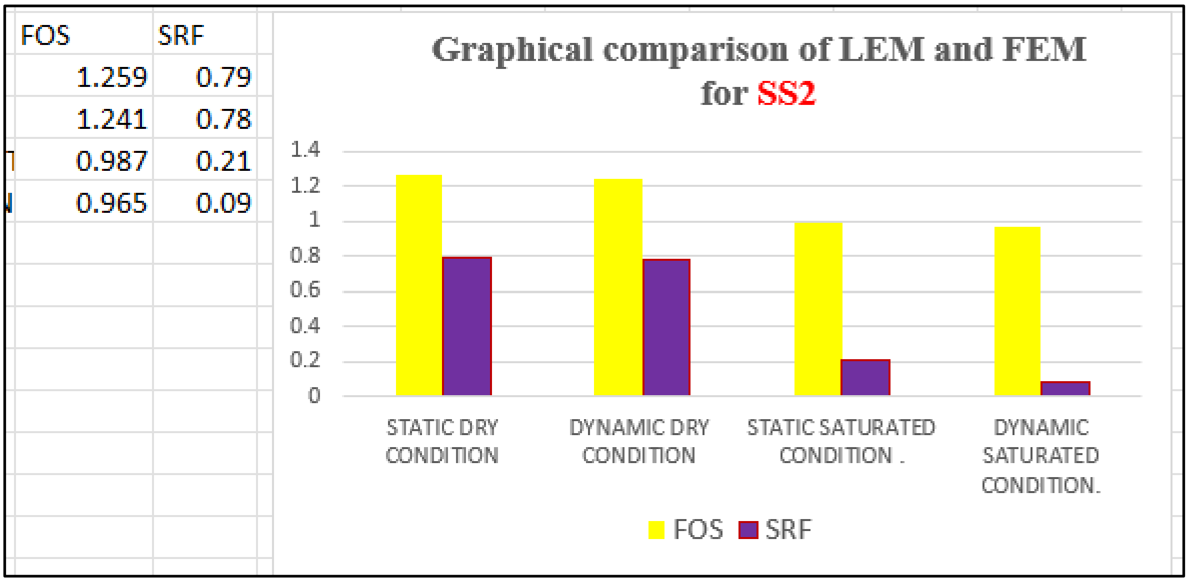

Figure 5. 31. Graphical comparison of LEM and FEM for SS2

5.14 REMEDIAL MEASURE

After conducting a field investigation and analyzing the results using selected methods, the study determined the actual stability condition of the slope and recommended three remedial measures. These measures include modifying the slope geometry, installing a well-designed drainage system, and constructing an engineering retaining structure to ensure the stability of the critical slope sections in the study area. According to (Kazmi, *et al* . 2017) surface protection and drainage, subsurface drainage, slope regarding, retaining structures, structural reinforcement, strengthening of slope-forming material, vegetation and bioengineering, removal of hazards and others are the remedial measures generally considered to stabilize unstable slope.

5.14.1 Adjustment of the shape and angle of a slope.

Th study area cross hill to steep landscape due the reason the most of the slope section were steep which cause instability due to gravity force of the material. According to Koca, (2023) the proposed solutions for modifying the geometry of a slope included remedial measures such as evaluating the impact of slope height, slope angle, and benching slope using slide software

5.14.2 Lowering of Slope Angle and Slope Height

In the study area, it was found that lowering the slope angle and height were crucial due to the high occurrence of slope instability. The stability of slopes can be impacted by changes in slope angle and height, as increasing these parameters can lead to an increase in shear stress on the potential failure plane while decreasing the shear strength (Zewdu, 2021). The analysis showed that slopes with high angles and heights had low FOS in static dry conditions, indicating that the slope angle itself impacts stability. Figure 5.25 demonstrates that as the slope angle decreases, the slope becomes more stable, resulting in an increase in FOS.

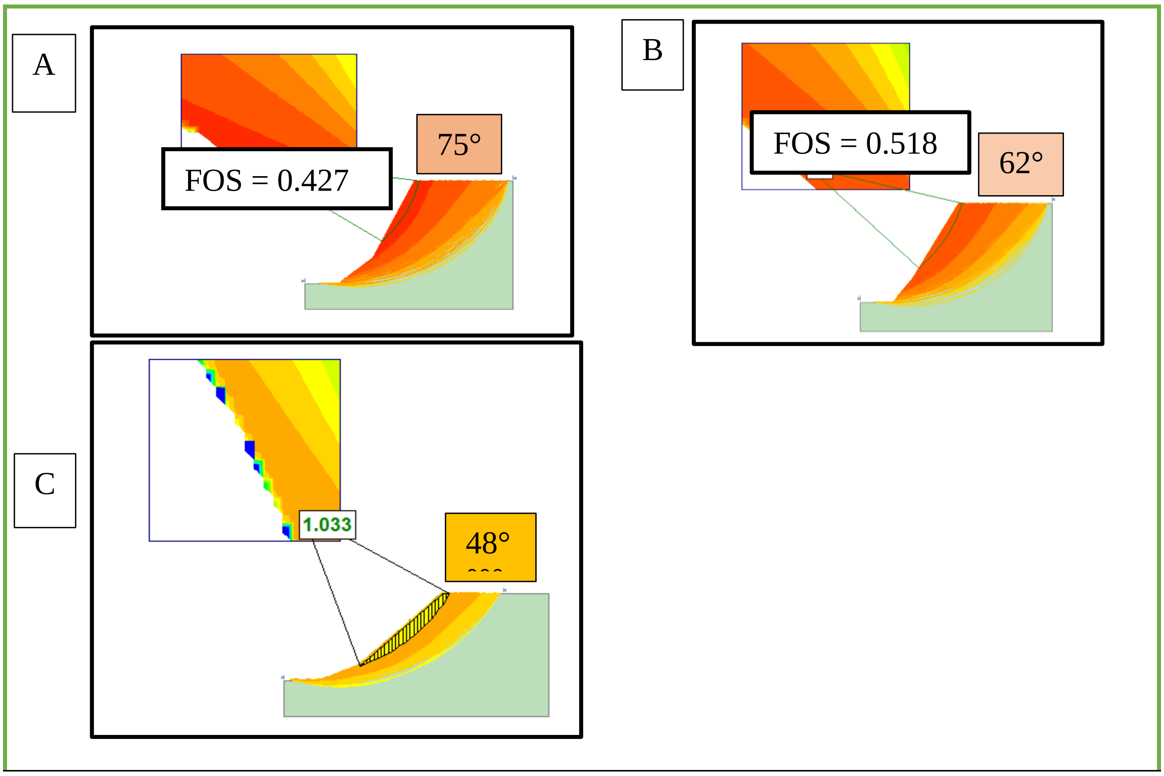

Figure 5. 32. Effects of slope angle on factor of safety (FOS) analysis using slide software, a) 75, b) 62 and c) 48

5.14.3 Benching the slope

Benching is a technique used to convert a steep slope into multiple smaller ones, and it is often used as a remedial measure for critical slope sections (Tiedeu et al., 2020). In this study, benching was conducted on the R3SS1 slope to increase the number of benches under worst-case scenarios, such as dynamic saturated conditions. The results of the factor of safety (FOS) analysis for three types of benching systems (bench one, two, and three) showed that the FOS increased from low to high as the number of benches increased. This indicates that the slope became more stable with an increase in the number of benching systems.

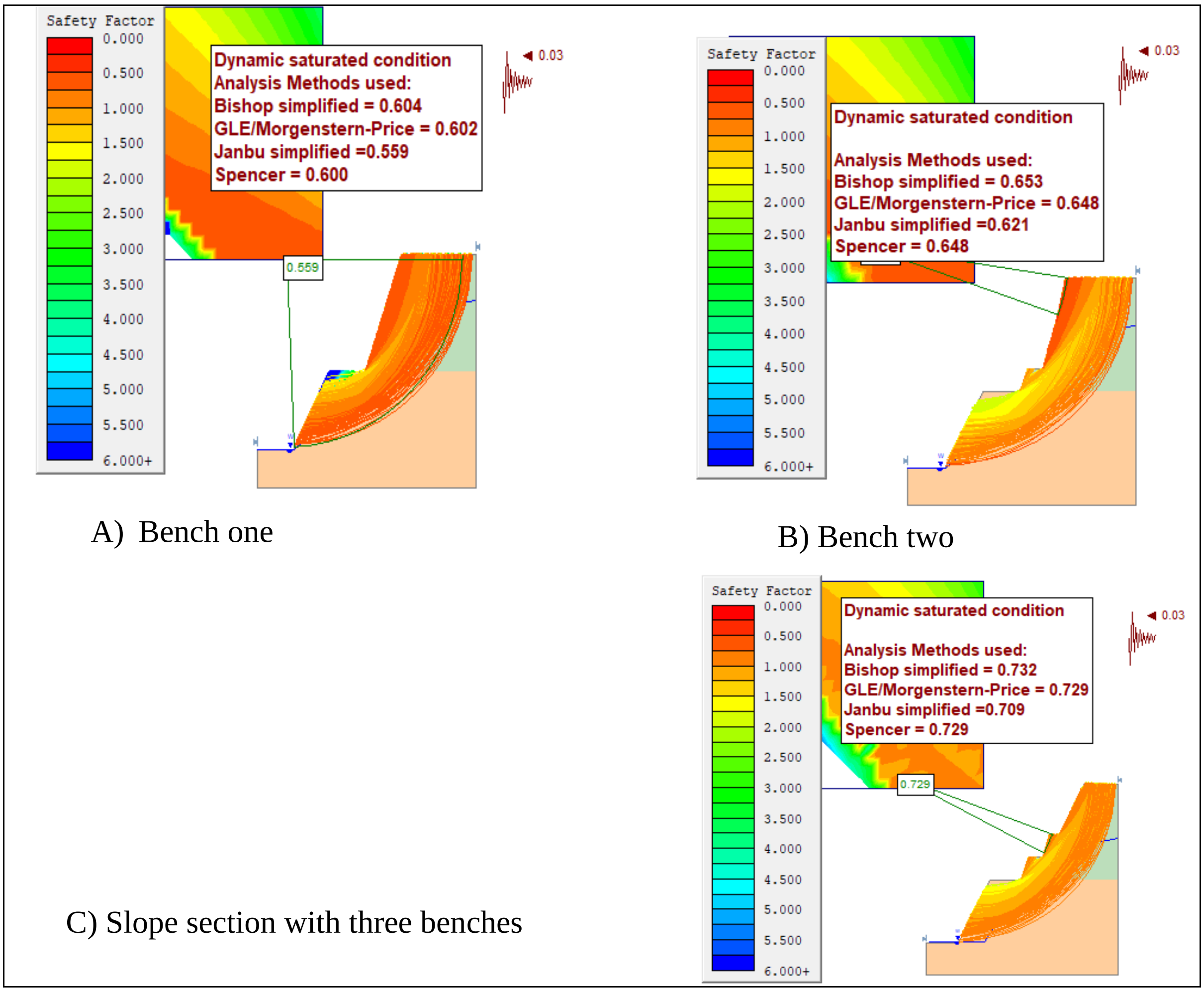

Figure 5. 33. Effects of benching on the critical slope section by using slide software

5.14.4 Installing a well-designed drainage system

In the study area, there was a poorly installed and designed drainage system that failed to prevent erosion problems during rainfall, leading to slope sliding. To mitigate these issues, provide surface drainage along the top side of the slide area from east to west and limiting runoff will be reduce the continuity of slope failure selected critical slope section from Agarfa town to Wabe river bridge.

CHAPTER SIX

CONCULUSSION AND RECOMMENDATION

CONCLUSION

The present study was carried out along the road Agarfa town to Wabe river bridge which connect the Bale with East Arsi zone. The area is located northern part of Bale zone which 30km from Robe bale town, Oromia region, southeastern Ethiopia. This road cross though steep slope to gentle which is greater occurrence of slope failure at the road-cut slope section. The local geology of my study categorized as basalt, and pyroclastic deposit.

From field surveying eight critical slope section viz two homogenous rock slope, three heterogenous rock with base soil and two homogenous soil slope was identified. The stability analyses were conducted for these critical slope section by different methods such as kinematic analysis, limit equilibrium, finite element methods, field surveying and rock mass classification. To determine the FOS of these critical slope section different software was undertaken. Furthermore, results of kinematic analysis done by dip software show that two planar mode failure occurred on R1SS2 slope section and one wedge. One planar and toppling mode of failure was identified on slope section R3SS1. After mode of failure identified was done the FOS of determine by Rockplane and swedge. The results of these two software that in all anticipated condition the rock slope section R3SS1 show less values which in interval of 0.73 to 0.47 for planar mode of failure and the slope section R1SS2 show that les FOS from the planar mode of failure along joint two (J2) show the slope was unstable in all condition and on J4 the slope was stable under static and dynamic dry condition but, unstable under static and dynamic saturated condition.

The parameter of the next two methods includes both from field survey and laboratory analysis. The slope orientation and in situ- strength test conducted by Schmidt hammer in the field, and laboratory test was conducted for both rock and soils. For soils shear parameter was done by direct shear test and unit weight from remolded soils. The unit weight of rock done by buoyancy techniques. In additionally the FOS and SRF for homogenous, heterogamous rock slope section and soil was done by determistic (slide software) and finite element method (Phase 2d software). Thes results of these all-analysis show that the FOS and SRF for critical slope section decrease from static dry to dynamic saturated condition. From those result the study area more prone by groundwater variation when correlate with dynamic since the dynamic force less.

6.2 RECOMMENDATION

From the present study's results and findings, the following recommendations were formulated:

The study area passes through hill to steep slope section and highly affect by poor drainage due the reason the area requires well designed drainage system. As shown in the remedial measure the slope height was very crucial for the occurrence of the stability problems to reduce this cause benching and reshaping the slope geometry was recommended. Especial rock slope section R3SS1 of the study and well-designed engineering structure and reinforcement was recommended on the R2SS1 rock slope section. The combination of two or three methods with engineering and economic consideration is highly recommended.

RESEARCH FUND ACKNOWLEDGMENT

This research project is found by Adama Science and Technology University under grant number ASTU/SM-R/699/23, Adama, Ethiopia.

REFERENCES

Aksoy, H., & Ercanoglu, M. (2007). Fuzzified kinematic analysis of discontinuity-controlled rock slope instabilities. Engineering Geology, 89(3–4), 206–219.

Aleumu, T., & Abebe, T. (2007). Geology and tectonic evolution of the Pan African Tulu Dimtu Belt, Western Ethiopia. Online Journal of Earth Sciences, 1(1), 24–42.

Anbalagan, R., Chakraborty, D., & Kohli, A. (2008). Landslide hazard zonation (LHZ) mapping on meso-scale for systematic town planning in mountainous terrain.

Aryal, K., Sandven, R., & Nordal, S. (2005). Slope stability evaluation by limit equilibrium and finite element methods. In Proceedings of the 16th International Conference on Soil Mechanics and Geotechnical Engineering: Geotechnology in Harmony with the Global Environment (Vol. 4).

Asfaw, L. M., & Woldeyes, G. (1986). Catalogue of Ethiopian earthquakes, earthquake parameters, strain release and seismic risk. Geophysical Observatory, Faculty of Science, Addis Ababa University.

Aydin, A. (2014). ISRM suggested method for determination of the Schmidt hammer rebound hardness: Revised version. The ISRM suggested methods for rock characterization, testing and monitoring: 2007-2014, 25–33.

Azarafza, M., Bonab, M. H., & Akgün, H. (2021). Numerical analysis and stability assessment of complex secondary toppling failures: A case study for the South Pars Special Zone. Geomechanics and Engineering, 27(5), 481–495. https://doi.org/10.12989/gae.2021.27.5.481.

Barton, N., & Choubey, V. (1977). The shear strength of rock joints in theory and practice. Rock Mechanics, 10, 1–54.

Bayou, N. B. (2020). Evaluation of slope stability conditions by numerical analysis, a case of Otolo-Sawla Asphalt Road Project, Southern Part of Ethiopia.

Bekele, A. (2022). Slope stability analysis along selected road sections between Mertule Maryam and Mekane Selam Town, Upper Blue Nile Basin, Central Ethiopia. August.

Bekele, A., & Meten, M. (2022). Modeling rock slope stability using kinematic, limit equilibrium, and finite-element methods along Mertule Maryam–Mekane Selam Road, Central Ethiopia. Modeling Earth Systems and Environment.

https://doi.org/10.1007/s40808-022-01563-8

Bieniawski, Z. T. (1974). Geomechanics classification of rock masses and application in tunneling. Proc., 3rd Int. Cong. Rock Mechanics, 27–32.

Bieniawski, Z. T., & Hawkes, I. (1978). Suggested methods for determining tensile strength of rock materials. International Journal of Rock Mechanics and Mining Sciences, 15(3), 99–103.

Billi, P. (2015). World geomorphological landscapes: Landscapes and landforms of Ethiopia. http://www.springer.com/series/10852

Bogaard, T. A., & Greco, R. (2016). Landslide hydrology: From hydrology to pore pressure. Wiley Interdisciplinary Reviews: Water, 3(3), 439–459.

Broch, E., & Franklin, J. A. (1972). The point-load strength test. International Journal of Rock Mechanics and Mining Sciences, 9(6), 669–676. https://doi.org/10.1016/0148-9062(72)90030-7

Bushira, K. M., Gebregiorgis, Y. B., Verma, R. K., & Sheng, Z. (2018). Cut soil slope stability analysis along National Highway at Wozeka–Gidole Road, Ethiopia. Modeling Earth Systems and Environment, 4, 591–600.

Cao, Z., Wang, Y., & Li, D. (2016). Probabilistic approaches for geotechnical site characterization and slope stability analysis. In Probabilistic Approaches for Geotechnical Site Characterization and Slope Stability Analysis. https://doi.org/10.1007/978-3-662-52914-0

Chala, T. (2017). Integrated geological and geophysical studies to investigate the landslide zones and study its impact: A case along the road section within Kurar Kebele, Dejen Woreda, Central Ethiopia. Addis Ababa University, Addis Ababa, Ethiopia.

Chopra, M., & Arboleda-Monsalve, L. G. (2020). Comparison of standard penetration test (SPT) N-value with alternative field test methods in determining moduli for settlement predictions.

Çobanoğlu, I., & Çelik, S. B. (2008). Estimation of uniaxial compressive strength from point load strength, Schmidt hardness, and P-wave velocity. Bulletin of Engineering Geology and the Environment, 67(4), 491–498. https://doi.org/10.1007/s10064-008-0158-x.

DH Consult & Golder Associates UK Ltd. (2021). The Federal Democratic Republic of

Ethiopia Ministry of Water and Energy Consultancy Service for Hydrogeological Mapping Using Remote Sensing, GIS and Geophysical Surveying Procurement Reference Number: Developing Groundwater Potential Map of 14.1125149.

Dhar, A. S. (1996). Behaviour of unplugged pipe piles in granular soil.

Durrani, A. J. (2005). The Kashmir earthquake of October 8, 2005: A quicklook report.

Dyson, A. P., & Tolooiyan, A. (2020). Comparative approaches to probabilistic finite element methods for slope stability analysis. Simulation Modelling Practice and Theory, 100, 102061. https://doi.org/10.1016/j.simpat.2019.102061

Equilibrium, L. (2017). Sechura Desert, Northern Peru: Sechura Desert, Northern Peru Olmos Water Conveyance and Irrigation Project, 433, 1–25.

Erener, A., & Düzgün, H. S. B. (2010). Improvement of statistical landslide susceptibility mapping by using spatial and global regression methods in the case of More and Romsdal (Norway). Landslides, 7, 55–68.

Fredlund, D. G., & Krahn, J. (1977). Comparison of slope stability methods of analysis. Canadian Geotechnical Journal, 14(3), 429–439. https://doi.org/10.1139/t77-045

Giannecchini, R., Naldini, D., Avanzi, G. D., & Puccinelli, A. (2007). Modelling of the initiation of rainfall-induced debris flows in the Cardoso Basin (Apuan Alps, Italy). Quaternary International, 171, 108–117.

Göktepe, F., & Keskin, I. (2018). A comparison study between traditional and finite element methods for slope stability evaluations. Journal of the Geological Society of India, 91(3), 373–379. https://doi.org/10.1007/s12594-018-0864-3

Goodman, Y. M. (1989). Roots of the whole-language movement. The Elementary School Journal, 90(2), 113–127.

Habtamu, M., Garo, T., Chemeda, Y. C., & Info, A. (2022). Engineering geological investigation of Jimma Town for engineering practice, 9(1).

Habtemariam, B. G., Shirago, K. B., & Dirate, D. D. (2022). Effects of soil properties and slope angle on deformation and stability of cut slopes. Advances in Civil Engineering, 2022. https://doi.org/10.1155/2022/4882095

Hoek, E., & Bray, J. D. (1981). Rock slope engineering. CRC Press.

Hoek, E., Kaiser, P. K., & Bawden, W. F. (1995). Rock mass rating. In Support of Underground Excavations in Hard Rock (pp. 34–37).

Hoek, E., Kaiser, P. K., & Bawden, W. F. (2000). Support of Underground Excavations in Hard Rock.

Hussain, G., Singh, Y., Bhat, G. M., Sharma, S., Sangra, R., & Singh, A. (2019). Geotechnical characterisation and finite element analysis of two landslides along the National Highway 1-A (Ladakh region, Jammu and Kashmir). Journal of the Geological Society of India, 94, 93–99.

Kabeta, W. F., Teshager, D. K., & Danie, K. T. (2020). Assessments of geotechnical conditions and slope stability analysis: Case study in Gedo Town, Ethiopia. International Journal of Scientific Research & Engineering Trends, 6(3), 1250–1258.

Kadakci Koca, T., & Koca, M. Y. (2020). Comparative analyses of finite element and limit-equilibrium methods for heavily fractured rock slopes. Journal of Earth System Science, 129(1), 49.

Kahraman, S. (2001). Evaluation of simple methods for assessing the uniaxial compressive strength of rock. International Journal of Rock Mechanics and Mining Sciences, 38(7), 981–994. https://doi.org/10.1016/S1365-1609(01)00039-9

Kazmi, D., Qasim, S., Harahap, I., & Irfan, F. (2017). Slope remediation techniques and overview of landslide risk management. April. https://doi.org/10.28991/cej-2017-00000084

Kazmi, D., Qasim, S., Harahap, I. S., Baharom, S., Mehmood, M., Siddiqui, F. I., & Imran, M. (2017). Slope remediation techniques and overview of landslide risk management. Civil Engineering Journal, 3(3), 180–189. https://doi.org/10.28991/cej-2017-00000084

Khanna, R., & Dubey, R. K. (2021). Comparative assessment of slope stability along road-cuts through rock slope classification systems in Kullu Himalayas, Himachal Pradesh, India. Bulletin of Engineering Geology and the Environment, 80(2), 993–1017. https://doi.org/10.1007/s10064-020-02021-4

Khursheed, A., & Sharma, A. (2020). A comparative study of slope stability methods using geotechnical software Geo5. International Research Journal of Modernization in Engineering, 01, 1121–1127. www.irjmets.com.

Kiros, T., Supervisors, M., Wohnlich, S., & Alber, I. M. (2020). Failure mechanisms and stability analysis of deep-seated landslides in the northwestern rift escarpment, Ethiopia.

Koca, T. K. (2023). The effect of geometrical features of release surfaces on the stability of tectonically disturbed deep rock slopes in an albite open pit mine. Sustainability, 15(2), 1425.

Komadja, G. C., Pradhan, S. P., Roul, A. R., Adebayo, B., Habinshuti, J. B., Glodji, L. A., & Onwualu, A. P. (2020). Assessment of stability of a Himalayan road cut slope with varying degrees of weathering: A finite-element-model-based approach. Heliyon, 6(11). https://doi.org/10.1016/j.heliyon.2020.e05297

Kumar, A., Mrinal, G., & Mukherjee, K. (2022). Evaluating road-cut slope stability using newly proposed stability charts and rock microstructure: An example from Dharasu-Uttarkashi roadway, Lesser Himalayas, India. Rock Mechanics and Rock Engineering, 55(7). Springer Vienna. https://doi.org/10.1007/s00603-022-02846-3.

Kundu, J., Sarkar, K., Singh, P. K., & Singh, T. N. (2018). Deterministic and probabilistic stability analysis of soil slope – A case study. Journal of the Geological Society of India, 91(4), 418–424. https://doi.org/10.1007/s12594-018-0874-1

Lamessa, G. (2019). Slope stability analyses along selected road section from Gutane Migiru town to Fincha'a Sugar Factory, Oromiya, Western Ethiopia. Addis Ababa Science and Technology University, Master's thesis, 1–130.

Lee, L. M., Gofar, N., & Rahardjo, H. (2009). A simple model for preliminary evaluation of rainfall-induced slope instability. Engineering Geology, 108(3–4), 272–285. https://doi.org/10.1016/j.enggeo.2009.06.011

Liang, W.-L. (2020). Dynamics of pore water pressure at the soil–bedrock interface recorded during a rainfall-induced shallow landslide in a steep natural forested headwater catchment, Taiwan. Journal of Hydrology, 587, 125003.

Lógó, B. A., & Vásárhelyi, B. (2019). Estimation of the Poisson's rate of the intact rock in the function of the rigidity. Periodica Polytechnica Civil Engineering, 63(4), 1030–1037.

Loka, W. P., Sumadja, W. A., & Resmi. (2017). Journal of Chemical Information and Modeling, 21(2), 1689–1699. https://www.oecd.org/dac/accountable-effective-institutions/governance-notebook-2.6-smoke.pdf

Marinos, P. G., Marinos, V., & Hoek, E. (2007). The Geological Strength Index (GSI): A characterization tool. Proceedings of the International Workshop on Rock Mass Classification in Underground Mining, 9498, 87.

Maula, B. H., & Zhang, L. (2011). Assessment of embankment factor safety using two commercially available programs in slope stability analysis. Procedia Engineering, 14, 559–566. https://doi.org/10.1016/j.proeng.2011.07.070

Mebrahtu, T. K., Heinze, T., Wohnlich, S., & Alber, M. (2022). Slope stability analysis of deep-seated landslides using limit equilibrium and finite element methods in Debre Sina area, Ethiopia. Bulletin of Engineering Geology and the Environment, 81(10). https://doi.org/10.1007/s10064-022-02906-6

Memon, Y. (2018). A comparison between limit equilibrium and finite element methods for slope stability analysis. Missouri University of Science & Technology, Rolla, Missouri, December, 1–18.

Mengesha Tefera, T. C., & Haro, W. (1996). Explanation of the Geological map of Ethiopia. Ministry of Mines and Energy, EIGS. Bull, 3.

Mite, H. W., Quezon, P. E. T., & Abebe, T. (2020). A study on the slope instability problems and mitigation measures for the road failure from Gebre Guracha to Lumame road segment. 8(10), 411–423.

Molla, S. (2011). School of Graduate Studies Faculty of Science slope stability analysis on a selected slope section along the road Gohatsion-Dejen. June.

Palmstrom, A. (1982). The volumetric joint count—A useful and simple measure of the degree of rock mass jointing. International Association of Engineering Geology. International Congress, 4, 221–228.

Pantelidis, L. (2009). Rock slope stability assessment through rock mass classification systems. International Journal of Rock Mechanics and Mining Sciences, 46(2), 315–325.

Park, H.-J., West, T. R., & Woo, I. (2005). Probabilistic analysis of rock slope stability and random properties of discontinuity parameters, Interstate Highway 40, Western North Carolina, USA. Engineering Geology, 79(3–4), 230–250.

Park, H., & West, T. R. (2001). Development of a probabilistic approach for rock wedge failure. Engineering Geology, 59(3–4), 233–251.

Popescu, M. E., & Sasahara, K. (2009). Engineering measures for Landslide Disaster Mitigation. Landslides - Disaster risk reduction, 609–631. Https://Doi.Org/10.1007/978-3-540-69970-5_32.

Pun, W. K., & Urciuoli, G. (2008). Soil nailing and subsurface drainage for slope stabilization. In Landslides and Engineered Slopes. From the Past to the Future, Two Volumes+ CD-ROM (pp. 107–148). CRC Press.

Rasti, A., Pineda, M., & Razavi, M. (2020). Assessment of soil moisture content measurement methods: Conventional laboratory oven versus halogen moisture analyzer. Journal of Soil and Water Science, 4(1), 151–160.

R. K, Umrao., Singh, R., Ahmad, M., & Tn, S. (2011). Stability analysis of cut slopes using continuous slope mass rating and kinematic analysis in Rudraprayag District, Uttarakhand. Geomaterials, 2011.

Salmanfarsi, A. F., Awang, H., & Ali, M. I. (2020). Rock mass classification for rock slope stability assessment in Malaysia: A review. IOP Conference Series: Materials Science and Engineering, 712(1), 12035.

Sarkar, S., & Chakraborty, M. (2021). Stability analysis for two-layered slopes by using the strength reduction method. International Journal of Geo-Engineering, 12(1). https://doi.org/10.1186/s40703-021-00153-4.

Satyanarayana, I., Budi, G., & Murmu, S. (2021). Stability analysis of a deep highwall slope using numerical modelling and statistical approach—A case study. Arabian Journal of Geosciences, 14(3). https://doi.org/10.1007/s12517-021-06476-x

Shahien, M. M. (1998). Settlement of structures on granular soils subjected to static and earthquake loads. University of Illinois at Urbana-Champaign.

Sharma, M., Sharma, S., Kumar, M., & Singh, S. K. (2019). Analysis of slope stability of road cut slopes of Srinagar, Uttarakhand, India. International Journal of Applied Engineering Research, 14(3), 609–615. http://www.ripublication.com

Siddque, T., & Pradhan, S. P. (2018). Stability and sensitivity analysis of Himalayan road cut debris slopes: An investigation along NH-58, India. Natural Hazards, 93, 577–600.

Singh, H. O., Ansari, T. A., Singh, T. N., & Singh, K. H. (2020). Analytical and numerical stability analysis of road cut slopes in Garhwal Himalaya, India. Geotechnical and Geological Engineering, 38, 4811–4829.

Stead, D., Eberhardt, E., & Coggan, J. S. (2006). Developments in the characterization of complex rock slope deformation and failure using numerical modelling techniques. Engineering Geology, 83(1–3), 217–235.

Tiedeu, W. N., Jiang, D., Chen, J., & Fan, J. (2020). A review on rock slope stability: Failure mechanisms, stabilization techniques and implications for mining engineering. Geotechnical Engineering, 51(4).

Tiwari, V. N., Pandey, V. H. R., Kainthola, A., Singh, P. K., Singh, K. H., & Singh, T. N. (2020). Assessment of Karmi landslide zone, Bageshwar, Uttarakhand, India. Journal of the Geological Society of India, 96, 385–393.

Torabi-Kaveh, M., Mehrnahad, H., Mohammadi, S., & Moosavizadeh, S. M. A. (2023a). Application of kinematic and distinct element methods to investigate instability mechanism of rock slopes containing weak and hard layers. Modeling Earth Systems and Environment, 1–14.

Torabi-Kaveh, M., Mehrnahad, H., Mohammadi, S., & Moosavizadeh, S. M. A. (2023b). Application of kinematic and distinct element methods to investigate instability mechanism of rock slopes containing weak and hard layers. Modeling Earth Systems and Environment. https://doi.org/10.1007/s40808-022-01672-4

Ullah, S., Khan, M. U., & Rehman, G. A. (2020). Brief review of the slope stability analysis methods. Geological Behavior (GBR), 4(2), 73–77.

Vatanpour, N., Ghafoori, M., & Talouki, H. H. (2014). Probabilistic and sensitivity analyses of effective geotechnical parameters on rock slope stability: A case study of an urban area in northeast Iran. Natural Hazards, 71(3), 1659–1678. https://doi.org/10.1007/s11069-013-0982-6

Woldearegay, K. (2013). Review of the occurrences and influencing factors of landslides in the highlands of Ethiopia: With implications for infrastructural development. Momona Ethiopian Journal of Science, 5(1), 3. https://doi.org/10.4314/mejs.v5i1.85329

Workineh Haro, Daba Bulto Mekonen Bekele, Desalegn Debelo, Muluken Kebede, & Mohamed Edris. (2020). Geology, geochemistry, and gravity survey of Asella area. 20(323). https://doi.org/10.5089/9781513564876.002

Wyllie, D. C. (2014). Rock fall engineering. In Rock Fall Engineering. https://doi.org/10.1201/b17470.

Wyllie, D. C., & Mah, C. (2004). Rock slope engineering.

Yokota, S., & Iwamatsu, A. (2000). Weathering distribution in a steep slope of soft pyroclastic rocks as an indicator of slope instability. Developments in Geotechnical Engineering, 84(C). https://doi.org/10.1016/S0165-1250(00)80016-4

Zewdie, M. M., & Asmare, D. (2023). Investigation and mapping of geological construction materials in parts of Chemoga River Sub Basin, Debre Markos, Ethiopia. Heliyon, 9(3).

Zewdu, A. (2021). Modelling of seepage and slope stability analysis of Ribb embankment dam, Ethiopia.

Zhang, L. (2016). Determination and applications of rock quality designation (RQD). Journal of Rock Mechanics and Geotechnical Engineering, 8(3), 389–397. https://doi.org/10.1016/j.jrmge.2015.11.008

Zheng, H. (2012). A three-dimensional rigorous method for stability analysis of landslides. Engineering Geology, 145, 30–40.

APPENDIXES

Appendix A: The location of the critical the rocks, soil and heterogenous (rock and soil) slope sections of the study area

Locations of slope section's		Sample ID	Northing (N)	Easting (E)	Elevation (m)	Rock types
Before Weyib river from Agarfa town to Wabe river bridge		R1SS1⁑	7° 18' 00″	39° 49 ' 03″	2440	SW-basalt
		R1SS2€				
Ija Doke village		R2SS1⁑	7° 18' 53″	39° 48' 04″	2425	MW-A. basalt
Sire Area	Left side of road from AT-WRB	R3SS1©	7° 21' 02″	39° 47 ' 52″	2345	SW-basalts
	Right side of road from AT-WRB	R3SS2€	7° 21' o4″	39° 47' 57″	2300	SW-basalts
	Right side of road from AT-WRB	R3SS3⁑	7° 21' 14″	39° 47' 04″	2260	W-SC to MW-Basalts
Side of Oda Chefo village		R4SS1¥	7° 25' 15″	39° 44' 17″	1600	Ignimbrite
Before Wabe river bridge		R5SS2©	7° 28' 09″	39° 42' 08″	1435	Alkali olivine basalts

RSS = Road slope section, AT- WRB = Agarfa town to Wabe river bridge

(⁑) - Heterogeneous rock slope without soil (©) - Heterogeneous rock slope with soil at the bottom of slope section

(€) – homogeneous rock slope section (structural control) (¥) – homogeneous rock slope section (non-structural control)

Appendix B: The location of the critical the soil slope sections of the study area

Locations of slope section	Sample ID	Northing(N)	Easting(E)	Elevation (m)	Soil sampling technique
Side of Sebaja village	SS1£	7° 18' 09″	39° 49' 04″	2400	Disturbed soil at depth > 2.5 m
Around Sire area	SS2*	7° 21' 03″	39° 47' 06″	2245	Disturbed soil at depth > 1m
Wanagaya village	SS3£	7° 25' 37″	39° 43' 39″	1550	Disturbed soil at depth >2m
Around Wabe river bridge	SS4*	7° 28' 2″	39° 42' 08″	1415	Disturbed soil at depth > 1m
SSS– Soil slope section					

SS1£ - SS3£ Homogeneous soil slope section	SS2* SS4* Soil sample side section of critical slope

Appendix C: Field surveying for discontinuity parameter of critical slope section

		Critical slope sections	
Discontinuity parameter		R1SS1	R3SS1
Joint spacing(cm)		60-100	50-80
Condition of discontinuity	Persistence (m)	0.3-1.0	2-5
	Joint aperture (cm)	0.05-0.1	0.1-1.5
	Filling materials	Soft filling>5mm	None
	Roughness	Moderately rough	Slightly rough
	Degree of Weathering	Slightly weathered	Slightly weathered
Groundwater condition		Dry	Dry

Appendix D: According to the Deere (1988) modification, the RQD values can be classified as follows:

Interval of RQD values (%)	Rock quality according to Deere (1988)
0- 25	Poor
25-50	Fair
50-75	Good
57-90	Very good
90-100	Excellent

Appendix E: Field estimated GSI values for identified rock

Road slope section	Rock Types	Estimated GSI values
R2SS1	Slightly weathered Aphanitic basalt	50
	Vesicular basalt	47
	scoria	35
R3SS1	Moderately weathered basalt	55
R4SS1	Ignimbrite	45
R5SS1	Alkali- olivine basalt	51

Appendix F: Dry unit weight of rock sample collected from field in laboratory result

Samples Id	Rock types	M (g)	V1(ml)	V2(ml)	V2(ml)-v1(ml)	P=m/v g/cm3	γ= p*g kg/m3	Average of dry unit weight
R1SS2	SW-B	711	650	850	200	3.56	34.87	28.4
		782	600	950	350	2.23	21.92	
	SC	167.5	500	590	90	1.86	18.26	13.5
		142.25	500	660	160	0.89	8.72	
R2SS1	MW-B	672	650	930	280	2.4	23.54	25.6
		564	650	850	200	2.82	27.66	
	MW-V. B	391	500	660	160	2.42	23.97	24.5
		433	650	820	170	2.55	24.99	
	SC	143.5	500	650	150	0.955	9.37	14.8
		123.5	500	560	60	2.06	20.19	
R3SS1	MW-A. B	627	600	830	230	2.73	26.74	23.6
		470	600	825	225	2.089	20.49	
R3SS2	W-SC	487	500	700	200	2.44	23.94	24.6
		465	500	680	180	2.58	25.34	
	SW-B	680	600	850	250	2.72	26.68	27.7
		878	600	900	300	2.93	28.71	
R4SS1	SW-B	662	600	870	270	2.45	24.05	22.0
		715	600	950	350	2.04	20.04	
R5SS2	MW-AOB	525	600	830	230	2.28	22.39	25
		477	650	730	80	5.96	58.49	

SW-B = Slightly weathered Basalts, SC= Scoria, MW-B= Moderately weathered Basalts MW-V. B = Moderately weathered Vascular Basalts, HW-A. B= Highly weathered Aphanitic Basalt, HW-B = Highly weathered basalts, MW-B= Moderately weathered Alkali Olivine Basalts

Appendix G: Laboratory results of Saturated unit weight of rock sample collected from critical slope section

Samples Id	Rock types	M (g)	V1(ml)	V2(ml)	V2(ml)-V1(ml)	ρ=m/v g/cm3	γ= p*g KN/m3	Average of saturated Unit weight (KN/m3)
R1SS2	SW-B	714.4	650	900	250	2.86	28.03	29
		792.3	650	910	260	3.05	29.89	
	SC	172.5	500	590	90	1.92	18.80	21.7
		150.25	500	560	60	2.50	24.57	
R2SS1	MW-B	680.9	600	830	230	2.96	29.04	29.2
		569	600	790	190	2.99	29.39	
	MW-V. B	403.1	650	790	140	2.879	28.25	26.91
		443	650	820	170	2.61	25.56	
	SC	153.25	500	580	80	1.92	18.79	21.13
		143.5	500	560	60	2.39	23.46	
R3SS1	HW-A. B	634	650	830	180	3.52	34.55	30.71
		479.2	650	825	175	2.74	26.86	
R3SS2	W-SC	495	500	700	200	2.48	24.33	25.12
		475	500	680	180	2.64	25.92	
	MW-B	684	650	825	175	3.91	38.34	33.25
		890	600	910	310	2.87	28.16	
R4SS1	MW-B	664.5	650	870	220	3.02	29.63	28.89
		717.5	600	850	250	2.87	28.15	
R5SS2	MW-POB	526.5	600	780	180	2.93	28.69	29.95
		477	600	750	150	3.18	31.19	

Appendix H: The values of Schmidt Rebound and UCS obtained from various critical slope sections.

Slope sections		Schmidt hammer rebound value from each critical slope sections	Average of Rebound value for rock slopes (R)	UCS (Mpa)
R1SS2	SW-B	36, 42, 42.5, 43.5, 46, 48, 48.5, 51.5, 52, 53	46.3	146.89
	SC	15.25, 16, 16.5, 18.25, 19, 20, 21, 21.75, 22, 24	19.375	17.38
R2SS1	MW-B	28, 29, 31.2, 32, 32.5, 33, 34.5, 35.9, 36, 38	32.99	56.67
	SC	11.25, 12, 13, 13.5, 14, 15.5, 16, 17.35, 18.5, 21	15.21	16.14
R3SS1	MW-B	11.25, 12, 13, 13.5, 14, 15.5, 16, 17.35, 18.5, 21	41.975	76.28
R3SS2	W-SC	24, 25, 26, 29, 32, 33, 34.5, 39, 40, 41	32.35	19.09
	MW-B	32, 32.5, 34, 34.5, 36, 36.5, 38, 41.5, 46, 52	37.1	82.08
R4SS1	SW-B	41.5, 42, 42.2, 46, 46.5, 48, 48.5, 51.75, 52, 53	47.325	84.75
R5SS2	SW-AOB	36, 42, 42.5, 43.5, 45, 46.6, 48, 48.5, 50, 51.5	43.61	92.86

Appendix I: The assessed shear strength parameters of critical failure planes (joints) using the Barton-Bandis method

R1SS2---J1

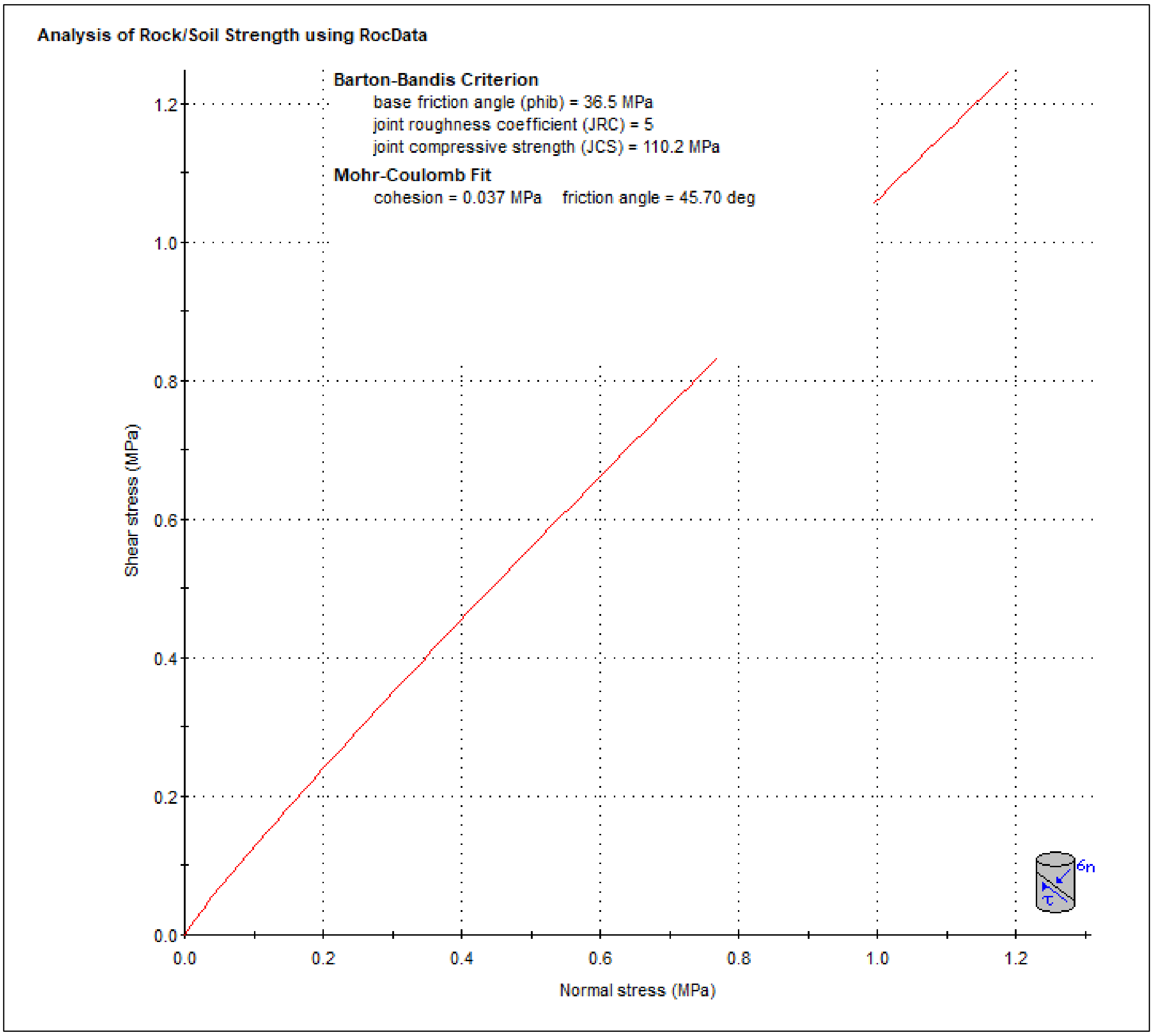

R1SS2---J2

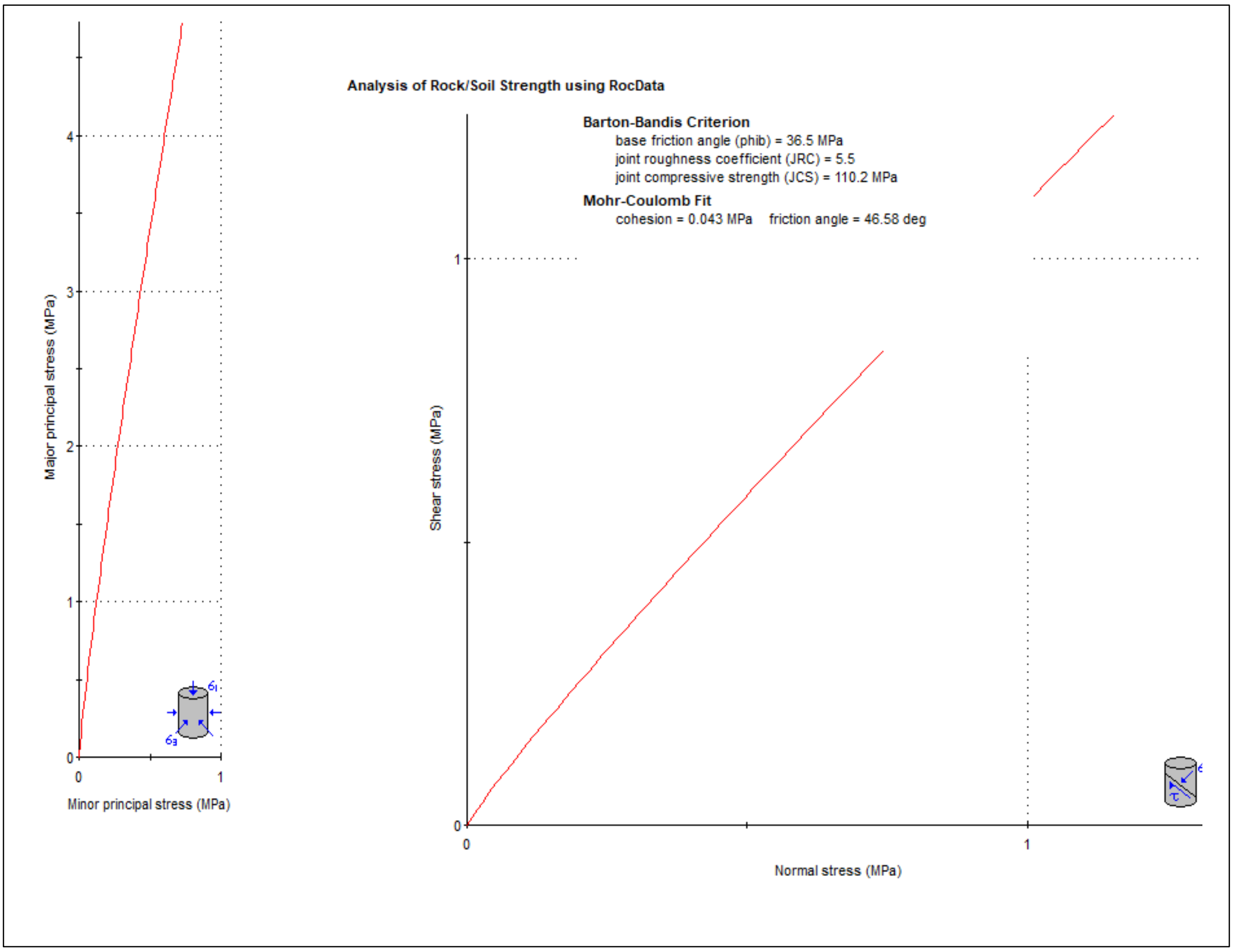

R1SS2- J3

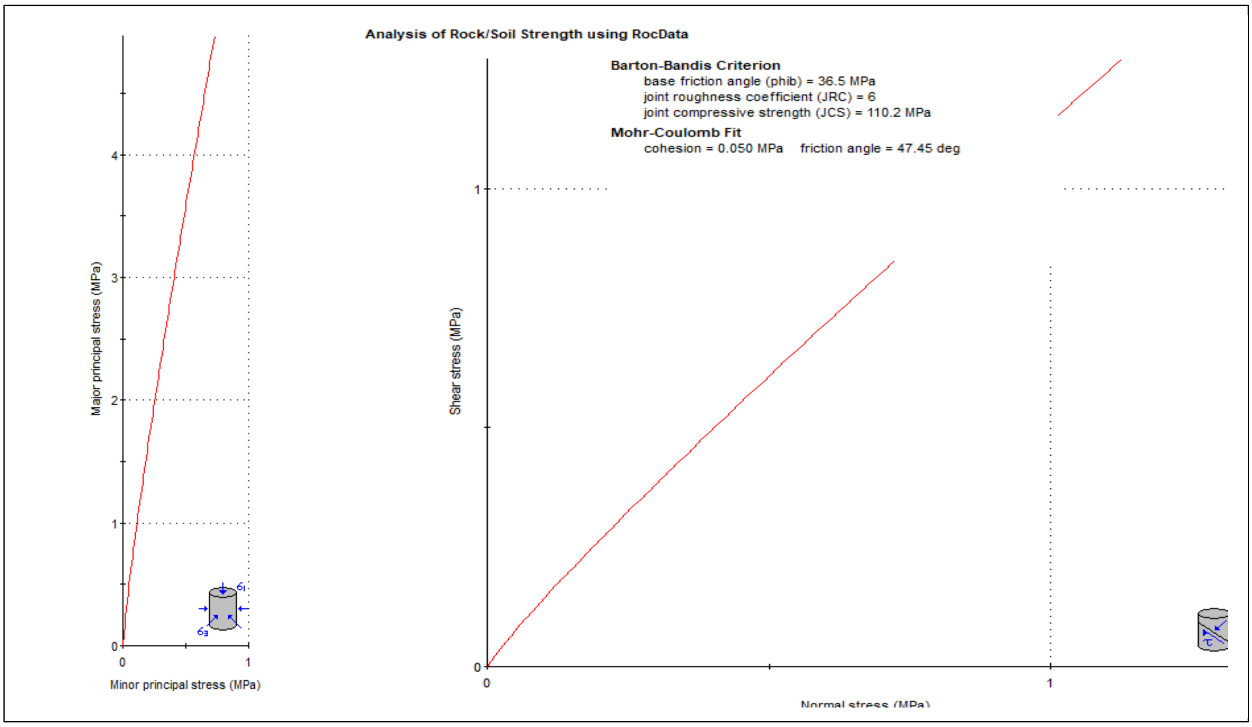

R1SS2- J4

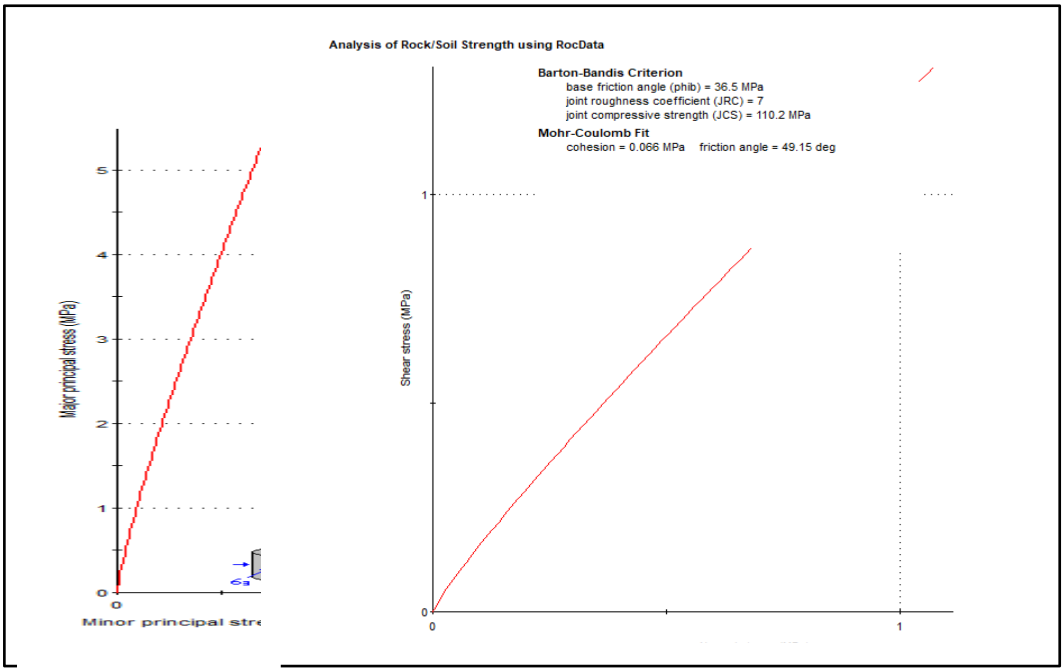

R3SS1……J1

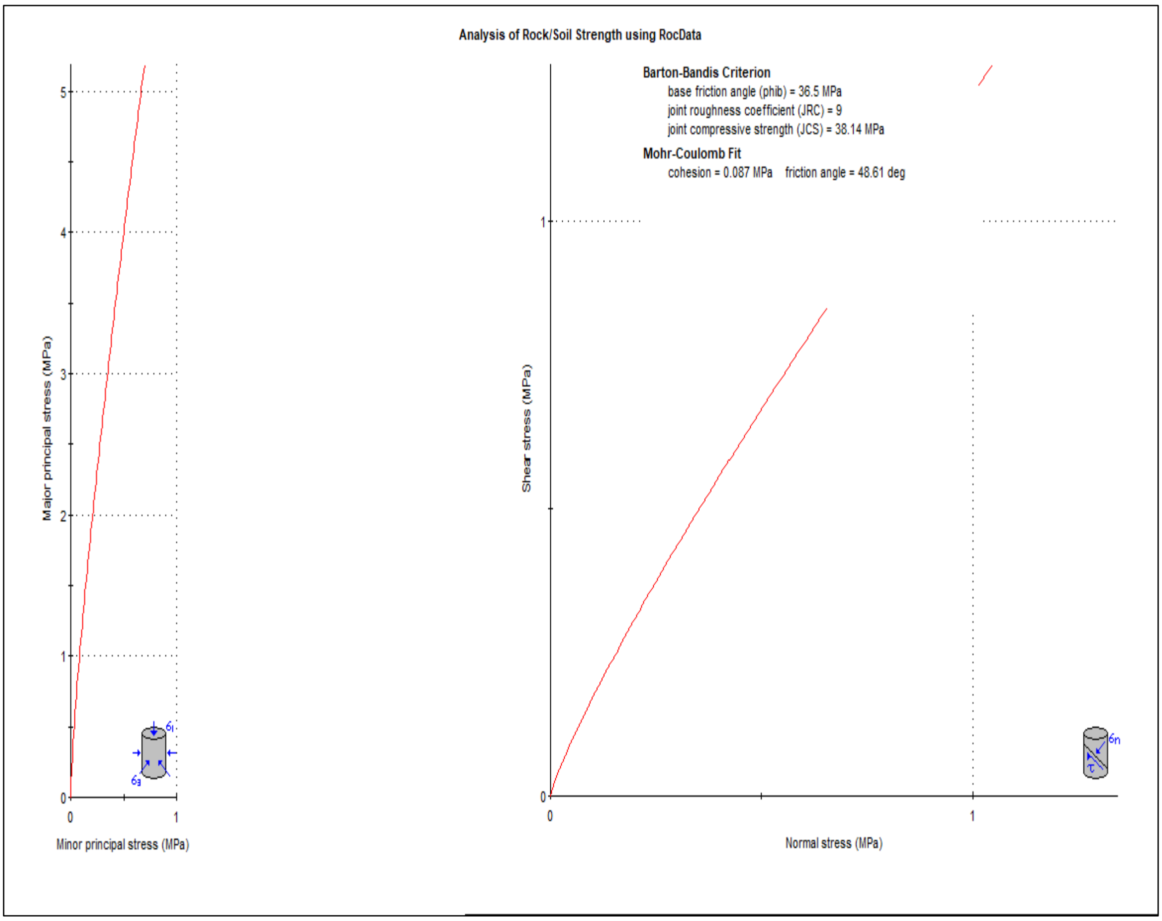

APPENDIX J: The shear strength parameters of the rock mass in critical slope sections were estimated using Rocdata software (Hoek-Brown methods).

R2SS1 MW-A. basalts

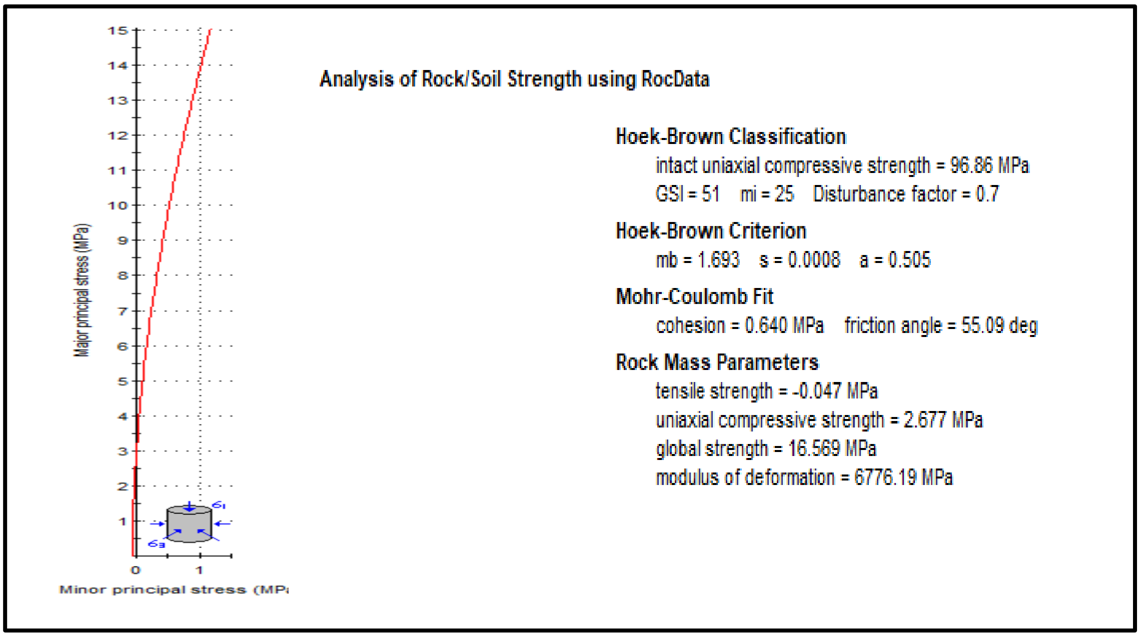

R2SS1 MW-V. basalts

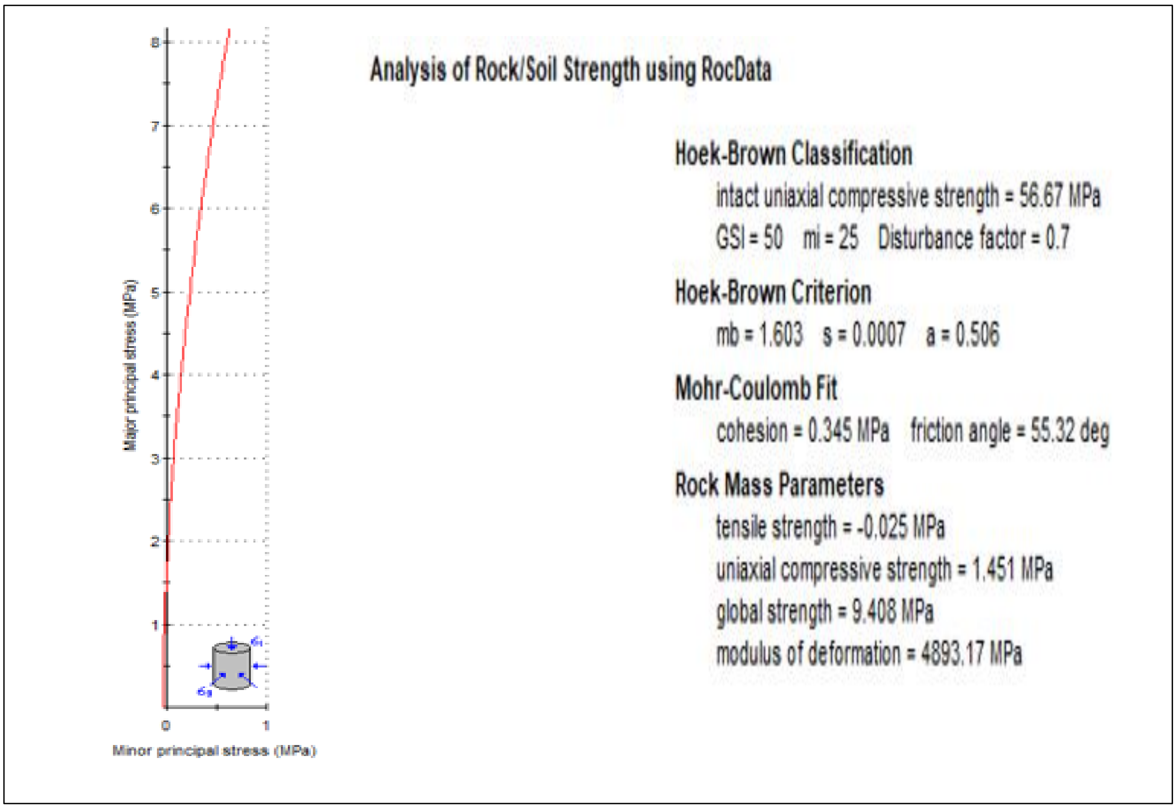

Appendix Ka: Monthly Rainfall data of the study area (Agarfa station) (2010-2022)

Months	Jan	Feb	Mar	Apr	May	Jun	Jul	Aug	Sep	Oct	Nov	Dec	Annual total
2010	41.82	29.61	57.03	60.45	45	11.82	32.22	41.82	16.53	13.77	0.54	0	2360.61
2011	0	0	1.05	14.88	41.13	0	24.03	20.73	22.05	12.99	21.15	0	2169.01
2012	0	0	11.28	39.9	20.16	7.02	21.39	43.53	0	18.06	3.42	3	2179.76
2013	3.27	0.24	60.18	22.11	6.12	5.61	36.75	73.59	25.02	17.82	17.73	0	2281.44
2014	0	0	6.6	5.64	16.05	13.65	16.47	29.1	24.03	38.19	12.57	1.05	2177.35
2015	0	0	7.53	14.7	22.53	19.62	14.64	20.22	21.12	14.88	13.14	0.09	2163.47
2016	8.82	3.06	9.48	0	31.68	14.76	13.44	44.58	0	24.12	23.64	0	2189.58
2017	0	2.28	3.6	10.56	18.16	0	0	0	0	0	0	0	2051.6
2018	37.4	16.8	43.18	45.32	46.75	21.7	65.5	141.13	81.0	93.97	19.22	0.88	2631
2019	2.84	0	36.93	26.9	42.65	13.44	64.12	52.46	52.08	91.61	1.8	9.18	2413.01
2020	0	0	29.79	41.9	56.59	19.175	33.95	84.46	48.16	59.5	11.45	15.77	2420.8
2021	7.56	0	43.28	56.37	39.62	28.16	34.19	57.08	44.97	35.35	4.61	43.56	2415.77
2022	8.9	0	17.45	51.95	18.4	17.95	12.925	24.75	31.25	18.85	0	25.78	2250.2
AV	8.5	4.0	25.18	30.05	31.14	13.3	28.43	48.72	28.17	33.78	9.94		

Appendix Kb: Monthly Rainfall data of the study area (Gobesa station) (2010-2018)

Months	Jan	Feb	Mar	Apr	May	Jun	Jul	Aug	Sep	Oct	Nov	Dec	Annual total
2010	27	12.04	40.24	35.37	6.67	26.067	0	0	0	0	0	147.4	
2011	0	0	1.8	16.38	0	23.82	44.13	57.93	37.62	6.51	28.68	0.36	217.23
2012	0.45	0	0	50.88	19.17	17.88	62.46	54.78	81.6	23.01	4.29	4.41	318.93
2013	3.93	0	39.34	39.2	12.85	16.99	67.37	63.92	40.07	47.74	19.21	0.12	350.74
2014	0	11.52	25.38	29.01	49.05	9.15	30.51	59.7	53.4	68.64	15.3	0	351.66
2015	12.98	11.92	11.92	42.96	15.57	20.26	17.79	44.34	11.94	26.79	5.28	0	221.75
2016	15.75	4.5	0	66	35.52	0	6.99	46.89	0	0	0	0	175.65
2017	57.6	23.1	50.4	131.1	0	0	0	0	0	0	0	0	262.2
2018	0	0	0	0	0	352.5	456.3	350.1	458.4	317.1	0	0	1934.4
average	117.71	63.08	169.08	410.9	138.83	114.167	229.25	327.56	224.63	172.69	72.76	4.89	